Deposit & Copying of Dissertation Declaration

UNIVERSITY OF CAMBRIDGE

Board of Graduate Studies

Please note that you will also need to bind a copy of this Declaration into your final, hardbound copy of thesis - this has to be the very first page of the hardbound thesis.

1 Surname (Family Name)	Forenames(s)	Title
Watson	Laura Pippa Emily	Ms

2 Title of Dissertation as approved by the Degree Committee

Characterisation of human metabolism in physiological and pathophysiological states.

In accordance with the University Regulations in *Statutes and Ordinances* for the PhD, MSc and MLitt Degrees, I agree to deposit one print copy of my dissertation entitled above and one print copy of the summary with the Secretary of the Board of Graduate Studies who shall deposit the dissertation and summary in the University Library under the following terms and conditions:

1. Dissertation Author Declaration

I am the author of this dissertation and hereby give the University the right to make my dissertation available in print form as described in 2. below.

My dissertation is my original work and a product of my own research endeavours and includes nothing which is the outcome of work done in collaboration with others except as declared in the Preface and specified in the text. I hereby assert my moral right to be identified as the author of the dissertation.

The deposit and dissemination of my dissertation by the University does not constitute a breach of any other agreement, publishing or otherwise, including any confidentiality or publication restriction provisions in sponsorship or collaboration agreements governing my research or work at the University or elsewhere.

2. Access to Dissertation

I understand that one print copy of my dissertation will be deposited in the University Library for archival and preservation purposes, and that, unless upon my application restricted access to my dissertation for a specified period of time has been granted by the Board of Graduate Studies prior to this deposit, the dissertation will be made available by the University Library for consultation by readers in accordance with University Library Regulations and copies of my dissertation may be provided to readers in accordance with applicable legislation.

3 Signature	Date
	18/04/2018

Corresponding Regulation

Before being admitted to a degree, a student shall deposit with the Secretary of the Board one copy of his or her hard-bound dissertation and one copy of the summary (bearing student's name and thesis title), both the dissertation and the summary in a form approved by the Board. The Secretary shall deposit the copy of the dissertation together with the copy of the summary in the University Library where, subject to restricted access to the dissertation for a specified period of time having been granted by the Board of Graduate Studies, they shall be made available for consultation by readers in accordance with University Library Regulations and copies of the dissertation provided to readers in accordance with applicable legislation.

Characterisation of human metabolism in physiological and pathophysiological states.

Laura Felgate (nee Watson)

Wolfson College

University of Cambridge

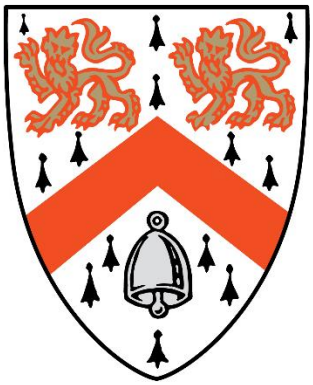

This dissertation is submitted for the degree of Doctor of Philosophy.

September 2017.

Declaration

I hereby declare that this dissertation:

Is the result of my own work and includes nothing which is the outcome of work done in collaboration except as declared in the Preface and specified in the text:

Is not substantially the same as any that I have submitted, or, is being concurrently submitted for a degree or diploma or other qualification at the University of Cambridge or any other University or similar institution except as declared in the Preface and specified in the text. I further state that no substantial part of my dissertation has already been submitted, or, is being concurrently submitted for any such degree, diploma or other qualification at the University of Cambridge or any other University or similar institution:

Does not exceed the word limit of 60,000 (excluding figures, tables, appendices, and references) prescribed by the Degree Committee of the Faculty of Clinical Medicine.

Laura Felgate (nee Watson)

September 2017

Acknowledgements

Throughout my PhD I have been incredibly lucky to meet and work with various people that have contributed to my learning experience. I would like to express my deepest gratitude to Peter Murgatroyd for the opportunity to learn from him and for creating the opportunity to pursue a PhD with his support. I would not be in the position I am today without his guidance, encouragement and patience. Special thanks also goes to Krishna Chatterjee, for agreeing to be my primary supervisor and both David Savage and Krishna for giving me the opportunity to work with their teams. This has provided invaluable added perspective to my PhD and is the part of my research which I have enjoyed the most.

Of course I will remain forever indebted to Les Bluck for all of the scientific contributions and humorous conversations throughout my PhD before his untimely death. His guidance is greatly missed. I would also like to thank Michelle Venables, not only for taking on responsibilities as my co-supervisor, but also her collaboration, the frequent trips to my house to help me with writing up whilst I was on maternity leave and for also being a great colleague.

My PhD would also not have been possible without the support from my colleagues at the CRF. Without the support of Caroline Saunders I would not have progressed at an early stage. She also allowed me the opportunity to present my research in America, which resulted in an award and a publication. Her support towards my research has enabled me to also progress my career as a metabolic physiologist. Lastly to my team and the nurses, without whom, my research would never have been possible. Especially to Katie Carr, for being an amazing colleague and friend who knows how much I have appreciated this.

Finally, I would like to thank my family, especially my husband without whose support, encouragement and shoulder, I would not have completed the dissertation. The addition of my daughter Molly during year 4 makes me even more proud of what I have achieved with everyone's help.

Summary. Laura Watson. Wolfson College.

Characterisation of human metabolism in physiological and pathophysiological states.

The aim of this thesis was to describe the relationships between energy expenditure and body composition in healthy adults and children and in patients with metabolic disorders. In a healthy population resting energy expenditure (REE) is highly influenced by body composition, specifically lean mass (LM). Prediction equations can therefore accurately predict REE from body composition in healthy individuals. However, application of these equations to clinical patients, in whom metabolism is disordered, risks miscalculation of energy metabolism due to their dissociation between body composition and energy expenditure. Therefore new prediction equations were derived based on precise body composition measurements in healthy adults and children. Then, in patients with metabolic disorders, differences between their measured and equation-predicted REE and LM were presented as standardised Z scores.

REE in healthy adults was predicted by the coefficients: age, fat mass and fat-free mass. LM in healthy adults was predicted by the coefficients: bone mineral content and height^2 in men; and by fat and height^2 in women. In healthy children, REE was predicted using gender specific models: by fat and LM in boys; and by solely LM in girls. REE and LM were then measured in adult and paediatric patients with metabolic disorders (Lipodystrophy, Thyrotoxicosis and Resistance to Thyroid Hormone β or α), and Z scores were calculated to highlight their deviations from the healthy populations.

In adults, thyrotoxicosis patients displayed the highest REE Z scores (5.8), followed by lipodystrophy (2.9) and RTHβ cases (1.8), with RTHα demonstrating the lowest REE Z scores (-2.3). For LM, lipodystrophy patients exhibited with the highest Z scores (4.2), followed by RTHα patients (2.1), with RTHβ patients showing normal LM Z scores (-0.2) and thyrotoxicosis patients presenting with the lowest LM Z scores (-1.2). In the paediatric patients, RTHβ patients demonstrated REE Z scores similar to healthy controls (males; -0.15, females; 0.15), but RTHα patients displayed lower REE Z scores (male; -0.82, female; -2.2) compared to RTHβ patients and healthy controls.

These studies highlight the disassociation between REE and body composition in patients with metabolic disorders. The application of a prediction equation for REE to calculate Z scores between measured and predicted values allows quantification of the differences between patients with metabolic disorders and healthy populations, and is a new and important concept.

Abbreviations

Acronym	Definition
2-C	Two-component
4-C	Four – Component model
ADP	Air displacement plethysmography
ADRA2A	Adrenoreceptor Alpha 2A
AGL	Acquired general lipodystrophy
AGPAT2	Acylglycerol-3-phosphate acyltransferase 2
AKT2	Protein Kinase B2
APL	Acquired partial lipodystrophy
BA	Bone area
BIA	Bioelectrical impedance analysis
BMC	Bone mineral content
BMD	Bone mineral density
BMI	Body mass index
BMR	Basal metabolic rate
BSA	Body surface area
BSCL	Berardinelli-Seip congenital lipodystrophy
BSCL2	Berardinelli-Seip congenital lipodystrophy 2
BV	Body volume
BW	Body weight
CAV1	Caveolin 1
CGL	Congenital generalised lipodystrophy
CHO	Carbohydrate
CI	Confidence interval
CIDEC	Cell death-inducing DFFA-like effector C
CRF	Clinical Research Facility
CV	Coefficient of variance
Db	Density
DIT	Diet induced thermogenesis
DXA	Dual energy X-ray absorptiometry
ECG	Electrocardiogram

ECW	Extracellular water
FFM	Fat-Free mass (kg)
FM	Fat mass
FPLD	Familial partial lipodystrophy
FSH	Follicle-stimulating hormone
GEM	Gas exchange measurement
GH	Growth hormone
GnRH	Gonadotropin-releasing hormone
HIV	Human immunodeficiency virus
HPG	Hypothalamic pituitary gonadal axis
HPT	Hypothalamic-pituitary-thyroid axis
ICW	Intracellular water
IGF1	Insulin-like growth factor 1
IRMS	Isotope ratio mass spectroscopy
ISCD	International society of clinical densitometry
KJ/min	Kilo Joules per minute
LD	Lipodystrophy
LH	Luteinizing hormone
LIPE	Lipase, hormone sensitive
LM	Lean mass
LMNA	Lamin A and C
LSC	Least significant change
M	Body mass
MJ/d	Mega Joules per day
N	Nitrogen
NHANES	National Health and Nutrition Examination Survey
P	Pressure
PAEE	Physical activity energy expenditure
PAL	Physical activity level
PCOS	Polycystic Ovary Syndrome
PETCT	Positron emission tomography-computed tomography
PPARγ	Peroxisome proliferator-activated receptor γ

PTRF	Polymerase 1 and transcript release factor
PVN	Paraventricular nucleus
QC	Quality check
REE	Resting energy expenditure
RMS-SD	Root mean square standard deviation
RQ	Respiratory quotient
RTH	Resistance to thyroid hormone
SD	Standard deviation
SDC	Standard deviation scores
SHGB	Sex hormone-binding globulin
SPA	Single photon absorptiometry
SSA	Surface area artefact
STP	Standard temperature pressure
SXA	Single energy X-ray absorptiometry
T3	Triiodothyronine
T4	Thyroxine
TBW	Total body water
TDEE	Total daily energy expenditure
TH	Thyroid hormone
THRA	Thyroid hormone alpha gene
THRB	Thyroid hormone beta gene
TRN	Thyrotropin-releasing hormone
TRα	Thyroid hormone receptor alpha
TRβ	Thyroid hormone receptor beta
TSH	Thyroid stimulating hormone
VSMOW	Vienna Standard Mean Ocean Water
WHO	World Health Organisation
ZMPSTE24	Zinc metallopeptidase STE24

Table of Contents

1. General Introduction.

1.1. Measurement of body composition

Body composition describes approximately 60-80% of the variability in resting energy expenditure (REE), with the majority of the contribution from lean or fat-free mass (FFM (lean plus bone mass)) and a much smaller, but significant, contribution from fat mass. Dual-energy X-ray absorptiometry (DXA) is the method used throughout this thesis to explore both whole body and regional fat, lean and bone mass.

Throughout the history of DXA, developments in science and technology have facilitated advances in bone density and body composition measurement instruments. Single-photon technology was first introduced in 1963, using a single gamma ray radionuclide source with the ability to image peripheral skeleton sites [1]. Dual-photon technology was later developed, making it possible to scan the axial skeleton using the transmission of gamma rays of two different energies. However, both of these instruments had limitations: the use of radionuclides that decayed quickly, long scanning times and poor resolution [2 3]. As the technology advanced further, these instruments were replaced with single and dual-energy X-ray absorptiometry (SXA, DXA). Both instruments used a low dose X-ray tube instead of a radionuclide source, had shorter scanning times, and benefited from higher resolution and thus improved precision. Because SXA uses only a single X-ray beam, it is necessary to correct for soft tissue by laying the site of interest in a water bath. DXA was introduced in 1987 and has become the "gold standard" for clinical bone density measurements. The use of X-ray beams of two energies enables distinction of soft tissue and bone without the need for a water bath [4 5]. The abilities of the latest DXAs to accurately assess both whole body and regional soft tissue, fat and lean mass, as well as bone mineral density, has encouraged the utilisation of DXA within body composition research. Based on the successful use of DXA in research studies, this technology is now migrating into clinical practice.

1.1.1 DXA precision

Precision within this thesis is defined as the repeatability of measurements, with % Coefficient of Variance (%CV) and Least Significant Change (LSC) reported. Instrument precision is important not only for ensuring confidence in the data acquired but also for avoiding misinterpretation of changes in measurements over time. The precision of an instrument is usually established upon installation through repeated measurements in vitro, using a phantom, or in vivo, on participants. The International Society of Clinical Densitometry

(ISCD) has oversight of most policies and procedures issued by DXA manufacturers. In their guidelines, they suggest 30 repeated scans or 15 triplicated scans on the new instrument to explore its repeatability [6 7]. A least significant change (LSC) value is calculated from repeated measures on each region and site scanned twice; this represents the difference in measurements between two scans before a true biological change can be assumed [8].

1.1.2. DXA accuracy

In addition to repeated measurements on each scanner for establishment of precision, measurements should also be performed against different instruments to determine their accuracy. Instrument accuracy is ascertained by comparing the measurements on one instrument to the same measurements collected by another appropriate technique. This scenario typically occurs when new instruments are released by the same or a competing manufacturer. Determining the accuracy of a new instrument is essential before it can be used clinically for patients requiring repeated measures over a period of time and also in research spanning longitudinally where an unavoidable change in instrument occurs in the middle of data collection. Verifying the accuracy of a new instrument against the existing instrument will highlight any differences or biases between them and allow existing data to be corrected for any differences by the derivation and application of cross-calibration equations [7].

Exploring the accuracy of a DXA instrument compared to highly regarded reference methods, such as magnetic resonance imaging (MRI), positron emission tomography–computed tomography (PETCT) or a four-component (4-C) model, can further contribute to the understanding of the DXA instrument's accuracy. The 4-C model incorporates measurements of bone mineral density by DXA, total body mass and body volume by air displacement plethymography (ADP) and total body water by deuterium dilution. This approach can be used to assess whole body fat or lean mass. The benefit of this approach for whole body composition is the inclusion of total body water, which is assumed to be constant at 73% in two-component models (e.g. DXA and ADP). Previous studies have demonstrated differences in body composition measurements between DXA and 4-C models: Tylavsky *et al* [9] compared fat-free mass (FFM) and fat mass measured by the Hologic QDR4500A DXA to measurements obtained using a 4-C model (Lohman 4-C model [10] and Going 4-C model [11]). Their findings demonstrated that DXA overestimated FFM and underestimated fat mass compared to 4-C (Lohman) derived measures. In contrast, using a more recent DXA instrument, Gately *et al* [12] demonstrated significant differences in body fat percentage

between DXA (Prodigy) and 4-C (Lohman) with DXA overestimating fat percentage in overweight and obese children. A similar study of obese children by Wells *et al* [13] also demonstrated that DXA (Prodigy) significantly overestimated fat mass and underestimated lean mass compared to a 4-C model. The relationship between 4-C and the latest DXA model from GE healthcare, the iDXA, is yet to be explored in children and adults.

Cross-calibration is performed by applying regression equations that describe the difference between two instruments or software versions and have been described extensively in the literature for various models of DXA [14-31]. This permits comparison of data from multiple DXA instruments, thus allowing the adoption of new DXA technology in research and clinical settings without negatively impacting the data generated over time.

1.2. Predicting resting energy expenditure and body composition in adults and children

Total daily energy expenditure (TDEE) is divided into three components: resting energy expenditure (REE), the minimum amount of energy needed to maintain normal function; diet-induced thermogenesis (DIT), the amount of energy used to process recently ingested food; and physical activity energy expenditure (PAEE), energy expended by physical movement [32]. REE constitutes 60-80% of TDEE in healthy adults and is most commonly used as an indirect estimate of TDEE, in combination with a physical activity score (PAL) and daily energy intake requirements. REE is often referred to as basal metabolic rate (BMR), but the terms can only be used interchangeably if the conditions of measurement are the same, i.e. at complete rest upon waking. REE can be measured by indirect calorimetry, but it is commonly predicted by multiple regression equations that are applicable to the population being studied [33-35].

1.2.1. Predicting REE in adults and children

Regression equations for the prediction of REE are common throughout the literature. They are used in clinical settings for estimating energy requirements within dietetics or establishing whether an individual's REE is normal compared to the prediction, which may give insight into a disease state.

The most common prediction equations for adults and children are the WHO Schofield equations [33], Oxford equations by Henry [34], Harris and Benedict [35], Mifflin [36], Owen [37] and Molnar [38]. These equations are based on simple anthropometric measurements (age, height, gender and weight), making them easy to apply in most settings and populations. As with any form of methodology, it is essential to recognise how the equations were derived, the population on which they were based and the accuracy of the variables within them.

Starting with the WHO requisitioned equations by Schofield [33], these equations were computed based on 114 published studies of BMR. This amalgamated dataset consisted of approximately 11,000 BMR values, mainly from European or North American participants, with nearly half of the data points from Italian subjects[34]. When applied to some populations outside of these regions, there is a common overestimation of BMR [39] [40] [41]. Henry [34] attributes this to the large number of Italian males in the dataset, as they demonstrated a higher BMR per kg of body weight compared to other populations within the dataset. Although Henry is highly critical of the WHO equations, his development of the Oxford predictive equations utilised data from 166 published studies and excluded all Italian participants, outliers and extreme data points, suggesting that, like the WHO equations, the Oxford equations are not appropriate for all populations.

Total body weight is often used as a coefficient in prediction equations because it is easy and convenient to measure, thus it allows computation of predicted REE at any facility. However, it assumes that there is a consistent contribution of fat, lean and bone mass to the estimation of REE, which may be true for a healthy population of adults but may not be the case in other populations such as disease groups, the elderly and children. Instead, prediction equations using lean or fat-free mass may be more appropriate for describing the variation in REE, especially in those who display atypical lean or fat mass.

Prediction equations such as those derived by Neilson *et al* [42], Nelson *et al* [43], Cunningham [44], Mifflin *et al* [36] and Goran *et al* [45] (in children) offer the means to use either lean or fat-free mass to predict REE. However, some studies have still found significant differences between REE predicted by the aforementioned equations and measured REE [46 47]. The differences between measured and estimated REE may suggest that there are variables other than lean mass and fat-free mass that explain some existing variation in REE. Fat mass and age have been shown to hold small but significant contributions to REE, as have thyroid hormone levels and physical activity parameters [44 48]. The differences in bias seen in REE prediction equations may also lie in the method used for assessment of lean mass, such as DXA, bioelectrical impedance analysis (BIA) or the amalgamation of FFM estimates from existing literature.

1.2.2. Predicting body composition in adults

In the literature, predictions of body composition have primarily focused on body fat as this has been directly linked to obesity and other health issues. Predictions of lean or fat

free mass are typically derived from BIA methods [49-53], which have the advantages of being easy to use and relatively low cost, but as a result, the measurements obtained are less accurate compared to criterion methods such as DXA or 4-C models [54-56]. Accurate prediction of lean mass or FFM may improve the accuracy of REE predictions if the lean mass or FFM variable were to be inserted into a regression equation. However, again, caution should be applied when using regression equations derived from populations that differ from the population being studied and variables are obtained using measurement techniques of questionable accuracy.

When presented in the literature, REE is often divided by lean mass in order to exclude the influence of lean mass on any variation in REE. In a healthy population, REE should increase with lean mass and vice versa [57]. For example, in healthy obese populations, weight gain is associated with a higher REE, because of both an increase in fat mass and a curvilinear increase in fat-free mass as a result of the increased energy cost of carrying more body weight [58]. The elderly often present with low REE and lean mass as a result of an age-associated decline in mobility and physical activity levels [59].

1.2.3. Describing resting energy expenditure in children

In children, lean mass is the primary determinant of variation in REE across the age groups. However, during puberty, REE increases; this can largely be accounted for by FFM, but other factors such as growth and pubertal hormones also play a role [60]. Age is often used as a proxy for maturation, but children do not enter puberty at the same age; girls tend to enter puberty from the ages of 8 to 12 years old and boys 9-14 years old [61]. Therefore, the timing and tempo of pubertal changes in body composition and REE vary considerably.

Puberty is characterised by the development of secondary sex characteristics, gonadal maturation and reaching reproductive capacity [61]. The onset of puberty is initiated by a gonadotropin-releasing hormone from the hypothalamus, marked by an increase in amplitude of luteinising hormone (LH) and follicle-stimulating hormone (FSH) pulses [62 63], which in turn act on the gonads to produce sex steroids such as growth hormone (GH) and oestradiol. The increase in sex steroids is crucial for linear growth and increases in mass of bone and muscle [64]. The timing of puberty varies greatly and is influenced by both environmental and genetic factors.

In boys and girls, puberty induces changes such as a growth spurt, changes in body composition and pubic hair growth. In girls, menarche is a key marker for the timing of

puberty, along with breast development, increases in body fat mass and altered fat distribution. In boys, puberty presents with testicular and penile enlargement and an increase in whole body muscle mass [61].

Physical developments associated with puberty can be assessed using a variety of techniques: self-assessment questionnaires, physical assessment or biochemical assessment. Self-assessed questionnaires, first proposed by Tanner *et al* [65], contain pictures of different stages of breast and pubic development in girls and testicular, penile and pubic development in boys; images are selected by the participant based on their interpretation of their own development [66].

Previous validation studies of pubertal assessment questionnaires have highlighted a risk of under and over-interpretation of self-reported development compared to parental or clinician interpretations [67]. In girls, age at menarche is commonly reported in addition to physical sex characteristics. A physical assessment by a qualified health professional can also be undertaken to assess the development of secondary sex characteristics but may be deemed too intrusive for research into healthy participants and may reduce recruitment of participants onto studies if this were an integral part of the data collection. Finally, this leaves the assessment of hormonal markers of puberty, such as LH or FSH, by a small blood test. Increases in LH and FSH concentrations in the plasma may be an indicator of the production of sex hormones and an early marker of the onset of puberty before the appearance of secondary sex characteristics. This may be the most reliable marker of pubertal status; however, the pulsatile nature of gonadal hormones may make a single assessment difficult, as these hormones are subject to diurnal fluctuations and individual variability [61].

The inclusion of a pubertal score or stage of puberty in predicting REE is rare; instead, age is used as an indicator of puberty. Lazzer *et al* [68] developed prediction equations in over 800 healthy obese children and adolescents and included a pubertal score by Tanner assessment within the analysis. The model that explained the greatest variation in REE consisted of pubertal stage, FFM and fat mass (R^2 = 0.70).

1.2.4 Standard deviation and Z-score use in interpretation

Describing what is “normal” in anthropometry and body composition is more common in the paediatric literature than the adult literature. Growth charts are used to establish normal growth and development for paediatric age ranges using percentiles, with 0.4th being

the lowest, 50th regarded as average and 99.6th as the highest percentile displayed on many such charts [69].

Bone density interpretation within the adult and paediatric literature uses an age- and gender-matched Z-score based on data-points from large, healthy cohorts (WHO/NHANES) to distinguish normal bone density trends with age, tracking the increase in bone density with age in paediatrics and the decline with advancing age in adults. It also identifies, in adults, where osteoporosis and osteopenia begin.

The use of Z-scores or percentiles in other areas of body composition and energy expenditure is less common and has only recently been explored in DXA and 4-C measurements in order to determine "normal" in the adult and paediatric literature. Kelly *et al* [70], using the National Health and Nutrition Examination Survey (NHANES) from 1999-2004, developed Z-scores and percentiles for DXA-measured body composition. These data provide reference ranges for multiple components of body composition, including fat mass, lean mass and bone mineral content (BMC), for regions including arms, legs and trunk for populations of white, black and Mexican American origins. Percentiles were derived from Z-scores calculated from the standard deviation of each measurement for the whole population. The measurements were performed on Hologic QDR4500 DXA scanners. More recently, Imboden *et al* [71] derived healthy adult reference percentiles (n=3327, 1251 men and 2076 women) based on fat mass measurements performed on recent models of GE DXA scanners to replace the existing NHANES (1999-2004) dataset. Although its application may be restricted to GE systems and Caucasian populations, it is a useful up-to-date tool for providing meaningful interpretation of DXA fat mass measurements in healthy adults.

In children, Wells *et al* and Atherton *et al* [56 72] have generated Z-scores and standard deviation scores (SDC) in measures such as fat mass and FFM using robust and accurate methods of measurement (DXA and 4-C) in children aged 3-23 years. Reference data Z-scores in energy expenditure are yet to be found within the paediatric or adult literature.

1.3. Metabolic disorders

Clinical examples of metabolic disorders focus on thyroid hormone (TH) disorders and lipodystrophy as these complex genetic conditions present with very different dissociations in body composition and REE compared to each other and healthy controls.

1.3.1. Resistance to thyroid hormone

Thyroid hormones (TH), thyroxine (T4) and triiodothyronine (T3), are essential for normal growth, development and metabolism of most cell and tissues. The hypothalamic-pituitary-thyroid (HPT) axis controls the synthesis and secretion of TH from the thyroid. Circulating TH feedback at hypothalamic and pituitary levels to regulate their own synthesis. Thyrotropin-releasing hormone (TRH) neurons in the PVN secrete TRH in response to low circulating T4 and T3 levels. Consequently, TRH signalling in the pituitary stimulates the secretion of thyroid-stimulating hormone (TSH), which triggers the release of T4 and T3 from the thyroid gland into the blood stream [73]. These signals maintain the complex mechanisms involved in TH homeostasis. The effect of TH on physiological processes are mediated by thyroid hormone receptor (TR) proteins. TRα and TRβ are encoded by genes THRA and THRB on chromosomes 17 and 3 [74 75]. Two proteins are generated from THRA; TRα1 and TRα2. TRα1 is particularly abundant in the central nervous system, myocardium, gastrointestinal tract and skeletal muscle. TRα2 is expressed in a variety of tissues such as the brain and testis but does not bind thyroid hormone, so its physiological role is unclear. THRB generates two thyroid hormone receptors, TRβ1 and TRβ2. TRβ1 is widely expressed, predominantly in the liver and kidney whilst TRβ2 is present in the hypothalamus, pituitary, inner ear and retina [76].

Thyroid hormone also has profound effects on skeletal muscle. Hyperthyroidism often presents with reduced muscle mass and myopathy [77]. Skeletal muscle is one of the main determinants of resting energy expenditure (REE). REE is also closely dependent on thyroid hormone status and altered by small changes in thyroid hormone. Thyroid hormones are known to upregulate many genes involved in metabolism and are also known to increase mitochondrial uncoupling, thereby providing a mechanism for increasing energy expenditure [78].

Thyroid hormones also have important interactions with adipose tissue and this is important for weight control and energy balance [79]. Hormonal signals from adipose tissue (e.g. leptin) act on the central nervous system to regulate energy intake and also the activity of the HPT axis. Thyroid hormones, in particular T3, regulates adipogenesis of white adipose tissue (WAT) and brown adipose tissue (BAT) and genes involved in lipid metabolism; lipogenesis and lipolysis. The lipolytic effects of thyroid hormones can be indirect. Specifically, hyperthyroidism enhances tissue sensitivity to catecholamines and this includes

adipose tissue lipolysis. The isoforms of thyroid hormone receptors TRα1 and TRβ1 are present in both WAT and BAT [80]. Mutations in human TRα1 are associated with increased body fat, visceral adiposity and reduced adaptive thermogenesis [81]. Within BAT, whose function is the production of heat under cold exposure, T3 is known to regulate uncoupling protein 1 gene expression via TRβ1 thereby increasing fatty acid oxidation in BAT and its metabolism [82].

Thyroid hormone resistance (RTH) is a rare dominantly-inherited syndrome caused by mutations in either of two different thyroid hormone receptor isoforms, TRα and TRβ, [74 75]. The mutant receptors exhibit reduced function and also inhibit their wild type counterparts in a dominant negative manner [83]. Mutations in these receptors cause RTHα and RTHβ, respectively.

RTHβ is characterised by elevated circulating free thyroxine (T_4) and triiodothyronine (T_3) and normal or slightly elevated thyroid-stimulating hormone (TSH). The incidence of RTHβ is approximately 1 in 40,000 [84]. Clinically, RTHβ is highly heterogeneous and ranges from asymptomatic to highly symptomatic. The majority of individuals with RTHβ achieve normal growth and development because high TH levels compensate for tissue resistance. However, due to divergent expressions of TRα and TRβ in different tissues, some individuals with RTHβ exhibit features of hyperthyroidism, such as tachycardia and weight loss, or osteoporosis (Figure 1.1) [85]. Both total cholesterol and LDL cholesterol are raised in RTHβ [86], which may reflect hepatic resistance to the effect of thyroid hormone, and dyslipidaemia improves with thyroxine treatment [86]. Hypothyroidism is also known to increase intrahepatic lipid levels, which can lead to non-alcoholic fatty liver disease (NAFLD).

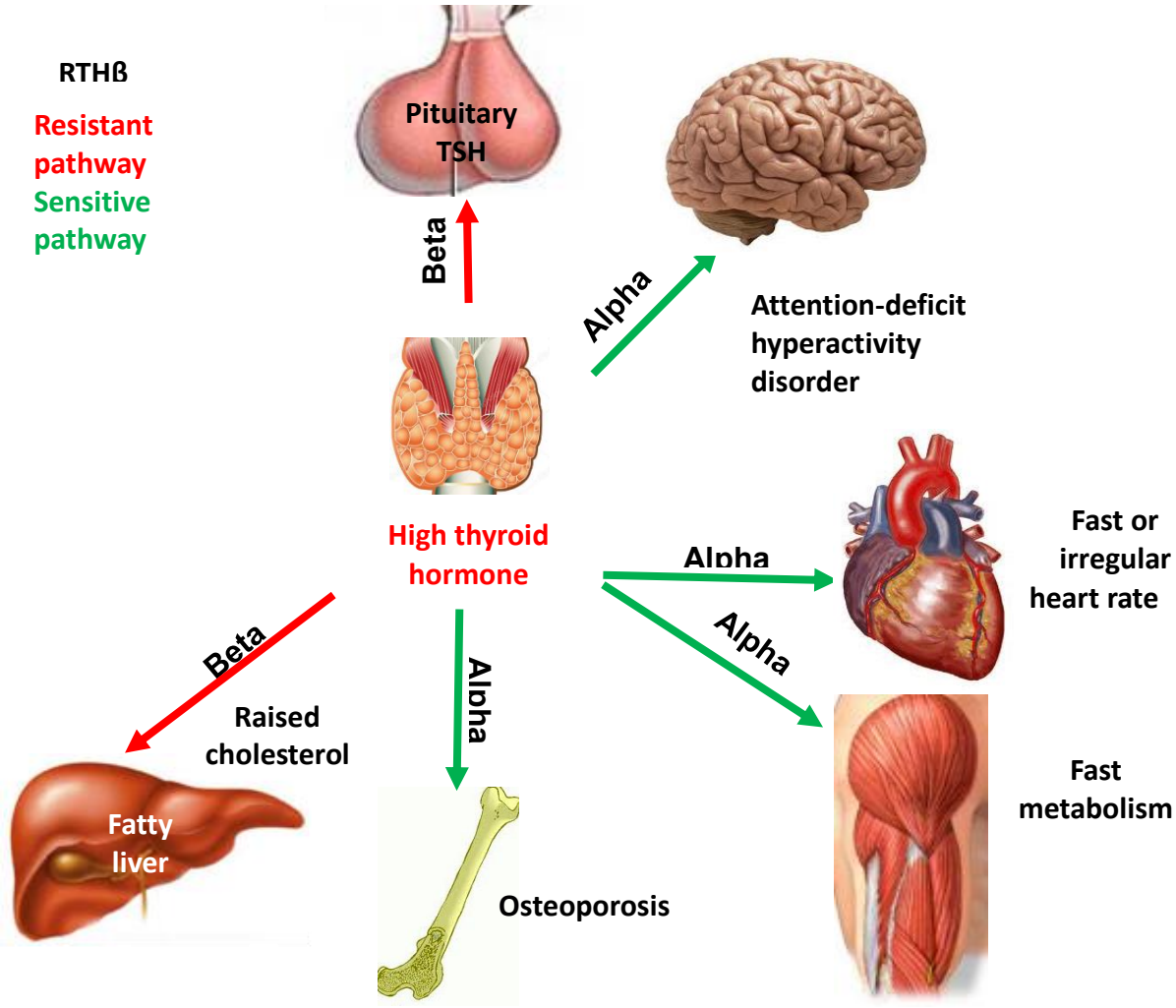

Figure 1.1. Resistance to thyroid hormone due to defective thyroid receptor beta. TRβ mutations markedly increase liver mass with an excess deposition of lipids, so patients consequently present with fatty liver and raised cholesterol. TSH = thyroid stimulating hormone

RTHα mutations are much rarer, with just fourteen cases having been identified to date. Patients exhibit hypothyroid features, such as delayed growth, neuro-developmental retardation, weight gain and a slow heart rate, reflecting hormone resistance in TRα-expressing tissues, in the face of near-normal circulating TH levels (figure 1.2) [87].Common findings in the reported RTHα patients include short stature, high BMI and low muscle tone [75 88-90]. Body composition and energy expenditure are not always reported, but some RTHα cases demonstrate high fat mass and low resting energy expenditure [87 88]. In contrast, Mitchell *et al* [78] reported elevated REE in RTHβ patients compared to controls.

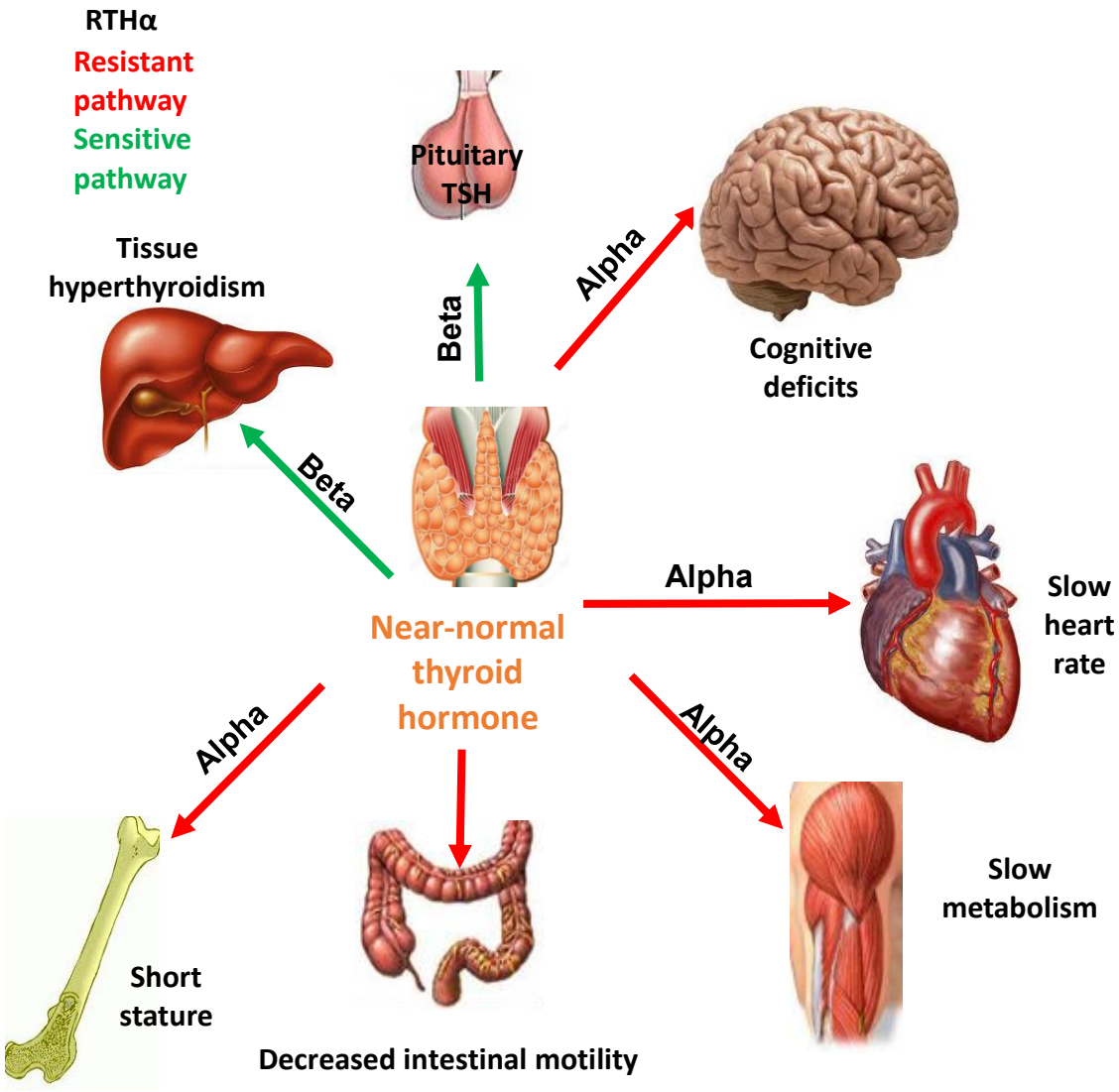

Figure 1.2. Resistance to thyroid hormone due to defective thyroid receptor alpha. TSH = thyroid stimulating hormone

3.2. Thyrotoxicosis

Thyrotoxicosis is a state of thyroid hormone excess, encompassing hyperthyroidism where the thyroid secretes and synthesises excessive quantities of thyroid hormone. Both T_4

and T_3 concentrations are elevated and TSH is undetectable because of negative feedback inhibition. Extremely elevated TH concentrations cause weight loss (mediated by raised metabolic rate), fast heart rate, and muscle weakness due to catabolic tissue effects (figure 1.3) [91]. The most common cause of thyrotoxicosis is Graves' disease, which is an autoimmune condition. Physical characteristics of Graves' disease depend on the severity of the disorder, but common symptoms include weight loss, fatigue, muscle weakness, decreased appetite and cardiac arrhythmias.

Hyperthyroidism is associated with increased REE [92] and decreased fat and lean mass [93 94], demonstrating a dissociation between energy expenditure and body composition in this disease cohort. The increased REE has been correlated with elevated TH levels, which can be treated with anti-thyroid drugs, radioactive iodine or surgery to restore the euthyroid state; however, these treatments result in reduced REE, which may contribute to weight gain and increased fat and lean mass after thyrotoxicosis treatment.

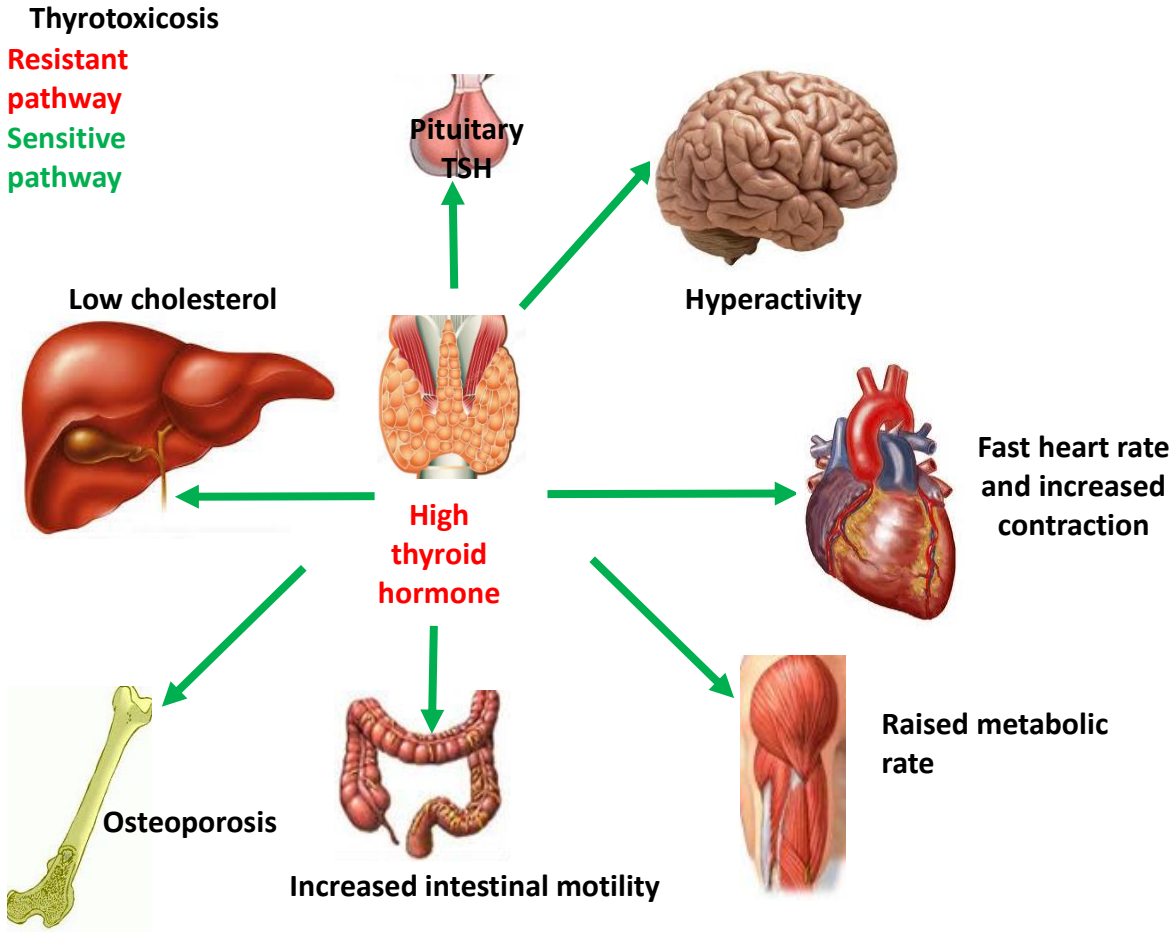

Figure 1.3. Hyperthyroidism due to thyrotoxicosis. TSH = thyroid stimulating hormone.

1.3.3. Lipodystrophy

Lipodystrophy (LD) is a disorder characterised by a lack of adipose tissue or fat tissue. In contrast to 'leanness', a state characterised by 'empty' but otherwise healthy adipocytes (fat cells), in LD the adipocytes are either absent or dysfunctional. LD is categorised in terms of aetiology (genetic or acquired) and the extent of fat loss (generalised or partial). The major metabolic consequences of LD, which include severe insulin resistance, dyslipidaemia and hepatic steatosis, are consistent across the forms of LD but vary in severity depending on the extent of adipocyte loss/dysfunction [95]. The types of LD are explained below, and the clinical and metabolic features of LD are detailed in figure 1.4.

Inherited lipodystrophies:

1) Congenital generalised LD (CGL), also known as Berardinelli-Seip congenital lipodystrophy (BSCL), is a rare autosomal recessive disorder, characterised by a general loss of adipocytes, therefore it is considered the most severe form of LD. A loss of function in several genes (AGPAT2, BSCL2, CAV1 and PTRF) has been identified as the basis of CGL [95 96].

2) Familial partial LD (FPLD) is characterised by a partial lack and/or re-distribution of adipocytes and is often more prominent peripherally, in the limbs [97]. The loss of adipose tissue often becomes apparent around the time of puberty, whereas CGL is usually observed from birth. Loss-of-function mutations in the LMNA, PPARG, ZMPSTE24, AKT2, CIDEC, PLIN1, LIPE and ADRA2A genes have been identified as contributing factors in the development of FPLD [95], [98-100].

Acquired lipodystrophies:

1) Acquired partial LD (APL) is the most common form of partial LD. It is associated with the use of antiretroviral therapy for the treatment of human immunodeficiency virus (HIV) and is found in approximately 50% of HIV patients undergoing treatment.

2) Acquired generalised lipodystrophy (AGL), also known as Lawrence syndrome, is characterised by a gradual loss of subcutaneous fat in the face, trunk and extremities. It can be recognised during childhood or adulthood, and it often occurs in conjunction with other auto-immune disorders.

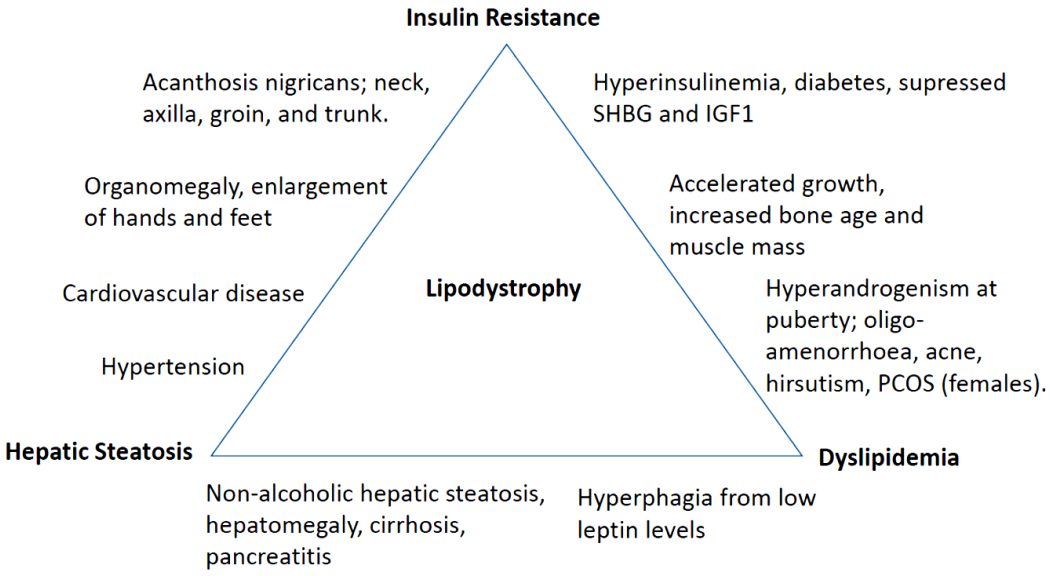

Figure 1.4. Triad of the effects, symptoms and consequences of lipodystrophy, dependent on severity, in inherited or acquired forms. SHBG = sex hormone binding-globulin, IGF1 = insulin-like growth factor 1, PCOS = polycystic ovary syndrome.

Typically, LD has been associated with an absolute increase in muscle mass and an accompanying increase in REE [101]. The increase in REE has predominantly been explained by high lean body mass; however, there is a lack of information on the relationship between body composition and REE in different forms of LD. Other metabolic contributions, such as from organomegaly, may be more evident in different genetically-defined subtypes of the disorder.

1.4. Aims and objectives

The aims of this thesis are:

- To develop a new approach to describe resting energy expenditure and body composition in healthy adults (Chapter 4).
- To further explore and develop an approach to describe resting energy expenditure in healthy children and adolescents (Chapter 5).
- To apply the above approaches to three metabolic conditions, resistance to thyroid hormone (alpha and beta forms), thyrotoxicosis and lipodystrophy, in order to describe divergence in energy expenditure and body composition in these disorders in comparison to healthy controls.

1.5. References

1. Adams JE. Single- and Dual-Energy: X-Ray Absorptiometry. In: Genant HK, Guglielmi G, Jergas M, eds. Bone Densitometry and Osteoporosis. Berlin, Heidelberg: Springer Berlin Heidelberg 1998:305-34.

2. Gluer CC. 30years of DXA technology innovations. *Bone* 2017

3. Lohman TGC, Z. Dual energy X-ray Absorptiometry. In: Heymsfield SL, T.G. Wang, Z. Going, S.G. , ed. Human Body Composition. USA: HUman Kinetics 2005.

4. Shepherd JA, Ng BK, Sommer MJ, et al. Body composition by DXA. *Bone* 2017

5. Fundamentals of Bone Densitometry. National Oesteoporosis Society National Training Scheme for Bone Densitometry; 2000; Bath. National Oesteoporosis Society.

6. Baim S, Wilson CR, Lewiecki EM, et al. Precision assessment and radiation safety for dual-energy X-ray absorptiometry: position paper of the International Society for Clinical Densitometry. *Journal of clinical densitometry : the official journal of the International Society for Clinical Densitometry* 2005;8(4):371-8.

7. Shepherd JA, Lu Y, Wilson K, et al. Cross-calibration and minimum precision standards for dual-energy X-ray absorptiometry: the 2005 ISCD Official Positions. *Journal of clinical densitometry : the official journal of the International Society for Clinical Densitometry* 2006;9(1):31-6.

8. Shepherd JA, Lu Y. A generalized least significant change for individuals measured on different DXA systems. *Journal of clinical densitometry : the official journal of the International Society for Clinical Densitometry* 2007;10(3):249-58.

9. Tylavsky F, Lohman T, Blunt BA, et al. QDR 4500A DXA overestimates fat-free mass compared with criterion methods. *Journal of applied physiology* 2003;94(3):959-65.

10. Lohman TG. Research progress in validation of laboratory methods of assessing body composition. *Medicine and science in sports and exercise* 1984;16(6):596-605.

11. Hewitt MJ, Going SB, Williams DP, et al. Hydration of the fat-free body mass in children and adults: implications for body composition assessment. *The American journal of physiology* 1993;265(1 Pt 1):E88-95.

12. Gately PJ, Radley D, Cooke CB, et al. Comparison of body composition methods in overweight and obese children. *Journal of applied physiology* 2003;95(5):2039-46.

13. Wells JC, Haroun D, Williams JE, et al. Evaluation of DXA against the four-component model of body composition in obese children and adolescents aged 5-21 years. *Int J Obes (Lond)* 2010;34(4):649-55.

14. Faulkner KG, Gluer CC, Estilo M, et al. Cross-calibration of DXA equipment: upgrading from a Hologic QDR 1000/W to a QDR 2000. *Calcified tissue international* 1993;52(2):79-84.

15. Genant HK, Grampp S, Gluer CC, et al. Universal standardization for dual x-ray absorptiometry: patient and phantom cross-calibration results. *Journal of bone and mineral research : the official journal of the American Society for Bone and Mineral Research* 1994;9(10):1503-14.

16. Eiken P, Kolthoff N, Barenholdt O, et al. Switching from DXA pencil-beam to fan-beam. II: Studies in vivo. *Bone* 1994;15(6):671-6.

17. Abrahamsen B, Gram J, Hansen TB, et al. Cross calibration of QDR-2000 and QDR-1000 dual-energy X-ray densitometers for bone mineral and soft-tissue measurements. *Bone* 1995;16(3):385-90.

18. Benmalek A, Sabatier JP. Comparison and cross-calibration of DXA systems: ODX-240 and Sophos L-XRA versus Hologic QDR-4500, for spinal bone mineral measurement. Translation of a reference database. *Osteoporosis international : a journal established as result of cooperation between the European Foundation for Osteoporosis and the National Osteoporosis Foundation of the USA* 1998;8(6):570-7.

19. Ellis KJ, Shypailo RJ. Bone mineral and body composition measurements: cross-calibration of pencil-beam and fan-beam dual-energy X-ray absorptiometers. *Journal of bone and mineral research : the official journal of the American Society for Bone and Mineral Research* 1998;13(10):1613-8.

20. Cawte SA, Pearson D, Green DJ, et al. Cross-calibration, precision and patient dose measurements in preparation for clinical trials using dual energy X-ray absorptiometry of the lumbar spine. *Br J Radiol* 1999;72(856):354-62.

21. Blake GM, Harrison EJ, Adams JE. Dual X-ray absorptiometry: cross-calibration of a new fan-beam system. *Calcified tissue international* 2004;75(1):7-14.

22. Saarelainen J, Honkanen R, Vanninen E, et al. Cross-calibration of Lunar DPX-IQ and DPX dual-energy x-ray densitometers for bone mineral measurements in women: effect of body anthropometry. *Journal of clinical densitometry : the official journal of the International Society for Clinical Densitometry* 2005;8(3):320-9.

23. Pearson D, Horton B, Green DJ. Cross calibration of DXA as part of an equipment replacement program. *Journal of clinical densitometry : the official journal of the International Society for Clinical Densitometry* 2006;9(3):287-94.

24. Covey MK, Smith DL, Berry JK, et al. Importance of cross-calibration when replacing DXA scanners: QDR4500W and Discovery Wi. *J Nurs Meas* 2008;16(3):155-70.

25. Hull H, He Q, Thornton J, et al. iDXA, Prodigy, and DPXL dual-energy X-ray absorptiometry whole-body scans: a cross-calibration study. *Journal of clinical densitometry : the official journal of the International Society for Clinical Densitometry* 2009;12(1):95-102.

26. Covey MK, Berry JK, Hacker ED. Regional body composition: cross-calibration of DXA scanners--QDR4500W and Discovery Wi. *Obesity (Silver Spring)* 2010;18(3):632-7.

27. Shepherd JA, Fan B, Lu Y, et al. A multinational study to develop universal standardization of whole-body bone density and composition using GE Healthcare Lunar and Hologic DXA systems. *Journal of bone and mineral research : the official journal of the American Society for Bone and Mineral Research* 2012;27(10):2208-16.

28. Malouf J, DiGregorio S, Del Rio L, et al. Fat tissue measurements by dual-energy x-ray absorptiometry: cross-calibration of 3 different fan-beam instruments. *Journal of clinical densitometry : the official journal of the International Society for Clinical Densitometry* 2013;16(2):212-22.

29. Hind K, Cooper W, Oldroyd B, et al. A cross-calibration study of the GE-Lunar iDXA and prodigy for the assessment of lumbar spine and total hip bone parameters via three statistical methods. *Journal of clinical densitometry : the official journal of the International Society for Clinical Densitometry* 2015;18(1):86-92.

30. Saarelainen J, Hakulinen M, Rikkonen T, et al. Cross-Calibration of GE Healthcare Lunar Prodigy and iDXA Dual-Energy X-Ray Densitometers for Bone Mineral Measurements. *Journal of osteoporosis* 2016;2016:1424582.

31. Reinhardt M, Piaggi P, DeMers B, et al. Cross calibration of two dual-energy X-ray densitometers and comparison of visceral adipose tissue measurements by iDXA and MRI. *Obesity (Silver Spring)* 2017;25(2):332-37.

32. Westerterp KR. Control of energy expenditure in humans. *European journal of clinical nutrition* 2017;71(3):340-44.

33. Schofield WN. Predicting basal metabolic rate, new standards and review of previous work. *Human nutrition Clinical nutrition* 1985;39 Suppl 1:5-41.

34. Henry CJ. Basal metabolic rate studies in humans: measurement and development of new equations. *Public Health Nutr* 2005;8(7A):1133-52.

35. Harris JA, Benedict FG. A Biometric Study of Human Basal Metabolism. *Proceedings of the National Academy of Sciences of the United States of America* 1918;4(12):370-3.

36. Mifflin MD, St Jeor ST, Hill LA, et al. A new predictive equation for resting energy expenditure in healthy individuals. *The American journal of clinical nutrition* 1990;51(2):241-7.

37. Owen OE, Holup JL, D'Alessio DA, et al. A reappraisal of the caloric requirements of men. *The American journal of clinical nutrition* 1987;46(6):875-85.

38. Molnar D, Jeges S, Erhardt E, et al. Measured and predicted resting metabolic rate in obese and nonobese adolescents. *The Journal of pediatrics* 1995;127(4):571-7.

39. Song T, Venkataraman K, Gluckman P, et al. Validation of prediction equations for resting energy expenditure in Singaporean Chinese men. *Obes Res Clin Pract* 2014;8(3):e201-98.

40. Wahrlich V, Teixeira TM, Anjos LA. Validity of a population-specific BMR predictive equation for adults from an urban tropical setting. *Clin Nutr* 2016

41. Muller MJ, Bosy-Westphal A, Klaus S, et al. World Health Organization equations have shortcomings for predicting resting energy expenditure in persons from a modern, affluent population: generation of a new reference standard from a retrospective analysis of a German database of resting energy expenditure. *The American journal of clinical nutrition* 2004;80(5):1379-90.

42. Nielsen S, Hensrud DD, Romanski S, et al. Body composition and resting energy expenditure in humans: role of fat, fat-free mass and extracellular fluid. *International journal of obesity and related metabolic disorders : journal of the International Association for the Study of Obesity* 2000;24(9):1153-7.

43. Nelson KM, Weinsier RL, Long CL, et al. Prediction of resting energy expenditure from fat-free mass and fat mass. *The American journal of clinical nutrition* 1992;56(5):848-56.

44. Cunningham JJ. Body composition as a determinant of energy expenditure: a synthetic review and a proposed general prediction equation. *The American journal of clinical nutrition* 1991;54(6):963-9.

45. Goran MI, Kaskoun M, Johnson R. Determinants of resting energy expenditure in young children. *The Journal of pediatrics* 1994;125(3):362-7.

46. Tverskaya R, Rising R, Brown D, et al. Comparison of several equations and derivation of a new equation for calculating basal metabolic rate in obese children. *Journal of the American College of Nutrition* 1998;17(4):333-6.

47. Hofsteenge GH, Chinapaw MJ, Delemarre-van de Waal HA, et al. Validation of predictive equations for resting energy expenditure in obese adolescents. *The American journal of clinical nutrition* 2010;91(5):1244-54.

48. Goran MI, Beer WH, Wolfe RR, et al. Variation in total energy expenditure in young healthy free-living men. *Metabolism: clinical and experimental* 1993;42(4):487-96.

49. Loenneke JP, Wilson JM, Wray ME, et al. The estimation of the fat free mass index in athletes. *Asian J Sports Med* 2012;3(3):200-3.

50. Ramsey R, Isenring E, Daniels L. Comparing measures of fat-free mass in overweight older adults using three different bioelectrical impedance devices and three prediction equations. *The journal of nutrition, health & aging* 2012;16(1):26-30.

51. Hughes JT, Maple-Brown LJ, Piers LS, et al. Development of a single-frequency bioimpedance prediction equation for fat-free mass in an adult Indigenous Australian population. *European journal of clinical nutrition* 2015;69(1):28-33.

52. Luke A, Bovet P, Forrester TE, et al. Prediction of fat-free mass using bioelectrical impedance analysis in young adults from five populations of African origin. *European journal of clinical nutrition* 2013;67(9):956-60.

53. Stewart AD, Hannan WJ. Prediction of fat and fat-free mass in male athletes using dual X-ray absorptiometry as the reference method. *Journal of sports sciences* 2000;18(4):263-74.

54. Xu L, Cheng X, Wang J, et al. Comparisons of body-composition prediction accuracy: a study of 2 bioelectric impedance consumer devices in healthy Chinese persons using DXA and MRI as criteria methods. *Journal of clinical densitometry : the official journal of the International Society for Clinical Densitometry* 2011;14(4):458-64.

55. Gaba A, Kapus O, Cuberek R, et al. Comparison of multi- and single-frequency bioelectrical impedance analysis with dual-energy X-ray absorptiometry for assessment of body composition in post-menopausal women: effects of body mass index and accelerometer-determined physical activity. *J Hum Nutr Diet* 2015;28(4):390-400.

56. Atherton RR, Williams JE, Wells JC, et al. Use of fat mass and fat free mass standard deviation scores obtained using simple measurement methods in healthy children and patients: comparison with the reference 4-component model. *PloS one* 2013;8(5):e62139.

57. Speakman JR, Selman C. Physical activity and resting metabolic rate. *The Proceedings of the Nutrition Society* 2003;62(3):621-34.

58. Deriaz O, Fournier G, Tremblay A, et al. Lean-body-mass composition and resting energy expenditure before and after long-term overfeeding. *The American journal of clinical nutrition* 1992;56(5):840-7.

59. Bosy-Westphal A, Eichhorn C, Kutzner D, et al. The age-related decline in resting energy expenditure in humans is due to the loss of fat-free mass and to alterations in its metabolically active components. *The Journal of nutrition* 2003;133(7):2356-62.

60. Cheng HL, Amatoury M, Steinbeck K. Energy expenditure and intake during puberty in healthy nonobese adolescents: a systematic review. *The American journal of clinical nutrition* 2016;104(4):1061-74.

61. Abreu AP, Kaiser UB. Pubertal development and regulation. *Lancet Diabetes Endocrinol* 2016;4(3):254-64.

62. Choi JH, Yoo HW. Control of puberty: genetics, endocrinology, and environment. *Curr Opin Endocrinol Diabetes Obes* 2013;20(1):62-8.

63. Grumbach MM. The neuroendocrinology of human puberty revisited. *Hormone research* 2002;57 Suppl 2:2-14.

64. Federico G, Baroncelli GI, Vanacore T, et al. Pubertal changes in biochemical markers of growth. *Hormone research* 2003;60(Suppl 1):46-51.

65. Tanner J. Growth at adolescence: with a general consideration of the effects of hereditary and environmental factors upon growth and maturation from birth to maturity. Oxford: Blackwell Scientific Publications 1962.

66. Taylor SJ, Whincup PH, Hindmarsh PC, et al. Performance of a new pubertal self-assessment questionnaire: a preliminary study. *Paediatr Perinat Epidemiol* 2001;15(1):88-94.

67. Rasmussen AR, Wohlfahrt-Veje C, Tefre de Renzy-Martin K, et al. Validity of self-assessment of pubertal maturation. *Pediatrics* 2015;135(1):86-93.

68. Lazzer S, Patrizi A, De Col A, et al. Prediction of basal metabolic rate in obese children and adolescents considering pubertal stages and anthropometric characteristics or body composition. *European journal of clinical nutrition* 2014;68(6):695-9.

69. Cole TJ. A chart to link child centiles of body mass index, weight and height. *European journal of clinical nutrition* 2002;56(12):1194-9.

70. Kelly TL, Wilson KE, Heymsfield SB. Dual energy X-Ray absorptiometry body composition reference values from NHANES. *PloS one* 2009;4(9):e7038.

71. Imboden MT, Swartz AM, Finch HW, et al. Reference standards for lean mass measures using GE dual energy x-ray absorptiometry in Caucasian adults. *PloS one* 2017;12(4):e0176161.

72. Wells JC, Williams JE, Chomtho S, et al. Body-composition reference data for simple and reference techniques and a 4-component model: a new UK reference child. *The American journal of clinical nutrition* 2012;96(6):1316-26.

73. Mendoza A, Hollenberg AN. New insights into thyroid hormone action. *Pharmacology & therapeutics* 2017;173:135-45.

74. Chatterjee VK, Nagaya T, Madison LD, et al. Thyroid hormone resistance syndrome. Inhibition of normal receptor function by mutant thyroid hormone receptors. *The Journal of clinical investigation* 1991;87(6):1977-84.

75. Moran C, Chatterjee K. Resistance to thyroid hormone due to defective thyroid receptor alpha. *Best practice & research Clinical endocrinology & metabolism* 2015;29(4):647-57.

76. Schoenmakers N, Moran C, Peeters RP, et al. Resistance to thyroid hormone mediated by defective thyroid hormone receptor alpha. *Biochimica et biophysica acta* 2013;1830(7):4004-8.

77. Finsterer J, Stollberger C, Grossegger C, et al. Hypothyroid myopathy with unusually high serum creatine kinase values. *Hormone research* 1999;52(4):205-8.

78. Mitchell CS, Savage DB, Dufour S, et al. Resistance to thyroid hormone is associated with raised energy expenditure, muscle mitochondrial uncoupling, and hyperphagia. *The Journal of clinical investigation* 2010;120(4):1345-54.

79. Santini F, Marzullo P, Rotondi M, et al. Mechanisms in endocrinology: the crosstalk between thyroid gland and adipose tissue: signal integration in health and disease. *European journal of endocrinology / European Federation of Endocrine Societies* 2014;171(4):R137-52.

80. Obregon MJ. Adipose tissues and thyroid hormones. *Front Physiol* 2014;5:479.

81. Liu YY, Schultz JJ, Brent GA. A thyroid hormone receptor alpha gene mutation (P398H) is associated with visceral adiposity and impaired catecholamine-stimulated lipolysis in mice. *The Journal of biological chemistry* 2003;278(40):38913-20.

82. Lahesmaa M, Orava J, Schalin-Jantti C, et al. Hyperthyroidism increases brown fat metabolism in humans. *The Journal of clinical endocrinology and metabolism* 2014;99(1):E28-35.

83. Olateju TO, Vanderpump MP. Thyroid hormone resistance. *Annals of clinical biochemistry* 2006;43(Pt 6):431-40.

84. Lafranchi SH, Snyder DB, Sesser DE, et al. Follow-up of newborns with elevated screening T4 concentrations. *The Journal of pediatrics* 2003;143(3):296-301.

85. Chiesa A, Olcese MC, Papendieck P, et al. Variable clinical presentation and outcome in pediatric patients with resistance to thyroid hormone (RTH). *Endocrine* 2012;41(1):130-7.

86. Duntas LH. Thyroid disease and lipids. *Thyroid : official journal of the American Thyroid Association* 2002;12(4):287-93.

87. Moran C, Schoenmakers N, Agostini M, et al. An adult female with resistance to thyroid hormone mediated by defective thyroid hormone receptor alpha. *The Journal of clinical endocrinology and metabolism* 2013;98(11):4254-61.

88. Bochukova E, Schoenmakers N, Agostini M, et al. A mutation in the thyroid hormone receptor alpha gene. *The New England journal of medicine* 2012;366(3):243-9.

89. van Mullem AA, Visser TJ, Peeters RP. Clinical Consequences of Mutations in Thyroid Hormone Receptor-alpha1. *Eur Thyroid J* 2014;3(1):17-24.

90. Demir K, van Gucht AL, Buyukinan M, et al. Diverse Genotypes and Phenotypes of Three Novel Thyroid Hormone Receptor-alpha Mutations. *The Journal of clinical endocrinology and metabolism* 2016;101(8):2945-54.

91. Franklyn JA, Boelaert K. Thyrotoxicosis. *Lancet* 2012;379(9821):1155-66.

92. Bech K, Damsbo P, Eldrup E, et al. beta-cell function and glucose and lipid oxidation in Graves' disease. *Clin Endocrinol (Oxf)* 1996;44(1):59-66.

93. Gomez Acotto C, Schott AM, Hans D, et al. Hyperthyroidism influences ultrasound bone measurement on the Os calcis. *Osteoporosis international : a journal established as result of cooperation between the European Foundation for Osteoporosis and the National Osteoporosis Foundation of the USA* 1998;8(5):455-9.

94. Acotto CG, Niepomniszcze H, Mautalen CA. Estimating body fat and lean tissue distribution in hyperthyroidism by dual-energy X-ray absorptiometry. *Journal of clinical densitometry : the official journal of the International Society for Clinical Densitometry* 2002;5(3):305-11.

95. Huang-Doran I, Sleigh A, Rochford JJ, et al. Lipodystrophy: metabolic insights from a rare disorder. *The Journal of endocrinology* 2010;207(3):245-55.

96. Garg A. Clinical review#: Lipodystrophies: genetic and acquired body fat disorders. *The Journal of clinical endocrinology and metabolism* 2011;96(11):3313-25.

97. Hegele RA, Joy TR, Al-Attar SA, et al. Thematic review series: Adipocyte Biology. Lipodystrophies: windows on adipose biology and metabolism. *Journal of lipid research* 2007;48(7):1433-44.

98. Agarwal AK, Garg A. A novel heterozygous mutation in peroxisome proliferator-activated receptor-gamma gene in a patient with familial partial lipodystrophy. *The Journal of clinical endocrinology and metabolism* 2002;87(1):408-11.

99. George S, Rochford JJ, Wolfrum C, et al. A family with severe insulin resistance and diabetes due to a mutation in AKT2. *Science* 2004;304(5675):1325-8.

100. Peters JM, Barnes R, Bennett L, et al. Localization of the gene for familial partial lipodystrophy (Dunnigan variety) to chromosome 1q21-22. Nature genetics 1998;18(3):292-5.

101. Savage DB, Murgatroyd PR, Chatterjee VK, et al. Energy expenditure and adaptive responses to an acute hypercaloric fat load in humans with lipodystrophy. The Journal of clinical endocrinology and metabolism 2005;90(3):1446-52.

2. Methods.

This chapter explores the principles of each method of measurement used throughout this thesis, including the equipment's accuracy and precision.

2.1. Body Composition

The term body composition, used frequently within this thesis, refers to four main compartments of the body; fat, lean, bone mineral and water. These compartments can be assessed at a whole body level or can be further compartmented into components, regions or depots, depending on the measurement technique applied.

Within this thesis, the method of measuring body composition; fat, lean and bone mineral, is **dual energy X-ray absorptiometry (DXA)**. Its accuracy for whole body fat assessment, however, is challenged by the comparison to a technique incorporating **four components** of body composition, body volume, mass, water and bone mineral (Chapter 3). DXA can also provide regional analysis of bone and soft tissue, a significant benefit of the method which cannot be compared to a four component model.

2.1.1. Dual Energy X-ray Absorptiometry (DXA)

DXA is a 2-Component (2-C) method and has the ability to separate body mass into soft tissue and bone mineral. With the help of scientific algorithms based on known densities of different tissue it is able to differentiate between lean and fat tissue. Two DXA machines have been used throughout this thesis, a GE Lunar Prodigy, encore software version 12.3 and a GE Lunar iDXA, encore software version 15 and 16 (GE Healthcare, Madison, WI, USA).

The fundamental principles of DXA consist of passing two X-ray beams at different high and low photon energies, through bone and tissue in the body. The beams are split by a thin sheet of metal in the beam to create two separate peaks in the X-ray spectrum [1]. The attenuation, reduction in intensity of the X-ray beam, by body tissues is measured by the detector and converted to a thickness of bone mineral and attenuation of soft tissue around the bone. For a given thickness the attenuation increases with the density of the material, bone indicating a higher attenuation than soft tissue [2]. It is the difference in attenuation of the two energies which determines bone density and body composition [3]. When a DXA scan is analysed the data creates a pixel-by-pixel map of bone density and soft tissue. An edge detection algorithm is used to find the bone edge and then bone mineral content (BMC) is calculated from multiplying bone mineral density (BMD), calculated as the mean BMD over all

the pixels identified as bone, by bone area (BA), derived by summing the pixel from within the bone edge [4]. Unpublished algorithms derived by the manufacturer provide the fat, lean and bone mass interpretation. Different versions of software with algorithm updates can be controversial during a longitudinal study [5]. There are substantial differences between the two DXA machines, Prodigy and iDXA, especially in body composition measures possibly due to the development not only of the software but the element technology of the iDXA. The iDXA has the same narrow-angle fan beam as the Prodigy but with a greater number of detectors, providing an improved resolution (1.05mm longitudinally, 0.6mm laterally) and image quality [2]. It also has a new metal filter to create a greater spectrum allowing more attenuation being detected resulting in greater bone edge and tissue detection [6 7].

The iDXA also comes with an increased radiation dose compared to the Prodigy which along with the detector improvements helps to provide greater precision in the images. A whole-body scan on the Prodigy administers an effective radiation dose of 0.08 µSv and takes approx 6-10 min depending on scan mode. There are three scan modes on both the Prodigy and the iDXA which can be applied to a participant based on the weight entered; thin, standard and thick which in turn use differing radiation doses and length of time to scan. On the iDXA using the standard scan mode, the radiation dose is greater, 1uSv for an adult and 1.6uSv for a child. Both the prodigy and the iDXA use a method called smart-scan which means only the area covered by the participant is scanned, limiting excess radiation exposure. The doses on both scanner are still considered low in the context of daily reported background radiation of 6-7 µSv around Cambridgeshire [8].

For the studies reported in this thesis, whole-body scans are performed in both adults and children to acquire whole-body fat mass, lean mass and bone mineral content (BMC). Furthermore, bone mineral density (BMD), bone area (BA) and BMC measures were made on additional sites, femoral hip and lumbar spine, in adults. These additional sites are recognised areas of degradation of bone density with age [9].

2.1.1.1. Precision

Precision values for iDXA are presented in Chapter 3 along with accuracy data for iDXA and Prodigy.

2.1.2 Four-Component (4-C) model

The 4-C model expresses fat mass in terms of body volume (BV), total body water (TBW), bone mineral (BMC) and body mass (M). Body volume can be determined by under-water weighing or from **air-displacement plethysmography** (ADP) using the BODPOD. Total body water is estimated using the deuterium dilution method by **Isotope ratio mass spectroscopy (IRMS)** and bone mineral content (BMC) from **dual energy X-ray Absorptiometry.** Body mass can be measured by either a simple set of calibrated scales, the mass measurement taken at the point of ADP assessment or derived from the sum of DXA measured masses; fat, lean and BMC. The study within this thesis (chapter 3) used mass from the ADP assessment as this closely resembled a naked weight measurement. Combined, these measures derive values for the estimation of fat mass by coefficients of mineral, water, fat and protein. A 4-C model is commonly used as a reference comparison for other 2 or 3-C methods because of its incorporation of further components of whole body composition. The 4-C equation used for the estimation of fat mass within the work presented in this thesis is based on the Fuller *et al* analysis [10].

$$\mathrm{FM\ (kg)} = [2.747 * \mathbf{BV}) - (0.710 * \mathbf{TBW})] + [(1.460 * \mathbf{BMC}) - (2.050\ \mathbf{M})] \quad \textbf{(1)}$$

Other 4-C models are available ranging from Selinger *et al* 1977 [11] to the most recent developed models such as Wang *et al* [12]. The models display similar coefficients for the components but the recent models have derived the measurements from newer techniques such as iDXA. Wang *et al* used the latest DXA model from GE to generate the expressions compared to Selinger who used single photon absorptiometry (SPA), a predecessor to DXA. Body volume was also measured by under-water weighing in the early studies compared to ADP, and TBW has been estimated by the deuterium dilution method which has superseded $H_2{}^{18}O$ due to its expense and tritium (^3H_2O) due to its radioactive properties. Other models have attempted to incorporate a 5th or 6th components such as extracellular (ECW) and intracellular water (ICW) or a glycogen factor [11]. Selection of the appropriate formula will be based on the methods used to derive the equations and the techniques available in the current research. The equation by Fuller *et al* [10], was chosen for analysis within this thesis because the methods applied to derive the 4-C model were applicable to the methods available in the current research studies.

2.1.3. Air Displacement Plethysmography (ADP)

ADP is a 2-C model that considers the body as having fat and fat-free compartments characterised by their densities. For fat this density was set by Siri (1956) at 0.9kg/l and 0.1 kg/l for fat-free mass. From the measurement of body mass (M) and body volume (V), body density may be derived (D_b) and proportioned to fat and fat-free compartments.

The trade name for the instrument is BODPOD (Life measurement, Inc, Concord, CA) which is a system that provides the means of determining body volume using Poisson's Law. This describes the pressure – volume relationship under conditions that allow gains and losses of temperature and pressure (unlike Boyles law) during expansion and compression (adiabatic), although the total heat content of the air remains constant:

$$P_1 / P_2 = (V_2 / V_1)^{\gamma} \quad \textbf{(2)}$$

where γ is the ratio of the specific heat of the gas at constant pressure to that of constant volume and is equal to 1.4 for air [13-15].

The BODPOD consists of two chambers, a test chamber and a reference chamber, connected by a diaphragm, in which oscillations can produce pressure changes in the chambers. The ratio of the pressures is a measure of the ratio of the test chamber to the ratio of the chamber volume. Some of volume of air, however, is still maintained under isothermal rather than adiabatic conditions and must be accounted for independently, for example air contained in the lungs, and near skin/hair or clothing. For this reason, tight fitting clothing is worn along with a swimming hat to contain the hair and minimise the surface area artefact (SSA). SSA, which is typically -1.0 L for an average sized adult [13], is generated automatically by the BODPOD as:

$$SSA\ (L) = k\left(\frac{L}{cm^2}\right) * BSA\ (cm^2) \quad \textbf{(3)}$$

Where k is a constant derived by the manufacturer and body surface area (BSA) is calculated by body weight and height using DuBois and DuBois [16]

The volume of air in the lungs can be measured or predicted from built in equations in the BODPOD software. In the studies reported in this thesis predicted lung volumes were used. Ottersletter *et al* [17] found no significant differences in body volume when lung volume was measured and predicted.

The *measurement* of body volume using the BODPOD involves 3 steps

1. A 2-point calibration process starting with the chamber empty to establish a baseline volume and then with a 50 L calibration cylinder.
2. The participant's volume in the chamber is measured (Vb_{raw}) not corrected for thoracic gas volume (V_{TG}) or surface area artefact (SSA).
3. The last step is then repeated to check for agreement that the measurements are within 0.2 % or 150 mL, if the first two are inconsistent then a 3rd measurement is taken.

The participant's volume is then corrected for SSA and V_{TG} (VB_{corr}) by estimations based on predictions by Crapo *et al* [18].

Body volume by BODPOD is therefore calculated by:

$$Vb_{corr}(L) = Vb_{raw}(L) - SAA(L) + 40\%\, V_{TG}(L) \quad \textbf{(4)}$$

Where Vb_{corr} is body volume corrected for V_{TG} and SAA, Vb_{raw} is body volume before correction for V_{TG} and SSA.

2.1.3.1. Precision and Accuracy

The precision and accuracy of the BODPOD have been widely reported for the assessment of %body fat [19-21] but not as widely for body volume. Our own precision calculations from two repeated measures across body volumes ranging from 16 – 103 L, demonstrate %CV of 0.44 and a least significant change (LSC) of 1.2 L (unpublished). The cohort of child body volumes ranging from 16-80 L demonstrates a %CV of 0.65 and LSC of 1.8 compared to %CV 0.28 and LSC of 0.78 L in the adults (range of 38-103 L).

2.1.4. Total Body Water (TBW)

Isotope dilution is the reference standard technique for measuring the volume or mass of large quantities of water [16]. Isotopes are elements that are chemically identical but have

different masses due to different numbers of neutrons [22]. In this thesis the deuterium dilution method (^2H) was used in chapter 3.

A known amount of deuterium oxide ($^2H_20$) is given orally (0.1g/kg body mass for mass spectroscopy), this equilibrates with body water typically reaching a plateau in enrichment after 2-5h [23]. In children, an equilibrium or plateau is reached sooner than in adults as their smaller size means they have a higher water turnover, therefore sampling may occur sooner than 2hrs. However, in the elderly turnover may be slower and therefore samples should be collected for longer [23].

Prior to dosing, a reference saliva sample is taken to establish natural abundance. Saliva is collected by absorption into cotton wool which is then syringed out into 1ml aliquots. Further saliva samples are taken from 2 hours and then 3, 4, and 5 hours *post dose*. The rationale for this is to observe the plateau ^2H enrichment in body water. Once the labelled saliva samples have been collected, they are refrigerated on collection and then frozen for future analysis by IRMS.

The saliva samples are equilibrated with hydrogen gas in the presence of a platinum catalyst and heated for 6 hours at 22°C before analysis by IRMS.

Total body water =

$$TBW\ (kg) = \left(W\ x \frac{A}{a}\right) x\ \frac{\left(\frac{\Delta DD}{\delta samp - \delta bk}\right)}{(1000x1.041)} - (cumulative\ fluid\ intake\ (kg)) \quad \textbf{(5)}$$

Where W and 'a' refer to a portion of the dose that has been diluted for analysis. W is the amount (g) of water used to make this dilution and 'a' is the amount (g) of the dose used in the dilution. 'A' is the dose (g) taken by the participant, ΔDD is the enrichment measured in the diluted dose (measured abundance in the diluted dose – abundance in the local drinking water used to dilute it) and δsamp-δbk is the enrichment measured in body water (Delta samp (relative to SMOW) – delta background). 1.041 represents a coefficient for deuterium that enters non-aqueous, distribution space, such as fat and protein. This is termed hydrogen exchange [24].

2.1.5. Isotope ratio mass spectrometer (IRMS).

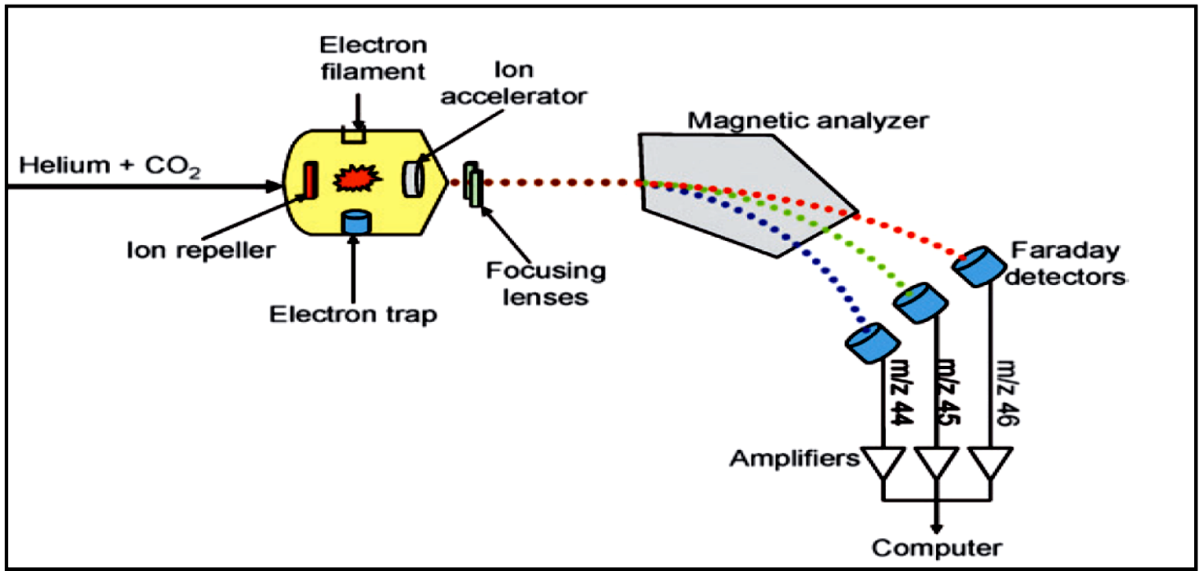

Figure 2.1. Schematic of an IRMS from Muccio *et al*, 2009.

Figure 2.1 illustrates the function of an IRMS. Firstly, the sample is introduced to the spectrometer in the form of a pure gas. The gas is then ionised by electrons emitted from a hot filament within a high vacuum. An ion repeller forces the ions to pass through a series of focusing lenses directing the ions into the magnetic analyser. The analyser separates the ions relative to their mass to charge ratio. The ions are then detected by the Faraday detectors [25]. IRMS measures the ratio of isotope in the sample relative to the ratio in a reference gas (equation 6).

The stages of the sample analysis by IRMS is as follows; firstly, the results off the IRMS are delta values relative to the reference gas (equation 6). Similarly, the machine will give the internal standard (MLO) relative to the reference gas (equation 7). Where R refers to the ratio of the mass 3 to mass 2.

$$\delta samp,ref = (Rsamp/ref - 1)10^3 \quad \textbf{(6)}$$

$$\delta MLO,ref = (RMLO/ref - 1)10^3 \quad \textbf{(7)}$$

The following calculations must then be applied to ultimately get the delta of the sample relative to VSMOW, the international standard.

Firstly, the δsamp needs to be made relative to MLO (equation 8).

$$\delta samp_{/MLO} = \left(\frac{\left(\delta samp_{/ref} + 10^3 \right)}{\left(\delta MLO_{/ref} + 10^3 \right)} - 1 \right) 10^3 \quad \textbf{(8)}$$

Then knowing that δMLO/SMOW, is a measured machine specific constant, δsamp relative to SMOW can be calculated (equation 9).

$$\delta samp_{/SMOW} = \left(\frac{\left(\delta samp_{/MLO} + 10^3 \right) \left(\delta MLO_{/SMOW} + 10^3 \right)}{10^6} - 1 \right) 10^3 \quad \textbf{(9)}$$

2.1.5.1. *Precision*

To determine the precision the IRMS measured deuterium (Delta samp ref) we calculated the %CV between QC standardised samples (MLO), corrected for SMOW, across 38 runs measured in duplicate. During each run two QC samples at delta 250 and 750 were performed. For the 250 samples we report a %CV of 0.54 and for the 750 samples we report a %CV of 0.26.

2.2. Measurement of Energy Expenditure

Energy expenditure can be defined as the rate at which heat is lost from the body (measured by direct calorimetry) or produced in the body (indirect calorimetry).

Direct calorimetry measures heat loss by radiation, convection, conduction and from the heat rising from the vaporisation of water [26]. This requires extremely technical equipment and expertise with the research interests in heat loss and heat storage. The physical properties of a direct calorimeter are determined by whether it is an isothermal system, heat sink or convection system [26]. Heat sink calorimeters are a heavily insulated chambers to prevent heat loss and liquid-cooled heat exchangers to collect the heat produced. Alternatively, in an isothermal system, the chamber can be lined with a thin layer of material of a constant thickness which is maintained at a constant temperature along with a network of other measures of evaporation and air conditioning [27]. This method of calorimetry is rarely employed in human physiology nowadays but exists mainly in animal research.

Indirect calorimetry describes the process of estimating heat production based on respiratory gas exchange and often including urea excretion. Measurements can be performed over short periods of time (10min) or as long as 24 hours or up to 7 days. There are two types of indirect calorimetry used within human metabolism; room/chamber calorimetry or ventilated canopy/mask calorimetry. In this thesis, energy expenditure is assessed using two methods of *indirect calorimetry*: whole body room calorimetry (chapter 4) and ventilated canopy calorimetry (chapters 4, 5).

Room calorimetry has the benefit of assessing oxygen and carbon dioxide gas exchange over longer durations in a reasonably comfortable controlled environment whilst maintaining a relatively normal level of habitation. Twenty four hour measurements can be broken down into smaller time frames and analysis periods. These can include sleeping metabolic rate (midnight to waking), basal or resting metabolic rate (upon waking, typically a 60min measurement), diet induced thermogenesis after the consumption of a meal or physical activity energy expenditure by inducing periods of exercise within the room (30min exercise). However, the room calorimeter is at a disadvantage for shorter analysis periods. The volume of the room results in a slow response between participant gas exchange and analysis of a sample which is also related to the flow rate needed for the size of the room. To minimise this,

the ventilated canopy method is used in addition to room calorimetry for the data collection of shorter periods of interest, such as resting energy expenditure.

The volume of the canopy is substantially less than the room, requiring a lower flow rate and therefore a smaller response time. The canopy is, however, only physically appropriate for shorter periods of time as it requires the participant to remain still and in a supine resting condition. For exercise testing that require gas exchange measurements during increased mobility and physical activity, a mask or mouth piece is used as the connector to the gas exchange instrument. With these instruments instead of there being a controlled constant flow rate, the flow rate is driven by expiration resulting in a breath-by-breath analysis.

Macronutrient oxidation can be derived from all gas exchange methods with appropriate energy conversion equations. This provides information about whole body fat, carbohydrate and protein oxidation (with the inclusion of urea and creatinine).

2.2.1 Indirect calorimetry

Indirect calorimetry can adopt a push or pressure ventilation system (room calorimetry) or a pull or suction ventilation system (ventilated canopy).

2.2.1.1. Whole-body room calorimeters

Figure 2.2.2 is a diagram of a modern room calorimeter, designed to mimic a normal bedroom, containing a bed, wash basin, portaloo, TV, DVD, computer with internet, telephone and a window. The floor area is 10.4m^2 and the room volume is 24m^3

.

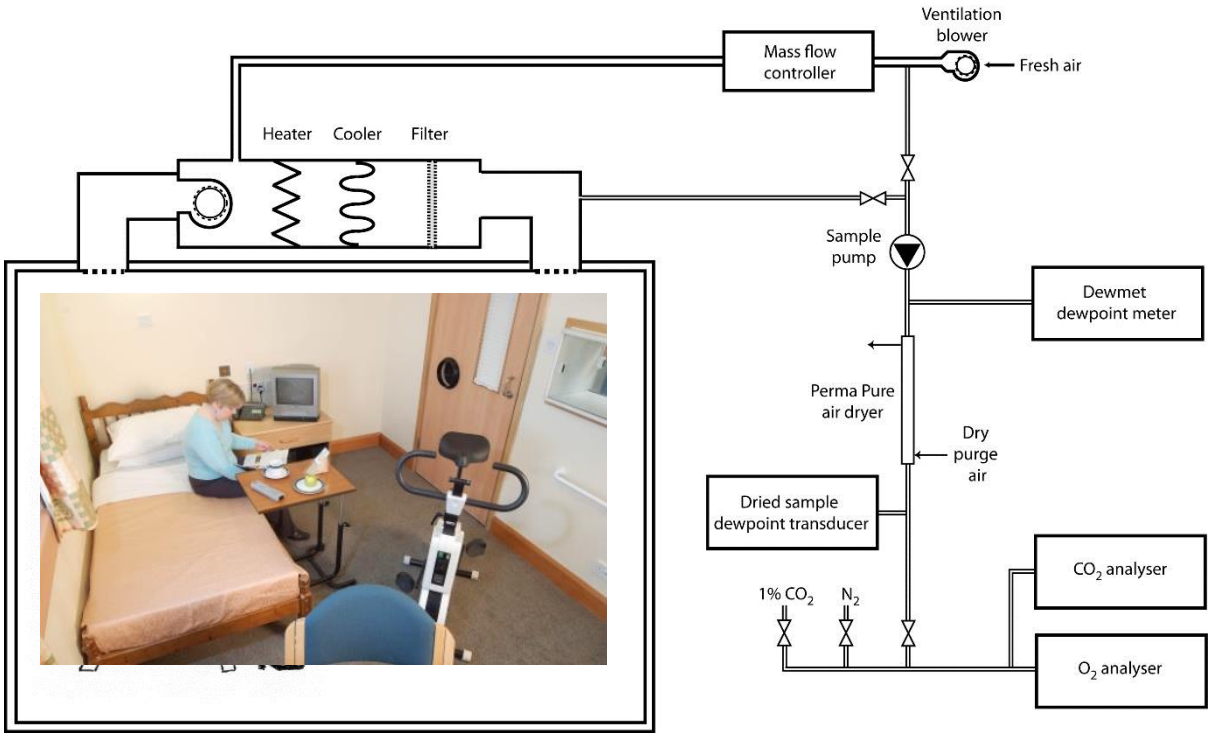

Figure 2.2. Diagram of a modern day room calorimeter for the measurement of 24 or 36 hour EE (Diagram by PR Murgatroyd).

The room is ventilated with a constant and measured supply of fresh air. All air entering the calorimeter is measured and controlled. This is referred to as "push" or pressure ventilation. A "pull" or suction ventilation method will control the air coming out of the chamber. The measurement of respiratory gas exchange has been described by Brown [28]. Where Fi and Fo are the flow rates of the moist air in and out of the chamber and R_G is the rate of respiratory gas exchange:

$$d/_{dt}(V\ \Psi_o f_{Go}) = (F_i\ \Psi_i\ f_{Gi}) + R_G - (F_o\ \Psi_o\ f_{Go)}$$

(10)

The rate of increase of volume of gas inside the chamber = rate of volume flow of gas into the chamber + rate of net volume production of gas by the subject – rate of volume flow of gas out of the chamber. Each calculation requires corrections which for simplicity are represented as Ψ. in the equation above:

1. The volume of dry air is converted to the proportion of the gas in wet air, which is then multiplied by the volume of the calorimeter to obtain the volume of gas under standard conditions

$$x\left(1-\frac{Pw}{P}\right) \tag{11}$$

where P_W is the vapour pressure of water in the air and P is the atmospheric pressure.

2. The resulting volume is then adjusted to standard temperature and pressure, STP, where T_S is 273 ^oK and P_S is 1013 mbar.

$$(x\frac{Ts}{Ps}x\frac{P}{T}) \tag{12}$$

Therefore:

$$\Psi=\left(1-\frac{Pw}{P}\right)x\frac{Ts}{Ps}\ x\ P/T \tag{13}$$

The analysers produce outputs that are proportional to the molecular density of the relevant gas in the analyser cell and therefore the resulting f_G value is directly related to the density of the air analysed [28]. f_G also needs to be corrected separately for changes in atmospheric pressure occurring after the time of calibration of the analyser.

The rate of gas production (R_G) for a push calorimeter is expressed as:

$$R_G=F_o\ \Psi_o\ f_{N20}+Vd/dt(\Psi_0 f_{N20}))\ \left(\frac{f_{Go}}{f_{N20}}-\frac{f_{Gi}}{f_{N2i}}\right)+V\Psi_o\ f_{N20}\frac{d}{dt}(\frac{f_{Go}}{f_{N20}}) \tag{14}$$

2.2.1.2. Ventilated canopy or portable indirect calorimetry.

Ventilated hood indirect calorimetry (Figure 2.3) share the basic principles with room calorimetry, however it instead uses a pull ventilation system rather than a push system and as the volume is significantly smaller than a room, it is not necessary account for it within the expression (15).

For a pull calorimeter (ventilated canopy) where the volume is expressed as 0 as the size is negligible:

$$R_G = F_i \, \Psi_i f_{N2i} \left(\frac{f_{Go}}{f_{N20}} - \frac{f_{Gi}}{f_{n2i}}\right) \quad \textbf{(15)}$$

Figure 2.3. Indirect calorimetry using a ventilated canopy and face mask techniques.

The ventilated hood technique of indirect calorimetry is typically the preferred method used to assess resting energy expenditure (REE). The concept of REE was developed by researchers such as Harris and Benedict [29], and Dubois [16]. REE and basal metabolic rate (BMR) are often used interchangeably, which is acceptable if the conditions of the measurement are the same. For accurate measurement of REE, the measurement conditions should be those of complete rest, preferably in the early morning on waking, 13 hours after the last meal and at thermoneutral temperature. The duration of the measurement can range from 10min to an hour depending on the protocol and how long the participant can remain still and comfortable for. The ventilated canopy fits over the participant's head whilst they are lying down.

2.2.2. Macronutrient Oxidation

Room calorimeter gas concentrations are measured every 200s by the analysers and then using software with built in expressions from Murgatroyd *et al* [30] the O_2 and CO_2 exchange are converted into carbohydrate, fat and protein oxidation rates:

$$Fat = [CO_2 - R_c\, O_2 + (R_c - R_p)V_p\, k\, N]/V_f\, (R_f - R_c)$$

(16)

$$CHO = [CO_2 - R_f\, O_2 + (R_f - R_p)V_p\, k\, N]/V_c\, (R_c - R_f)$$

(17)

[30]

Where R_f, is the ratio of carbon dioxide production to oxygen to consumption per gram oxidised for fat, R_c for CHO and R_p for protein, also referred to as respiratory quotients (RQ). V_f, V_c, and V_p are the volumes of oxygen consumed per gram oxidised for fat, CHO and protein. k is the constant that relates protein oxidation to nitrogen excretion, leaving N to represent protein oxidation. The primary method of nitrogen disposal is through urine excretion. Urine samples are analysed for Urea and Creatinine the main product in urine excretion. Nitrogen has the atomic weight of 14, and therefore 28g of nitrogen are lost with 1mol of urea and 42g are lost with 1mol of creatinine. Using this we can calculation *N* and therefore estimate protein oxidation.

Using the constants of Elia and Livesey [31] (Table 1), macronutrient oxidation can be calculated as follows:

$$Fat = -1.7\, [CO_2 - O_2 + 0.98\, N]$$

(18)

$$CHO = 4.6\, [CO_2 - 0.71\, O_2 - 0.74\, N]$$

(19)

$$Protein = 6.25\, N$$

(20)

Where Fat, CHO, Protein and Nitrogen are in grams when O_2 and CO_2 are in litres.

Table 2.1. Respiratory quotients (RQs) of macronutrients [31]

Macronutrient	RQ
Fat	0.710
Carbohydrate	1.000
Protein	0.835

Most dietary intakes consist of a combination of macronutrients, typically of 35% fat, 50% CHO and 15% protein by energy. Before assessing energy expenditure it is ideal that the participant is in a state of energy balance so that any manipulation within the diet (e.g. high CHO) are not influencing on the total oxidation rate or individual oxidation of macronutrients. However, to reach this state may require weeks of consuming standardised meals with known compositions. At the least, knowledge of the composition of the last meal eaten may prove helpful when analysing and interpreting the gas exchange the following morning.

Figure 2.4 demonstrates typical macronutrient oxidation rates generated from a 24 hr whole-body calorimeter visit for a healthy participant.

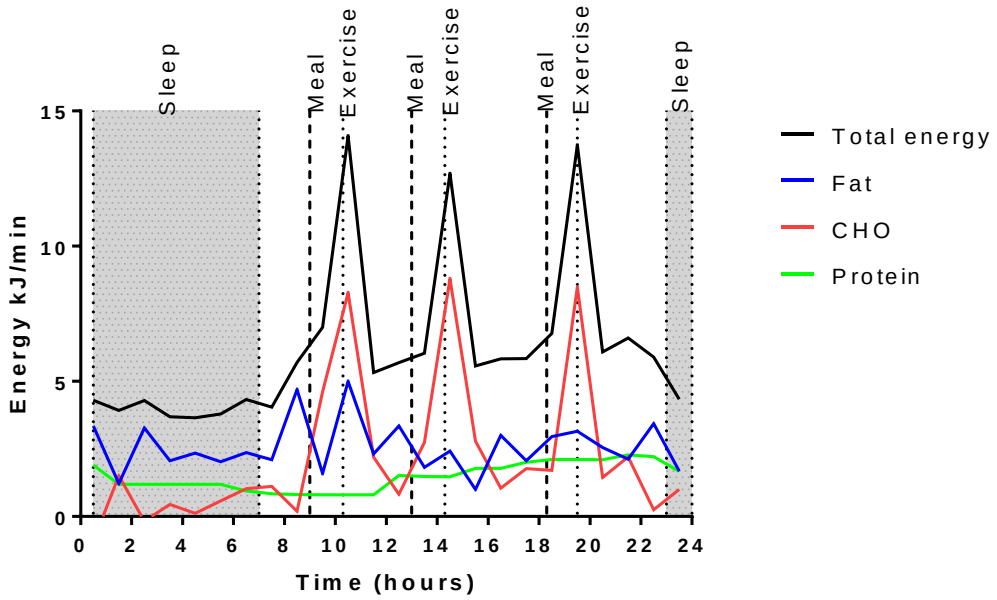

Figure 2.4. Macronutrient oxidation results from a 24 hour visit analysed at a 60min time interval. The three peaks in energy expenditure result from three exercise periods on a static bike (dashed line). For the shaded periods 0-7 hours and 23-24 hours, the participant is asleep.

2.2.3. Precision of indirect calorimetry

2.2.3.1. Room calorimetry

Repeated measurements of 24 hr whole body room calorimetry (unpublished) was calculated across 15 participants. This demonstrated a %CV of 7.1 and an LSC of 1.1 MJ/d. For repeated BMR measured by room calorimetry %CV was 4.68 and LSC 0.6 MJ/d.

2.2.3.2 Ventilated hood calorimetry

Repeated measurements of resting energy expenditure using the ventilated hood and portable gas exchange instrument demonstrated a %CV of 3.8 and LSC of 0.5 kJ/min (0.72 MJ/d). This was based on three repeated measurements on eight participants, all performed under the same conditions and using the same instrument.

2.3. References

1. Bazzocchi A, Ponti F, Albisinni U, et al. DXA: Technical aspects and application. *European journal of radiology* 2016
2. Toombs RJ, Ducher G, Shepherd JA, et al. The impact of recent technological advances on the trueness and precision of DXA to assess body composition. *Obesity (Silver Spring)* 2012;20(1):30-9.
3. Fischbach F, Bruhn H. Assessment of in vivo 1H magnetic resonance spectroscopy in the liver: a review. *Liver international : official journal of the International Association for the Study of the Liver* 2008;28(3):297-307.
4. Blake GM, Fogelman I. Technical principles of dual energy x-ray absorptiometry. *Seminars in nuclear medicine* 1997;27(3):210-28.
5. Hangartner TN, Warner S, Braillon P, et al. The Official Positions of the International Society for Clinical Densitometry: acquisition of dual-energy X-ray absorptiometry body composition and considerations regarding analysis and repeatability of measures. *Journal of clinical densitometry : the official journal of the International Society for Clinical Densitometry* 2013;16(4):520-36.
6. Hind K, Cooper W, Oldroyd B, et al. A Cross-Calibration Study of the GE-Lunar iDXA and Prodigy for the Assessment of Lumbar Spine and Total Hip Bone Parameters via Three Statistical Methods. *Journal of clinical densitometry : the official journal of the International Society for Clinical Densitometry* 2013
7. Longo R, Pollesello P, Ricci C, et al. Proton MR spectroscopy in quantitative in vivo determination of fat content in human liver steatosis. *Journal of magnetic resonance imaging : JMRI* 1995;5(3):281-5.
8. J C H Miles JDA, D M Rees, B M R Green, K A M Adlam, A H Myers. Indicative Atlas of Radon in England and Wales Chilton, Dicot, Oxfordshire: Health Protection Agency and British Geological Survey; 2007 [
9. Hamdy RC, Petak SM, Lenchik L, et al. Which central dual X-ray absorptiometry skeletal sites and regions of interest should be used to determine the diagnosis of osteoporosis? *Journal of clinical densitometry : the official journal of the International Society for Clinical Densitometry* 2002;5 Suppl:S11-8.
10. Fuller NJ, Jebb SA, Laskey MA, et al. Four-component model for the assessment of body composition in humans: comparison with alternative methods, and evaluation of the density and hydration of fat-free mass. *Clin Sci (Lond)* 1992;82(6):687-93.

11. Heymsfield SB, Ebbeling CB, Zheng J, et al. Multi-component molecular-level body composition reference methods: evolving concepts and future directions. *Obesity reviews : an official journal of the International Association for the Study of Obesity* 2015;16(4):282-94.
12. Wang Z, Heymsfield SB, Chen Z, et al. Estimation of percentage body fat by dual-energy x-ray absorptiometry: evaluation by in vivo human elemental composition. *Phys Med Biol* 2010;55(9):2619-35.
13. Fields DA, Goran MI, McCrory MA. Body-composition assessment via air-displacement plethysmography in adults and children: a review. *The American journal of clinical nutrition* 2002;75(3):453-67.
14. Heymsfield S. Human Body Composition. 2 ed. USA: Human Kinetics 2005.
15. Sly PD, Lanteri C, Bates JH. Effect of the thermodynamics of an infant plethysmograph on the measurement of thoracic gas volume. *Pediatric pulmonology* 1990;8(3):203-8.
16. Dubois D, Dubois EF. Nutrition Metabolism Classic - a Formula to Estimate the Approximate Surface-Area If Height and Weight Be Known (Reprinted from Archives Internal Medicine, Vol 17, Pg 863, 1916). *Nutrition* 1989;5(5):303-11.
17. Otterstetter R, Johnson KE, Kiger DL, et al. Comparison of air-displacement plethysmography results using predicted and measured lung volumes over a protracted period of time. *Clinical physiology and functional imaging* 2015;35(5):328-31.
18. Crapo RO, Morris AH, Clayton PD, et al. Lung volumes in healthy nonsmoking adults. *Bulletin europeen de physiopathologie respiratoire* 1982;18(3):419-25.
19. Gonzalez-Aguero A, Olmedillas H, Gomez-Cabello A, et al. Inter-Methods Agreement for the Assessment of Percentage of Body Fat Betweentwo Laboratory Methods in Male Adolescent Cyclists. *Nutricion hospitalaria : organo oficial de la Sociedad Espanola de Nutricion Parenteral y Enteral* 2013;28(4):1049-52.
20. Plasqui G, den Hoed M, Bonomi A, et al. Body composition in 10-13-year-old children: a comparison between air displacement plethysmography and deuterium dilution. *International journal of pediatric obesity : IJPO : an official journal of the International Association for the Study of Obesity* 2009;4(4):397-404.
21. Bentzur KM, Kravitz L, Lockner DW. Evaluation of the BOD POD for estimating percent body fat in collegiate track and field female athletes: a comparison of four methods.

Journal of strength and conditioning research / National Strength & Conditioning Association 2008;22(6):1985-91.

22. Kim IY, Suh SH, Lee IK, et al. Applications of stable, nonradioactive isotope tracers in in vivo human metabolic research. *Exp Mol Med* 2016;48:e203.
23. IAEA. Introduction to Body Composition Assessment Using the Deuterium Dilution Technique with Analysis of Saliva Samples by Fourier Transfrom Infrared Spectrometry. *IAEA Human Health Series* 2010;12:96.
24. IAEA. Assessment of body composition and total energy expenditure in humans using stable isotopes. Human Health Series Vienna, Austria, 2009:1-133.
25. Muccio Z, Jackson GP. Isotope Ratio Mass Spectrometry. *The Analyst* 2009;134(2):213-22.
26. Levine JA. Measurement of energy expenditure. *Public Health Nutr* 2005;8(7A):1123-32.
27. Blaxter K. Energy metabolism in animals and man. Cambridge: Cambridge University Press 1989:336.
28. Brown D, Cole TJ, Dauncey MJ, et al. Analysis of gaseous exchange in open-circuit indirect calorimetry. *Medical & biological engineering & computing* 1984;22(4):333-8.
29. Harris JA, Benedict FG. A Biometric Study of Human Basal Metabolism. *Proceedings of the National Academy of Sciences of the United States of America* 1918;4(12):370-3.
30. Murgatroyd PR, Sonko BJ, Wittekind A, et al. Non-invasive techniques for assessing carbohydrate flux: I. Measurement of depletion by indirect calorimetry. *Acta physiologica Scandinavica* 1993;147(1):91-8.
31. Elia M, Livesey G. Energy expenditure and fuel selection in biological systems: the theory and practice of calculations based on indirect calorimetry and tracer methods. *World review of nutrition and dietetics* 1992;70:68-131.

3. An investigation into the differences in bone density and body composition measurements between two GE Lunar densitometers and their comparison to a four component model.

Watson LPE, Venables MC, and Murgatroyd PR. An investigation into the differences in bone density and body composition measurements between two GE Lunar densitometers and their comparison to a four component model. *J Clin Densitometry;* 2017 Jul 27.

3.1 Abstract

Background. We describe a study to assess the precision of the GE Lunar iDXA and the agreement between the iDXA and GE Lunar Prodigy densitometers for measurement of regional and total body bone and body composition in normal to obese healthy adults. We compare the whole body fat mass by DXA to measurements by a four component (4-C) model.

Methods. Sixty nine participants, aged 37 ± 12 years, BMI 26.2 ± 5.1 kg/cm^2, were measured once on the Prodigy and twice on the iDXA. The 4-C model estimated fat mass from body mass, total body water by deuterium dilution, body volume by air displacement plethysmography and bone mass by DXA. Agreement between measurements made on the two instruments and by the 4-C model were analysed by Bland-Altman and linear regression. Where appropriate translational cross-calibration equations were derived. Differences between DXA software versions were investigated.

Results. iDXA precision was less than 2% of the measured value for all regional and whole body bone and body composition measurements with the exception of arm fat mass (2.28%). We found signifcant differences between iDXA and Prodigy ($P < 0.05$) whole body and regional bone, fat (FM) and lean mass (LM), with the exception of hip bone mass, area and density and spine area. Compared to iDXA, Prodigy over-estimated FM and under-estimated LM. However, compared to 4-C, iDXA showed a smaller bias and narrower limits of agreement than Prodigy. No significant differences between software versions in FM estimations existed.

Conclusion. Our results demonstrate excellent iDXA precision. However significant differences exist between the two GE Lunar instruments, Prodigy and iDXA measurement values. A divergance from the reference 4-C observations remains in FM estimations made by DXA even following the recent advances in technology. Further studies are particularly warranted in individuals with large fat mass content.

3.2. Introduction

Dual-energy X-ray absorptiometry (DXA) is widely used for bone density measurements within the clinical environment. Within the research community there is perhaps more emphasis on body composition measurement, driven by the increasing prevalence of obesity. In both contexts the ability to detect changes in measurements is arguably of more interest than the absolute value of the measurement so that an apparent change in bone or fat mass should not be generated and interpreted falsely.

DXA instruments have improved over time, most evidently in reduced scan times. As the technology has matured the focus of development has shifted to image quality, which has improved through advances in detector design yielding a higher pixel density. Major benefits of this are better discrimination of bone edges and better imaging of soft tissue, particularly in the thoracic region [1]. Both translate to improved repeated measures precision [2 3]. These benefits come at the cost of a new instrument, compounded by the complexities of managing the migration from old to new which involve performing cross-calibration assessments to identify any differences between instruments and account for them using translational regression equations [4].

The iDXA is the latest densitometer to come from GE Lunar, a development of the GE Lunar Prodigy and Prodigy Advance. A new detector and x-ray filter (producing different energy spectra) provide improved resolution and image quality by better bone edge detection [1]. This also suggests there may be improved soft tissue algorithms within the software compared to previous instruments. Repeated measures precision describes the variability between two measurements caused the instrument itself, by re-positioning and by operator error and so sets the threshold for discriminating biological change between two measurements [5]. Several authors have documented the iDXA's enhanced precision for repeated measures compared to previous models [2 3 6].

Here we report an investigation which extends the previously reported work. The primary purpose of this study is to evaluate the precision and accuracy of the iDXA. Secondly we aim to produce translational regression equations for relating scans between the Lunar Prodigy and iDXA. Further, we have determined accuracy of iDXA measured fat mass measurement by comparison with a four-component model (4-C) [7]. The 4-C model is widely accepted as a reference against which the accuracy of other body composition methodologies is evaluated.

3.3. Material and Method

3.3.1. Participants

Sixty nine healthy men (n = 33) and women (n=36) were recruited for the purposes of this study. Two participants were excluded from the hip analysis, one for poor positioning and one for an artificial joint. One participant was excluded from the total body water analysis because of an insufficient sample volume. The demographic data of the cohort is presented in Table 3.1. All participants were made aware of the risks associated with the measurements and provided informed consent in writing. Participants were healthy, free from disease and non-smoking; they were excluded if they were pregnant or receiving any metabolism-influencing medications. Participants were recruited locally from advertisements around Addenbrookes Hospital in Cambridge and Cambridge University. The study was approved by the Cambridge Central Ethics Committee.

Each participant arrived at NIHR/Wellcome Trust Clinical Research Facility, Addenbrooke's biomedical campus, Cambridge at noon on the day of their visit to undertake three procedures: whole body water determination using deuterium dilution; DXA; and body volume determination using air displacement plethysmography (ADP). The participants wore light, metal-free clothing and refrained from food and drink for 30 min before and during the measurements.

Table 3.1. Descriptive data of the participants

	Men n=33		Female n =36		(n=3 BMI >35)
	Mean ± SD	Range	Mean ± SD	Range	Mean, Range
Age (years)	38.0 ± 12.0	19.9 – 64.1	37.8 ± 12.7	19.2 – 57.9	33.7, 25.3 – 44.6
Height (m)	1.80 ± 7.9	1.62 – 2.01	1.66 ± 6.7	1.53 – 1.83	1.71, 1.66 – 1.78
Mass (kg)[1]	81.0 ± 12.0	54.1 – 106.9	73.9 ± 18.1	49.1 – 129.6	124.4, 120.7 – 129.6
BMI (kg/m^2)	25.3 ± 3.2	20.2 – 34.2	27.0 ± 6.3	18.4 – 47.5	43.06, 38.8 – 47.5
Fat mass (kg) (4-C)	16.8 ± 8.1	4.1 – 33.4	28.0 ± 14.4	9.6 – 71.5	66.8, 62.0 – 71.5
% Fat (4-C)	20.1 ± 8.0	5.8 – 34.4	36.0 ± 9.5	18.5 – 55.1	53.7, 51.4 – 55.1

SD; standard deviation, BMI; Body mass index, 4-C; 4 Component model (n=68). Hip analysis n = 67. Scan mode: Standard n =65, thick n=4. [1] ADP mass (mean difference ± SD in mass (kg) between ADP and iDXA; 0.15 ± 0.50, and Prodigy; -0.02 ± 0.65). Three female participants with the largest fat mass and BMI are also described in the last column but are included within the total female cohort.

3.3.2. Protocol

3.3.2.1. Deuterium dilution

A baseline saliva sample was obtained from the participant shortly after arrival. Height and weight were then measured. Height was measured on a stadiometer and recorded to the nearest millimetre (SECA 242 digital stadiometer, Seca, Hamburg, Germany). Weight was measured on electronic scales to the nearest gram (Kern & Sohn GmbH, Germany). The participant then consumed a dose of 70 mg per kg body mass of ^2H_2O (99.8 %, CK Isotopes Ltd., Ibstock, Leicestershire, UK) [8]. Further 1ml saliva samples were collected at 3, 4 and 5 hours post dose. Food and drink were withheld for 30 min prior to the collection of each saliva sample. The saliva samples were frozen at -20°C until later analysis using dual inlet isotope ratio mass spectrometry (Isoprime, GV Instruments, Wythenshawe, UK).

3.3.2.2. DXA

Each participant was scanned twice on the iDXA (GE Healthcare Lunar, Maddison, WI, USA, EnCore software version 16 (enhanced analysis)), with repositioning in between scans, and once on the GE Lunar Prodigy (EnCore software version 12.3). The Prodigy data (basic analysis) was re-analysed on the iDXA using software version 16 to provide enhanced Prodigy analysis. All three scans were performed on the same day by the same operator. Sites scanned were hip (left femur) and lumbar spine (L2-L4) for bone mass, area and density and whole-body for both whole body bone mass, area and density and body composition. Calibration block quality assurance and encapsulated spine phantom quality control scans were performed on each instrument at the start of each scanning day.

The scans were performed by three trained operators who performed scans according to the manufacturers positioning and scanning protocols (Precision for each operator, represented by %CV of repeated scans, ranged from 0.7 % to 1.5 % for lumbar spine and 0.5 % to 1.0 % for total hip, below the recommended 1.9 % for lumbar spine and 1.8 % for total hip by the International Society of Clinical Densitometry (ISCD) [4]). Subsequent analysis of all scans was carried out by a single operator to ensure consistency throughout the study. Inter-operator variability was not significant for hip BMD (F=0.322, P = 0.726) and spine BMD (F=0.676, P=0.512).

3.3.2.3. Air displacement plethysmography

The participants were asked to pass urine before the ADP procedure (BODPOD®, Cosmed Srl, Rome, Italy). Tight fitting swim wear and a swimming cap were worn to minimise air trapped in clothing and hair. Lung volume was estimated by the BODPOD software to provide a net body volume estimate. The weight obtained during the ADP procedure was used as the body mass value for the total body water and 4-C analysis.

3.4. Analysis and Calculations

3.4.1. TBW plateau method

TBW was calculated according to the method of [8]. In brief, aliquots of 0.2 ml, drawn from the saliva samples were placed in 3.7 ml glass bottles with rubber septa (non-evacuated vials, Labco Ltd, Lampeter, UK) and equilibrated with hydrogen in the presence of a platinum catalyst. Data was drift corrected off-line and all measurements were made relative to Vienna

standard mean ocean water (V-SMOW) using laboratory standards traceable to the international standard.

$^{2}H_2O$ dilution space was determined using the following equation [9]:

$$^{2}H_2O(kg)) = \left[\frac{D \times T \times (Ed - Et)}{d \times (Es - Ep)} \right] / 1000$$

Where: T and 'd' refer to a portion of the dose that has been diluted for analysis. T is the amount (g) of water used to make this dilution and 'd' is the amount (g) of the dose used in the dilution. 'D' is the dose (g) taken by the participant.

Ed is enrichment of the diluted dose d in T; *Et* is the enrichment of the tap water diluent; *Es* is the mean enrichment of saliva samples at 3, 4 and 5 hours; *Ep* is the enrichment of the pre dose sample.

Total body water (TBW (kg)) was then calculated by reducing $^{2}H_2O$ dilution space values by 4% to account for the exchange of deuterium with non-aqueous hydrogen [10].

3.4.2. Four component model (4-C)

Fat mass (FM, kg) using the 4-C model was calculated using the following equation of Fuller *et al* [7]:

$$FM = 2.747 \times BV - 0.710 \times TBW + 1.460 \times BMC - 2.050 \times BW$$

Where: BV is body volume and determined using ADP; TBW is total body water and determined using deuterium dilution; BMC is whole body bone mineral content and determined using DXA and BW is body weight determined during the ADP procedure.

3.5. Statistical analysis

Descriptive data are reported as mean ± (standard deviation) unless otherwise stated. Statistical analysis revealed the body composition data was normally distributed.

Precision of the iDXA was expressed as the root mean square standard deviation (RMS-SD) and % CV according to ISCD recommendations. Least significant change (LSC) was calculated (2.77 x RMS-SD) to establish the smallest change between repeated scans which could be identified with 95% confidence as originating from the participant rather than instrument and positioning variability [5].

Paired sample t tests were performed to determine the difference between instruments.

Bland-Altman analysis was performed to determine the association and agreement between the two instruments and between each instrument and 4-C derived fat mass. Where appropriate linear regression analysis was used to derive cross-calibration equations between Prodigy data, using enhanced analysis mode and iDXA data. It should be noted that enhanced analysis mode is only available on Lunar Prodigy Advanced and iDXA instruments running software versions 15 and 16. If an earlier version of the Lunar Prodigy instrument is being used, refer to Table 3.7 where we have given whole body and regional bone and body composition cross-calibration regression equations to translate from Lunar Prodigy measurements analysed in basic mode to Lunar iDXA measurements.

Repeated measures ANOVA was applied to test for significance in fat measurements. Post hoc comparisons with Bonferroni correction were applied to discover significance between methods (4-C, iDXA, Prodigy Enhanced and Prodigy Basic). iDXA values were calculated as the mean of two iDXA measurements.

GraphPad Prism (Version 6.00 for Windows, GraphPad Software, San Diego California USA) was used to generate Bland-Altman analyses and IBM SPSS (IBM Corp. Released 2012. IBM SPSS Statistics for Windows, Version 21.0. Armonk, NY: IBM Corp) was used for all other statistical analyses.

Significance was assumed for $p < 0.05$ for all statistical tests.

3.6. Results

3.6.1. iDXA precision

Precision error for repeated iDXA scans is shown in Table 3.2. Precision error, when represented by %CV, was less than 2% for all measures with the exception of arm fat mass (2.28%). A greater precision was demonstrated for lean mass compared to fat mass.

Table 3.2. Precision variables of two iDXA whole-body and regional body composition measurements.

Region	Variables	Mean ± SD	Mean Difference	RMS-SD	CV (%)	LSC
Hip	BMC (g)	35.98 ± 7.61	-0.07	0.46	1.05	1.29
	Area (cm^2)	33.21 ± 3.98	0.06	0.28	0.59	0.77
	BMD (g/cm^2)	1.08 ± 0.16	-0.00	0.01	0.72	0.03
Spine	BMC (g)	58.74 ± 12.09	-0.44	0.71	0.86	1.96
	Area (cm^2)	46.59 ± 5.61	0.02	0.42	0.54	1.16
	BMD (g/cm^2)	1.25 ± 0.15	-0.01	0.01	0.74	0.04
Whole Body	BMC (kg)	2.82 ± 0. 58	-0.00	0.02	0.44	0.04
Arms	Fat mass (kg)	2.26 ± 1.11	-0.01	0.06	2.28	0.16
	Lean mass (kg)	5.61 ± 1.78	0.01	0.09	1.20	0.25
Legs	Fat mass (kg)	8.38 ± 4.45	-0.05	0.18	1.32	0.50
	Lean mass (kg)	18.24 ± 4.00	-0.07	0.19	0.74	0.52
Trunk	Fat mass (kg)	6.12 ± 6.49	-0.00	0.26	1.58	0.72
	Lean mass (kg)	24.03 ± 4.64	0.11	0.29	0.93	0.80
Whole Body	Fat mass (kg)	23.57 ± 11.51	-0.07	0.24	0.86	0.65
	Lean mass (kg)	51.00 ± 10.39	0.07	0.28	0.42	0.78

RMS-SD, root mean square standard deviation; %CV, percent coefficient of variance; LSC, ideal least significant change.

3.6.2. iDXA fat mass accuracy

iDXA measured fat mass and 4-C derived fat mass are highly correlated (r^2 = 0.99, P<0.05) with a slope of 0.892 and an intercept of 3.39. However, there is a significant difference between iDXA measured fat mass and 4-C derived fat mass (mean difference (SD), -0.936 (1.83), P < 0.05) with wide limits of agreements (-4.53 – 2.65). It can be seen in Figure 3.1 that there is a significant positive proportional bias. Furthermore, at an average fat mass of 32.12 kg the iDXA shifted from over-measuring to under-measuring fat mass compared to 4-C derived fat mass.

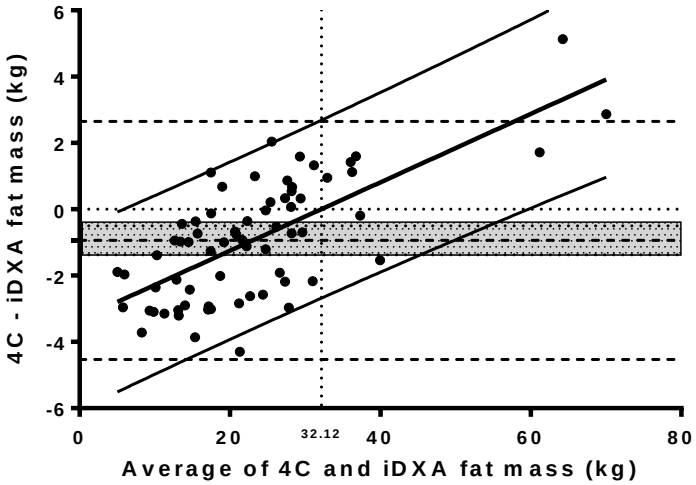

Figure 3.1. Bland-Altman plot of iDXA and 4 Component model derived fat mass (n=68). Solid black linear regression line demonstrates the systematic bias, hashed grey box corresponds to the 95% CI of the systematic bias, dashed lines represent the limits of agreements and the dotted lines present the crossover of over - to under - measuring fat mass at 32.12 kg.

3.6.3.iDXA vs Prodigy

There were significant differences in whole body and spine bone masses between iDXA and prodigy enhanced measurements, these differences were not seen in any hip measurements (Table 3.3).

The comparison of body composition measurements between the instruments reveals significant differences in fat and lean masses across all regions (Table 3.4).

Differences in whole body and regional bone and body composition measurements between Prodigy basic mode and iDXA enhanced mode analyses are presented in table 3.5 and 3.6. Significant differences were present in whole body and spine bone measurements and in all regions of body composition. Therefore relevant cross-calibration regression equations were derived and can be found in table 3.7. Hip and spine measurements for Prodigy basic and Prodigy Enhanced were identical.

Table 3.3. Whole body and regional iDXA and Prodigy enhanced bone density measurements.

Region	Variables	iDXA	Prodigy Enhanced	Bias	LOA
Whole Body	BMC (kg)	2.8 ± 0.6	2.8 ± 0.6	0.02 ± 0.05*	-0.07 – 0.12
	Area (cm^2)	2255.1 ± 234.3	2219.4 ± 236.9	35.8 ± 51.0*	-64.2 – 135.7
	BMD (g/cm^2)	1.24 ± 0.15	1.25 ± 0.16	-0.01 ± 0.02*	-0.06 – 0.04
Hip	BMC (g)	36.0 ± 7.6	36.1 ± 7.6	-0.07 ±1.148	-2.32 – 2.18
	Area (cm^2)	33.2 ± 4.0	33.2 ± 3.9	0.06 ± 0.87	-1.64 – 1.76
	BMD (g/cm^2)	1.08 ± 0.16	1.08 ± 0.15	-0.00 ± 0.02	-0.04 – 0.04
Spine	BMC (g)	58.7 ± 12.1	59.2 ± 12.3	-0.44 ± 1.21*	-2.82 – 1.93
	Area (cm^2)	46.6 ± 5.6	46.6 ± 5.6	0.02 ± 0.76	-1.48 – 1.51
	BMD (g/cm^2)	1.25 ± 0.15	1.26 ± 0.15	-0.01 ± 0.02*	-0.05 – 0.04

Mean ± standard deviation. * $P < 0.05$. BMC, bone mineral content; BMD, bone mineral density.

Table 3.4. Whole body and regional iDXA and Prodigy enhanced body composition measurements.

Region	Variables	iDXA	Prodigy enhanced	Bias	LOA
Whole body	Fat mass (kg)	23.6 ± 11.6	24.9 ± 11.7	-1.29 ± 0.56*	-2.53 – 0.05
	Lean mass (kg)	51.0 ± 10.4	49.9 ± 10.1	1.18 ± 0.57*	0.00 – 2.24
Arm	Fat mass (kg)	2.3 ± 1.1	2.5 ± 1.2	-0.25 ± 0.19*	-0.62 – 0.12
	Lean mass (kg)	5.6 ± 1.8	5.4 ± 1.8	0.20 ± 0.33*	-0.46 – 0.85
Leg	Fat mass (kg)	8.4 ± 4.5	8.9 ± 4.5	-0.54 ± 0.30*	-1.13 – 0.05
	Lean mass (kg)	18.2 ± 4.0	17.8 ± 3.9	0.46 ± 0.63*	-0.77 – 1.68
Trunk	Fat mass (kg)	12.1 ± 6.5	12.6 ± 6.4	-0.46 ± 0.42*	-1.28 – 0.35
	Lean mass (kg)	24.0 ± 4.7	23.6 ± 4.4	0.41 ± 0.72*	-1.00 – 1.81

Mean ± standard deviation, *P < 0.05.

Table 3.5. Difference between iDXA enhanced and Prodigy basic software analysis: whole-body and regional bone mass, area and density measurements

Region	Variables	iDXA	Prodigy	Difference
Total Body	BMC (kg)	2.8 ± 0.6	3.0 ± 0.7	-0.20 ± 0.14*
	BA (cm^2)	2.3 ± 0.2	2.4 ± 0.3	-0.14 ± 0.16*
	BMD (kg/cm^2)	1.24 ± 0.15	1.25 ± 0.13	-0.01 ± 0.04*
Hip	BMC (g)	36.0 ± 7.6	36.1 ± 7.6	-0.06 ± 1.15
	BA (cm^2)	33.2 ± 4.0	33.2 ± 3.9	0.06 ± 0.87
	BMD (g/cm^2)	1.08 ± 0.16	1.08 ± 0.15	0.00 ± 0.02
Spine	BMC (g)	58.7 ± 12.1	59.2 ± 12.3	-0.44 ± 1.21*
	BA (cm^2)	46.6 ± 5.6	46.6 ± 5.6	0.02 ± 0.76
	BMD (g/cm^2)	1.25 ± 0.15	1.26 ± 0.15	-0.01 ± 0.02*

Means ± Standard Deviations *P < 0.05

Table 3.6. Difference between iDXA enhanced and Prodigy basic software analysis: whole-body and regional body composition measurements

Region	**Variables**	iDXA	Prodigy	**D**ifference
Whole body	Fat mass (kg)	23.6 ± 11.6	26.0 ± 14.4	-0.79 ± 1.73*
	Lean mass (kg)	51.0 ± 10.4	49.9 ± 10.9	1.18 ± 1.99*
Arm	Fat mass (kg)	2.3 ± 1.1	2.1 ± 12.7	-0.16 ± 0.21**
	Lean mass (kg)	5.6 ± 1.8	5.4 ± 1.8	0.17 ± 0.23**
Leg	Fat mass (kg)	8.4 ± 4.5	8.8 ± 5.0	-0.44 ± 0.71**
	Lean mass (kg)	18.2 ± 4.0	17.4 ± 4.1	0.85 ± 0.89**
Trunk	Fat mass (kg)	12.1 ± 6.5	12.8 ± 6.7	-0.67 ± 1.11**
	Lean mass (kg)	24.0 ± 4.7	23.7 ± 4.9	0.29 ± 1.24

Means ± Standard Deviations *P < 0.05

Table 3.7. Cross calibration equations relating Prodigy data collected and analysed using Encore basic software versions to iDXA enhanced analysis.

	Variable	Slope	95% CI	Intercept	95% CI	r^2
Whole body	BMC (kg)	0.886	0.841-0.931	0.147	0.007-0.286	0.957
	BA (cm^2)	0.661	0.570-0.751	0.672	0.452-0.891	0.760
	BMD (kg/cm^2)	1.199	1.146-1.252	-0.254	-0.320- -0.187	0.968
	Fat mass (kg)	0.909	0.885-0.934	1.416	0.740-2.093	0.988
	Lean mass (kg)	0.941	0.899-0.983	4.117	1.969-6.265	0.967
Regional	Spine BMC (g)	0.978	0.954-1.001	0.877	-0.537-2.290	0.990
	Spine BA (cm^2)	0.990	0.956-1.023	0.504	-1.046-2.055	0.982
	Spine BMD (g/cm^2)	0.986	0.950-1.022	0.008	-0.038-0.054	0.978
	Arm fat mass (kg)	0.874	0.847–0.902	0.421	0.354-0.489	0.983
	Arm lean mass (kg)	0.973	0.943-1.004	0.317	0.141-0.493	0.984
	Leg Fat mass (kg)	0.882	0.864-0.901	0.599	0.407-0.791	0.992
	Leg Lean mass (kg)	0.963	0.910-1.015	1.500	0.565-2.434	0.953
	Trunk Fat mass (kg)	0.963	0.923-1.003	-0.201	-0.733-0.370	0.972

CI, Confidence intervals; adjusted r^2, model variance.

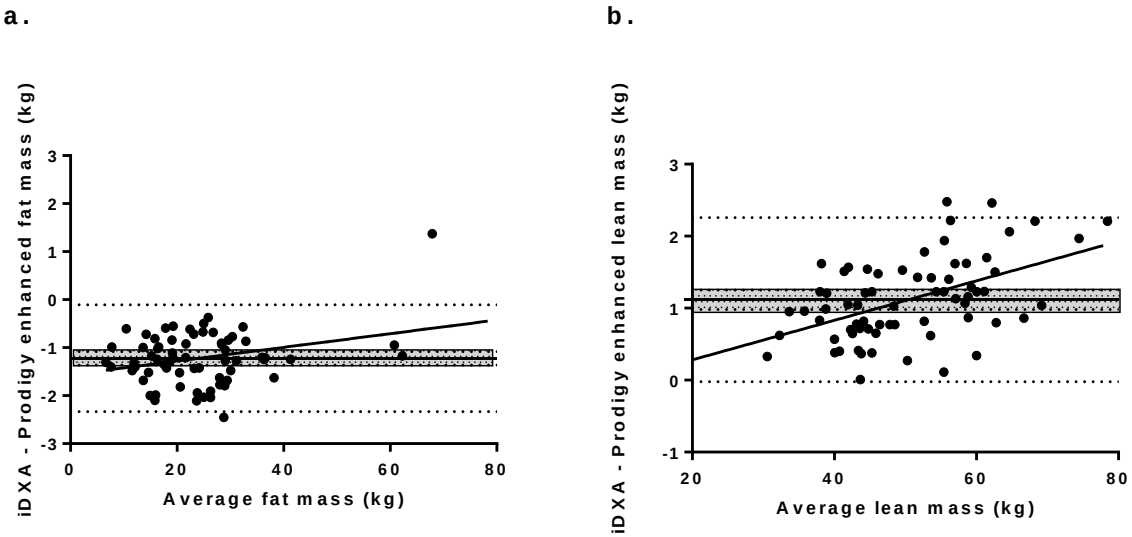

Figure 3.2. Bland-Altman analysis of the agreement between iDXA and Prodigy measured whole body fat (a) and lean mass (b).

Solid black line corresponds to the systematic bias, hashed grey box corresponds to the 95% CI of the systematic bias, and the dotted lines represent the limits of agreements.

Figure 3.2 illustrates the agreement between instruments in fat mass and lean mass by Bland-Altman analysis. Compared to iDXA, Prodigy overestimates fat mass (mean difference -1.29 kg) and underestimates lean mass (mean difference 1.18 kg).

Due to the observed differences between instruments (Table 3.3 and Table 3.4) linear-regression cross-calibration equations were derived where appropriate and can be seen in Table 3.8.

Table 3.8. Cross-calibration equations (Prodigy enhanced to iDXA).

	Variable	Slope	95% CI	Intercept	95% CI	r^2
Whole body	BMC (g)	1.003*	0.983 – 1.023	0.017	-0.041 – 0.074	0.993
	BA (cm^2)	0.966*	0.914 – 1.017	112.0	-3.543 – 227.6	0.953
	BMD (g/cm^2)	0.965*	0.928 – 1.001	0.035	-0.011 – 0.081	0.976
	Fat mass (kg)	0.991*	0.978 – 1.005	-1.016*	-1.393 – -0.639	0.997
	Lean mass (kg)	1.029	1.013 – 1.045	-0.262	-1.058 – 0.535	0.996
Spine	BMC (g)	0.978*	0.954 – 1.001	0.877	-0.537 – 2.290	0.990
	BA (cm^2)	0.990*	0.956 – 1.023	0.505	-1.045 – 2.055	0.981
	BMD (g/cm^2)	0.986	0.950 – 1.022	0.008	-0.038 – 0.054	0.978
Regional	Arm fat mass (kg)	0.962*	0.923 – 1.001	-0.155*	-0.262 - -0.048	0.973
	Arm lean mass (kg)	0.972*	0.927 – 1.016	0.350*	0.097 – 0.603	0.966
	Leg Fat mass (kg)	0.989*	0.973 – 1.005	-0.444*	-0.604 - -0.284	0.996
	Leg Lean mass (kg)	1.024*	0.985 – 1.063	0.036	-0.673 – 0.746	0.976
	Trunk Fat mass (kg)	1.010*	0.995 – 1.026	-0.591*	-0.811 - -0.372	0.996
	Trunk Lean mass (kg)	1.042*	1.003 – 1.080	-0.576	-1.494 – 0.341	0.978

CI, Confidence intervals; Adjusted r^2, model variance, *P < 0.05.

3.6.4. Prodigy Accuracy

Prodigy enhanced fat mass and 4-C derived fat mass are highly correlated (R^2 = 0.993), with a slope of 0.883 and intercept of 4.80. As observed with the iDXA (Figure 3.1), there is a significant difference between Prodigy enhanced fat mass and 4-C fat mass (mean difference (SD) -2.16 (2.05) kg). There are also wider limits of agreement (-6.17 – 1.86) and a more negative systematic bias than for the iDXA (Figure 3.3b & 3.3c)

3.6.5. Four method comparison

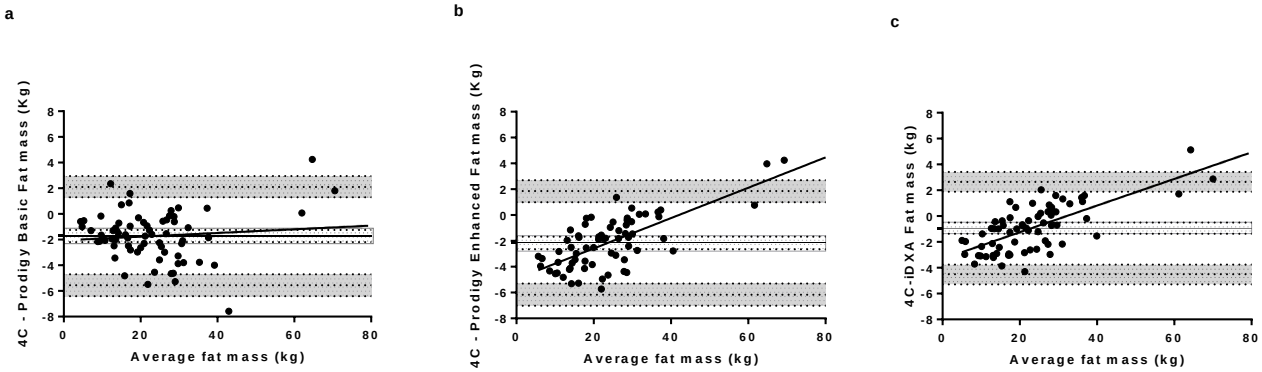

Figure 3.3. Demonstration of the difference and progression between 4-Component model and Prodigy Basic analysis (a), Prodigy Enhanced (b) and iDXA (c) with 95% limits of agreement. Solid black line corresponds to the systematic bias, hashed grey box corresponds to the 95% CI of the systematic bias, and the dotted lines represent the limits of agreements with corresponding 95% CI represented by grey boxes.

The measurement of fat mass was significantly affected by method ($F(3,201) = 41.057$, $P < 0.05$). There was a significant difference between 4-C derived fat mass and iDXA (mean diff -0.936, P = 0.000), Prodigy Enhanced (-2.157, P = 0.000) and Prodigy Basic (-1.720, P = 0.000) fat mass. However, there was no significant difference between Prodigy basic and Prodigy enhanced fat mass measurements (0.437, P = 0.275).

Figure 3.3 and Table 3.9 show that iDXA limits of agreement with 4-C (-4.78, 2.63) are narrower compared to Prodigy in basic mode (-5.56, 2.12) which in turn are narrower than Prodigy enhanced mode (-6.17, 1.86).

Table 3.9. Comparison of different measurement techniques against the four component model.

Model vs 4-C	Mean difference ± SD	RMS SD	LSC	CI Lower	CI Upper	LOA
iDXA	-0.9 ± 1.8	1.5	4.0	-3.4 to -1.9	3.8 to 5.3	-4.8 to 2.6
Prodigy Basic	-1.7 ± 2.0	2.1	5.8	-2.9 to -1.3	4.7 to 6.4	-5.6 to 2.1
Prodigy Enhanced	-2.2 ± 2.1	1.8	5.1	-2.7 to -1.0	5.3 to 7.0	-6.2 to 1.9

4-C; four-component model, SD; Standard deviation, RMS SD; Root mean square standard deviation, LSC; Least significant change, CI; Confidence Intervals, LOA; Limits of agreement.

3.7. Discussion

The aim of this study was two-fold: firstly, to determine the precision and accuracy of the GE Lunar iDXA and secondly, to determine if cross-calibration equations are necessary to relate data from the GE Lunar Prodigy to the iDXA densitometers. The difference between software versions for the Prodigy were also investigated.

When introducing a new DXA instrument the ISCD recommend that a cross-calibration of at least 30 participants, representative of the facility's patient population, should be performed. Participants should be scanned twice on the new system and once on the old, on those anatomical sites most commonly measured [4]. We compared the iDXA and Prodigy densitometers for regional and whole body bone mineral density, bone mineral content and bone area and, reflecting our interest in body composition, for lean and fat mass. Where cross-calibration equations were deemed necessary they were derived using linear regression.

3.7.1. iDXA Precision

Precision of the iDXA was assessed by %CV of repeated bone and body composition measurements. We found excellent precision in whole body and regional bone density with all values below 2 %. This was also observed for whole body and regional body composition measurements with the exception of arm fat mass, which had a lower precision of 2.28%.

Our findings support previously published literature which has reported similar precision data for whole body and regional bone density and body composition using iDXA [2 3 11 12]. Additionally, both Rothney *et al* [11] and Kaminsky *et al* [12] support our findings of a lower precision in arm fat mass (2.8% and 4.2% Rothney and Kaminsky respectively). The larger precision error may be due to re-positioning of the participants or the inclusion of breast tissue in the arm region of interest in some re-scans therefore offering the potential for larger errors [13]. To test this theory we separated arm fat by gender to determine whether breast tissue may have had an impact, but we found no significant differences in the precision of arm fat mass between genders.

Compared to the iDXA, previously published reports from its predecessor, the Prodigy have demonstrated similar precision for bone density with precisions reported below 2% by Oldroyd *et al* [14] and Krueger *et al* [15]. However, when exploring body composition, both Oldroyd *et al* and Bilsborough *et al* [16] reported whole body fat mass precision values of 2.5% for Prodigy. This is a much lower precision than that of 0.9% for the iDXA in the current study.

These comparisons suggest that the precision of iDXA when measuring bone density remains similar to the Prodigy. However, there appears to be a worthwhile improvement in precision in whole body and regional fat mass. This may be due to the improvement in soft tissue assessment as a result of enhanced bone edge detection technology [17].

3.7.2. iDXA vs Prodigy

When scan analysis was carried out using the same software version, significant differences between iDXA and Prodigy were identified in all regions of bone mass, area and density except for the femoral hip BMD and lumbar spine (L2-L4) BA, with Prodigy over-reading all values with the exception of hip area. This has been similarly observed in other studies [18-20] with Hull *et al* [19] reporting significantly higher mean BMC values in the Prodigy than the iDXA in both males and females (males; 3.11 kg *vs.* 3.06 kg, Prodigy *vs.* iDXA respectively and females; 2.37 kg *vs*. 2.31 kg, Prodigy *vs*. iDXA respectively). Rhodes *et al* [20] also found Prodigy BMC values were significantly higher compared to the iDXA in all regions of bone mass (BMC, 2842 g vs. 2651 g, Prodigy vs. iDXA respectively). Furthermore, Morrison *et al* [21] compared iDXA to Prodigy and found significant differences in whole body and regional bone density (mean whole body; 1.25 g/cm^2 *vs*. 1.22 g/cm^2, Prodigy *vs.* iDXA respectively). Prodigy basic comparisons to iDXA also displayed significant differences in whole body bone measurements, however hip and spine measurements were identical to hip and spine measurements analysed using Prodigy Enhanced mode. This suggests that any changes in software algorithms were not applied to regional bone analysis, only whole body bone measurements.

When investigating body composition, we also observed significant differences between iDXA and both Prodigy basic and enhanced, with Prodigy tending to over-read fat mass and under-read lean mass relative to iDXA. The only study we found in the literature to make a similar comparison was that of Morrison *et al* [21] who reported that only leg lean mass and arm soft tissue measurements were significantly different between instruments (leg lean mass mean difference (kg); 0.586, arm fat mass; -0.109, arm lean mass; -0.228).

The significant differences observed between the two DXA instruments warranted the development of cross-calibration regression equations. The differences and those observed across the published literature highlight the importance of generating instrument specific cross-calibration equations when undergoing a system upgrade. It is also important that the cross-calibration equations are relevant to the population under investigation as

demonstrated by the apparent outliers at the top end of the fat mass range. A possible limitation of the comparison of iDXA and Prodigy lies in the calculation of the mean of two iDXA measurements. This may lead to an unfair comparison against Prodigy due to a lower random error compared to a single measurement.

3.7.3. DXA accuracy

The accuracy of our DXA fat mass measurements was evaluated by comparing fat mass estimated by DXA to that derived from a four-component (4-C) model. The 4-C model, as well as whole body MRI, are recognised standards in body composition measurements as they account for inter-individual variability in total body water and bone mineral mass [22-24]. Our results demonstrated good correlation between iDXA and 4-C derived fat mass (r = 0.994) but a proportional bias between the two fat mass estimates was evident. The disadvantage of fixed and proportional bias is that the bias is driven by the measured variable, in this case fat mass, either by a constant amount or a proportional amount and therefore difficult to account for. To our knowledge there is no literature that discusses the accuracy of either iDXA or Prodigy fat mass measurement using the 4-C model. However, previous literature has reported significant differences between fat mass (%) measured by various DXA models (QDR2000, QDR2000W, DPX/L, and Lunar) and the 4-C model [25]. When comparing Prodigy and the 4-C model, Williams *et al* [25] found significant differences in fat mass (1.35, 1.21 and 1.58 kg in non-obese men, women and obese women, respectively). They also reported that the fat mass bias was positively associated with BMI. Although it appears that the accuracy of DXA has improved over the years, a systematic bias still remains between the iDXA and the 4-C model.

The differences identified between the two methods could have several origins. DXA assumes that the hydration value for fat-free mass remains constant [26], however this may not be true for participants across a range of masses. Participant mass itself may inflict a bias in soft tissue estimation because of the influence of tissue depth on bone edge detection by DXA, therefore as subject mass increases, so may the error in detecting soft tissue. Although 4-C is considered a reference measure against other methods there is still concern that errors arising from the individual methods may amalgamate to a large error in the final fat mass estimate. However, Fuller *et al* found a measurement error of less than 1% for fat and fat free mass derived from 4-C.

Comparisons between GE software versions (Basic and Enhanced) for Prodigy and a 4-C model have not been investigated before. There are many publications that demonstrate the transitions between instruments, but few that detail the differences when upgrading software versions. In the final part of this study we investigated the differences in whole body fat mass measurements between basic and enhanced software versions on the Prodigy and compared this to the iDXA and 4-C model.

Prodigy basic analysis mode compared to 4-C demonstrated a good agreement over a wide range of fat masses. However, in the highest fat masses the agreement was less good, consistent with previous studies [25 27 28]. As referred to earlier, Williams *et al* [25] reported the largest difference between 4-C and Prodigy (Encore 2002) in obese women (mean bias 1.58 kg) and Wells *et al* [27] (Software version not stated), reported that Prodigy significantly over-estimated FM compared to 4-C by 0.9 kg with the greatest variability being observed at the highest fat masses.

In summary, the latest DXA instrument from GE, the iDXA, comes with new hardware in the form of a more powerful X-ray tube, enhanced image resolution and therefore better bone edge detection. Furthermore the latest software, Encore version 15 & 16, comes with developed soft tissue algorithms. The enhancement in technology has led to an improvement in the accuracy and precision of iDXA compared to its predecessor Prodigy demonstrated by smaller differences between repeated iDXA measurements and compared to 4-C measurements in fat mass. However this means that differences exist between the iDXA and Prodigy instruments and therefore cross-calibration equations are essential if comparisons between instruments are unavoidable. Even with these improvements, accuracy issues remain at the highest fat masses, reinforcing the importance of deriving cross-calibration equations that are relevant to the population under investigation and also that further comparative studies are warranted in an obese population.

3.8. References

1. Toombs RJ, Ducher G, Shepherd JA, et al. The impact of recent technological advances on the trueness and precision of DXA to assess body composition. *Obesity (Silver Spring)* 2012;20(1):30-9.
2. Hind K, Oldroyd B, Truscott JG. In vivo precision of the GE Lunar iDXA densitometer for the measurement of total body composition and fat distribution in adults. *European journal of clinical nutrition* 2011;65(1):140-2.
3. Hind K, Oldroyd B, Truscott JG. In vivo precision of the GE Lunar iDXA densitometer for the measurement of total-body, lumbar spine, and femoral bone mineral density in adults. *Journal of clinical densitometry : the official journal of the International Society for Clinical Densitometry* 2010;13(4):413-7.
4. Shepherd JA, Lu Y, Wilson K, et al. Cross-calibration and minimum precision standards for dual-energy X-ray absorptiometry: the 2005 ISCD Official Positions. *Journal of clinical densitometry : the official journal of the International Society for Clinical Densitometry* 2006;9(1):31-6.
5. Baim S, Wilson CR, Lewiecki EM, et al. Precision assessment and radiation safety for dual-energy X-ray absorptiometry: position paper of the International Society for Clinical Densitometry. *Journal of clinical densitometry : the official journal of the International Society for Clinical Densitometry* 2005;8(4):371-8.
6. Chen X, Iqbal N, Boden G. The effects of free fatty acids on gluconeogenesis and glycogenolysis in normal subjects. *The Journal of clinical investigation* 1999;103(3):365-72.
7. Fuller NJ, Jebb SA, Laskey MA, et al. Four-component model for the assessment of body composition in humans: comparison with alternative methods, and evaluation of the density and hydration of fat-free mass. *Clin Sci (Lond)* 1992;82(6):687-93.
8. IAEA. Assessment of Body Composition and Total Energy Expenditure in Humans Using Stable Isotope Techniques. IAEA Human Health Series. Vienna, 2009:146.
9. Coward WA. Measurement of energy expenditure: the doubly-labelled-water method in clinical practice. *The Proceedings of the Nutrition Society* 1991;50(2):227-37.
10. Schoeller DA, Hnilicka JM. Reliability of the doubly labeled water method for the measurement of total daily energy expenditure in free-living subjects. *The Journal of nutrition* 1996;126(1):348S-54S.
11. Rothney MP, Martin FP, Xia Y, et al. Precision of GE Lunar iDXA for the measurement of total and regional body composition in nonobese adults. *Journal of clinical densitometry : the official journal of the International Society for Clinical Densitometry* 2012;15(4):399-404.

12. Kaminsky LA, Ozemek C, Williams KL, et al. Precision of total and regional body fat estimates from dual-energy X-ray absorptiometer measurements. *The journal of nutrition, health & aging* 2014;18(6):591-4.
13. Knapp KM, Welsman JR, Hopkins SJ, et al. Obesity increases precision errors in total body dual-energy x-ray absorptiometry measurements. *Journal of clinical densitometry : the official journal of the International Society for Clinical Densitometry* 2015;18(2):209-16.
14. Oldroyd B, Smith AH, Truscott JG. Cross-calibration of GE/Lunar pencil and fan-beam dual energy densitometers--bone mineral density and body composition studies. *European journal of clinical nutrition* 2003;57(8):977-87.
15. Krueger D, Vallarta-Ast N, Checovich M, et al. BMD measurement and precision: a comparison of GE Lunar Prodigy and iDXA densitometers. *Journal of clinical densitometry : the official journal of the International Society for Clinical Densitometry* 2012;15(1):21-5.
16. Bilsborough JC, Greenway K, Opar D, et al. The accuracy and precision of DXA for assessing body composition in team sport athletes. *Journal of sports sciences* 2014;32(19):1821-8.
17. Healthcare G. Lunar iDXA: Intelligent DXA. In: Healthcare G, ed. Belgium, 2006:10.
18. Hind K, Cooper W, Oldroyd B, et al. A cross-calibration study of the GE-Lunar iDXA and prodigy for the assessment of lumbar spine and total hip bone parameters via three statistical methods. *Journal of clinical densitometry : the official journal of the International Society for Clinical Densitometry* 2015;18(1):86-92.
19. Hull H, He Q, Thornton J, et al. iDXA, Prodigy, and DPXL dual-energy X-ray absorptiometry whole-body scans: a cross-calibration study. *Journal of clinical densitometry : the official journal of the International Society for Clinical Densitometry* 2009;12(1):95-102.
20. Rhodes LA, Cooper W, Oldroyd B, et al. Cross-calibration of a GE iDXA and Prodigy for total and regional body bone parameters: the importance of using cross-calibration equations for longitudinal monitoring after a system upgrade. *Journal of clinical densitometry : the official journal of the International Society for Clinical Densitometry* 2014;17(4):496-504.
21. Morrison SA, Petri RM, Hunter HL, et al. Comparison of the Lunar Prodigy and iDXA Dual-Energy X-ray Absorptiometers for Assessing Total and Regional Body Composition. *Journal of clinical densitometry : the official journal of the International Society for Clinical Densitometry* 2016;19(3):290-7.
22. Lohman TG, Harris M, Teixeira PJ, et al. Assessing body composition and changes in body composition. Another look at dual-energy X-ray absorptiometry. *Annals of the New York Academy of Sciences* 2000;904:45-54.

23. Muller MJ, Braun W, Pourhassan M, et al. Application of standards and models in body composition analysis. *The Proceedings of the Nutrition Society* 2016;75(2):181-7.
24. Heymsfield SB, Ebbeling CB, Zheng J, et al. Multi-component molecular-level body composition reference methods: evolving concepts and future directions. *Obesity reviews : an official journal of the International Association for the Study of Obesity* 2015;16(4):282-94.
25. Williams JE, Wells JC, Wilson CM, et al. Evaluation of Lunar Prodigy dual-energy X-ray absorptiometry for assessing body composition in healthy persons and patients by comparison with the criterion 4-component model. *The American journal of clinical nutrition* 2006;83(5):1047-54.
26. Wang Z, Deurenberg P, Wang W, et al. Hydration of fat-free body mass: review and critique of a classic body-composition constant. *The American journal of clinical nutrition* 1999;69(5):833-41.
27. Wells JC, Williams JE, Chomtho S, et al. Body-composition reference data for simple and reference techniques and a 4-component model: a new UK reference child. *The American journal of clinical nutrition* 2012;96(6):1316-26.
28. Wells JC, Haroun D, Williams JE, et al. Body composition in young female eating-disorder patients with severe weight loss and controls: evidence from the four-component model and evaluation of DXA. *European journal of clinical nutrition* 2015;69(12):1330-5.

4. An approach to quantifying abnormalities in energy expenditure and lean mass in metabolic disease.

Watson LPE, Raymond-Barker P, Moran C, Schoenmakers N, Mitchell C, Bluck L, Chatterjee VK, Savage D, and Murgatroyd PR. An approach to quantifying abnormalities in energy expenditure and lean mass in metabolic disease. *Eur J Clin Nutr* 2013, 1 – 7.

4.1 Abstract

Background*:* Our objective is to develop approaches to expressing resting energy expenditure (REE) and lean body (LM) mass phenotypes of metabolic disorders in terms of Z scores relative to their predicted healthy values.

Methods*:* Body composition and REE were measured in 135 healthy participants. Prediction equations for LM and REE were obtained from linear regression and the range of normality by the standard deviation of residuals. Application is demonstrated in patients from three metabolic disorder groups (Lipodystrophy n = 7, Thyrotoxicosis n = 16, and Resistance to Thyroid Hormone (RTH)β n = 46, RTHα n = 5) in which altered REE and/or LM were characterized by departure from the predicted healthy values, expressed as a Z-score.

Results*:* REE (kJ/min) = Prediction equations were derived for REE and LM. For REE the most significant contributing variables were age, fat mass (FM) and fat-free mass (FFM):
-0.010 x age (y) + 0.016 x FM (kg) + 0.054 x FFM (kg) + 1.736 (R^2 =0.732, RSD = 0.36 kJ/min). For LM, gender specific equations were derived. The most significant contributing varables were bone mineral content (BMC) and height^2 in the males and FM and height^2 in the females: LM (kg) = 5.30 x BMC (kg) + 10.66 x Height² (m) + 6.40 (Male), LM (kg) = 0.20 x FM (kg) + 14.08 x Height² (m) – 2.93 (Female) (Male R^2 = 0.55, RSD = 3.90kg; Female R^2 = 0.59, RSD = 3.85kg).
We found average Z scores for REE and LM of 1.77 and -0.17 in the RTHβ group, -2.25 for REE and 2.10 for LM in RTHα, 5.82 and -1.23 in the thyrotoxic group and 2.97 and 4.20 in the LD group.

Conclusion*:* This approach enables comparison of data from individuals with metabolic disorders with those of healthy individuals, describing their departure from the healthy mean by a Z score.

4.2. Introduction

Many metabolic disorders such as thyroid disease or lipodystrophy are associated with changes in body composition, energy expenditure or both [1 2]. In describing the phenotypes of such conditions it is often desirable to describe the extent to which body composition or energy metabolism deviates from that of healthy individuals, but this is not always straight forward. Comparisons against standard predictions of energy expenditure [3-5] may be compromised by atypical body composition, while comparisons based on body composition proxies such as body mass index (BMI) may not reveal unusual relationships between fat and lean masses.

Commonly used predictions of resting energy expenditure (REE) may be troublesome due to their dependence on age and gender as well as body mass and height [6]. Their piecewise-linear nature can lead to substantial differences between predicted REE just above and below the intersection of adjacent regression ranges. The use of fat free mass (FFM = lean mass (LM) + bone mineral content (BMC) in kg) as a predictor of REE is more accurate and is widely accepted [6] and, when allowed an intercept, is disassociated from gender differences in body composition.

Against this background, we have set out an approach to characterise REE and LM in metabolic disorders by reference to measurements in a metabolically healthy cohort. It utilises the accurate and precise measurements of body composition which are now widely available using dual-energy x-ray absorptiometry (DXA) [7-16]. The key to our approach is the quantification of the difference between measurements and predictions by the assignment of a Z score applied to patients with metabolic disorders. This allows us to quantify the probability of whether an individual data point observed lies within a healthy or metabolic disordered cohort, therefore allowing the discussion of whether a disorder presents with altered REE or body composition phenotype, or indeed both.

Three conditions (Resistance to thyroid hormone (RTHα and RTHβ), Thyrotoxicosis, and lipodystrophy (LD)) in which abnormal energy expenditure and lean body mass have been previously documented provide ideal examples to illustrate our method. RTH is a rare autosomal dominant genetic condition as a result of mutation in either the thyroid receptor TRα or TRβ which are encoded on the genes THRA and THRB [17 18]. TRα is most abundant in the central nervous system, myocardium and skeletal muscle. TRβ is largely expressed in

the liver and kidney. Mutations in these receptors lead to two different conditions, RTHα and RTHβ. RTHβ, a dominantly inherited disorder, with an incidence of 1 in 40,000 [19 20], characterised by elevated circulating thyroid hormones (TH) together with central (hypothalamo-pituitary) and variable peripheral tissue refractoriness to thyroid hormone action [21]. RTHα cases are much rarer with only 14 cases identified to date. The condition is characterised by hypothyroid tissue responses to near normal thyroid function and circulating TH levels [18]. The characteristics of the disorder are relatively consistent across patients.

Thyrotoxicosis (or hyperthyroidism) is due to excess TH secretion from the thyroid gland. Most commonly (50-80% of cases), thyrotoxicosis is caused by Grave's disease which affects ~0.5% of the population [22], and is due to autoantibodies causing excess TH production by stimulating the TSH receptor in the thyroid gland [23].

Lipodystrophy can be either genetic or acquired [24] and is characterised by reduced adipocyte storage capacity and loss of adipose tissue with significantly increased lean body mass, contributing to metabolic complications such as insulin resistance and diabetes mellitus [25]. We have extensive data in these disorders, which are of particular interest to us, and so have invoked them here for demonstration, though we believe our approach is more generally applicable.

4.3. Methods

4.3.1. Participants

Healthy volunteers were recruited by local advertisement in the East Anglian region of the UK. We recruited 135 male and female non-smokers, aged between 17 and 65 years who had no known medical conditions, were not taking any medications or supplements likely to influence energy expenditure or body composition and who did not normally exercise for over an hour a day. Volunteers were from different ethnic backgrounds (126 Caucasian, 2 Black, 6 Asian, and 1 Hispanic). All participants provided written, informed consent.

Volunteers from the metabolic disorder groups (LD n = 7, thyrotoxicosis n = 16, RTHα = 5 and RTHβ n = 46) were recruited following referral to Addenbrooke's hospital and provided written informed consent to participation in their studies. Participants were non-smoking, not on any beta-blockers or anti-arrhythmic treatment and had no current or past history of eating disorder. Thyrotoxic patients were identified based on thyroid function tests suggestive of thyroxicosis (serum TSH < 0.03mU/L, free T4 >22.5pmol/L) and had Graves' disease, as evidenced by elevated anti-TSH receptor antibody titres. Details on the recruitment of the lipodystrophic participants have been previously documented [26]. The lipodystrophic patients varied on genotype and extent of lipodystrophy. Three patients had partial lipodystrophy with C131Y, FS/PPP and R482W LMNA genotypes, and four patients had total lipodystrophy with R482L LMNA, AGPAT2, R482W LMNA and AGL genotypes.

Healthy participants and metabolically disordered participants were asked to refrain from strenuous physical activity, alcohol and caffeine for 24 hours prior to their visit. Each participant arrived at the NIHR/Wellcome Trust Clinical Research Facility (CRF) in Cambridge at 14:00 on day 0 and remained until 12:00 on day 1. After informed consent and medical examination on day 0, height, weight and body composition were measured. Body composition (fat mass, lean mass and bone mineral density) was assessed by dual energy x-ray absorptiometry (DXA; GE Lunar Prodigy GE Healthcare, Madison, WI, software version 12.2). At 18:00 a standardised dinner was served. The energy content of the meal was 1/3 of a participant's daily requirements estimated from predicted resting metabolic rate [3] multiplied by an activity factor of 1.35 [27]. Meal composition was 30-35% fat, 12-15% protein, and 50-55% carbohydrate by energy. The participant retired to bed at 23:00 and

was woken the next morning at 07:00. REE was measured between 07:00 and 08:00 by ventilated canopy respiratory gas exchange (GEM, GEMNutrition, Daresbury, UK). Measurements were recorded at 30s intervals over 20min. The lipodystrophy participants REE was measured by indirect room calorimetry for 60min and has been previously described [26]. All participants were asked to remain awake and still, without any interactions, for the duration of the measurement. Energy expenditure was calculated from the macronutrient respiratory quotients and energy equivalents of oxygen published by Elia and Livesey [28]. Following the REE measurement fasting blood samples were taken for renal and liver function tests, plasma glucose and thyroid function (free T3, T4 and TSH). Urinary metanephrines were also measured.

To determine least significant change (LSC) in REE measurement, three repeated measurements were performed on eight participants giving an LSC of 0.5kJ/min. For LSC in lean mass, previously reported values of 1.13kg [29] for Prodigy were used.

Body composition and REE measurements were performed in all healthy and metabolically disordered volunteers and are summarised in Table 4.1 - 4.4.

Table 4.1. Characteristics of metabolically healthy participants

Variable	*Female N = 88*		*Male N = 47*	
	Mean ± SD	*Range*	*Mean ± SD*	*Range*
Age (years)	34.8 ± 12.0	19.1-62.5	36.6 ± 12.9	17.4-62.2
Height (m)	1.65 ± 0.07	1.52-1.88	1.79 ± 0.7	1.62-1.92
Weight (kg)	66.4 ± 14.6	43.9-119.6	78.1 ± 10.9	56.6-102.8
BMI (kg/m²)	24.2 ± 4.6	17.6-38.6	24.3 ± 2.8	18.7-31.5
FM (kg)	22.8 ± 10.4	7.9-61.5	17.0 ± 8.2	3.9-38.4
LM (kg)	40.3 ± 5.7	28.6-55.6	57.5 ± 5.9	43.7-68.1
FFM (kg)	42.8 ± 6.0	30.5-57.8	60.7 ± 6.2	46.5-71.9
Fat %	33.4 ± 8.5	15.6-52.6	21.1 ± 8.3	6.1-37.7
BMC (kg)	2.5 ± 0.4	1.5-3.6	3.2 ± 0.4	2.3-4.1
REE (kJ/min)	4.1 ± 0.5	3.0-5.8	5.0 ±0.6	3.6-6.4
TSH mU/l (0.4-4.0)	1.6 ± 0.7	0.4-4.0	1.5 ± 0.6	0.5-3.1
Free T4 pmol/l (9.0 – 20.0)	13.0 ± 1.8	9.3-16.9	13.8 ±1.6	10.9-17.3
Free T3 pmol/l (3.0 – 7.5)	5.3 ± 0.6	4.0-7.3	5.8 ± 0.6	4.1-6.9
Plasma Glucose mmol/l	4.5 ± 0.4	3.7 – 6.2	4.7 ± 0.5	3.9 – 5.8

FM, fat mass, LM, Lean Mass, FFM, Fat-free mass, BMC, Bone mineral content, REE, Resting Energy Expenditure. Population reference range for Free T3 (3.0 – 7.5 pmol/l, Free T4 9.0-20.0 pmol/l, TSH 0.40-4.0 mU/l).

Table 4.2. Characteristics of RTHα group

Variable	*RTHα (n = 5)*	
	Female (n =2) (Mean) and range	*Male (n = 3)* (Mean) and range
Age (years)	(53.6) 45.9 to 61.4	(24.8) 17.1 to 30.8
Height (m)	(1.53) 1.48 to 1.58	(1.81) 1.76 to 1.86
Weight (kg)	(82.2) 72.2 to 92.2	(93.4) 72.2 to 85.3
BMI (kg/m²)	(35.6) 29.1 to 42.2	(28.7) 25.3 to 33.3
FM (kg)	(31.0) 24.4 to 37.7	(24.7) 15.8 to 31.3
%FM	(37.8) 34.0 to 41.6	(26.5) 18.3 to 31.6
LM (kg)	(47.7) 45.2 to 50.2	(64.4) 55.7 to 70.4
FFM (kg)	(50.1) 47.3 to 52.9	(67.8) 58.3 to 74.3
BMC (kg)	(2.4) 2.1 to 2.7	(3.4) 2.6 to 3.8
REE (kJ/min)	(3.5) 3.4 to 3.5	(4.8) 4.4 to 5.2
TSH mU/L (0.4 – 4.0)	(4.9) 4.3 to 5.4	(3.6) 2.9 to 4.4
Free T4 pmol/l (9.0 – 20.0)	(8.6) 8.3 to 8.8	(9.2) 9.0 to 9.3
Free T3 pmol/l (3.0 – 7.5)	(5.6) 5.2 to 6.0	(7.4) 6.8 to 8.0
Plasma glucose mmol/l	(4.6) 4.5 to 4.6	(4.2) 4.1 to 4.3

FM, fat mass, LM, Lean Mass, FFM, Fat-free mass, BMC, Bone mineral content, REE, Resting Energy Expenditure.

Table 4.3 Characteristics of the RTHβ and Thyrotoxic groups

Variable	*RTHβ (n = 46)*		*Thyrotoxicosis (n=16)*	
	Female (n =34)	*Male (n = 12)*	*Female (n = 10)*	*Male (n = 6)*
	Mean ± SD	Mean ± SD	Mean ± SD	Mean ± SD
Age (years)	39.4 ± 13.6	38.1 ± 16.8	45.8 ± 14.2	40.7 ± 14.4
Height (m)	1.61 ± 0.1	1.74 ±0.1	1.63 ± 0.1	1.76 ± 0.1
Weight (kg)	71.7 ± 14.4	72.8 ± 10.4	64.5 ± 9.4	74.1 ± 18.8
BMI (kg/m²)	27.6 ± 5.1	24.1 ± 3.8	24.2 ± 3.4	23.81 ± 3.6
FM (kg)	29.7 ± 10.0	18.2 ± 8.2	26.4 ± 7.6	20.9 ± 10.6
LM (kg)	38.6 ± 5.2	51.7 ± 4.8	35.6 ± 5.7	50.6 ± 9.6
FFM (kg)	40.9 ± 5.5	54.1 ± 5.1	38.1 ± 5.8	53.1 ± 10.1
BMC (kg)	2.3 ± 0.4	2.4 ± 0.5	2.5 ± 0.3	3.0 ± 0.6
REE (kJ/min)	4.6 ± 0.7	5.2 ± 0.6	5.5 ± 0.9	7.2 ± 1.4
TSH mU/L (0.4-4.0)	3.8 ± 3.4	2.2 ± 0.7	0.03 ± 0.0	0.4 ± 0.9
Free T4 pmol/l (9.0-20.0)	35.1 ± 13.1	29.5 ± 5.1	43.3 ± 19.6	32.4 ± 25.5
Free T3 pmol/l (3.0-7.5)	12.7 ± 4.3	10.5 ± 1.6	24.3 ± 11.3	22.4 ± 11.1
Plasma glucose mmol/l	5.0 ± 0.5	4.7 ± 0.8	4.9 ± 0.4	5.5 ± 0.3

FM, fat mass, LM, Lean Mass, FFM, Fat-free mass, BMC, Bone mineral content, REE, Resting Energy Expenditure.

Table 4.4. Characteristics of the Lipodystrophy group

Variable	*Female (n = 5)* Mean ± SD	*Male (n = 2)* (Mean) and range
Age (years)	48.8 ± 13.2	(34.2) 17.6 to 50.8
Height (m)	1.64 ± 0.05	(1.75) 1.65 to 1.84
Weight (kg)	66.2 ± 6.9	(78.8) 69.7 to 88.0
BMI (kg/m²)	24.5± 2.4	(25.8) 25.6 to 26.0
FM (kg)	9.3 ± 6.8	(5.6) 3.5 to 7.6
%Fat	13.6 ± 9.2	(6.8) 5.0 to 8.6
LM (kg)	54.2 ± 6.2	(70.0) 62.6 to 77.5
FFM (kg)	56.9 ± 6.0	(73.3) 66.1 to 80.4
BMC (kg)	2.7 ± 0.6	(3.2) 2.9 to 5.3
REE (kJ/min)	5.6 ± 0.7	(6.3) 5.7 to 6.9
TSH mU/L (0.4-4.0)	0.7 ± 0.4	(1.2) 1.1 to 1.3
Plasma Glucose mmol/l	6.9 ± 4.5	(10.4) 8.1 to 10.3

FM, fat mass, LM, Lean Mass, FFM, Fat-free mass, BMC, Bone mineral content, REE, Resting Energy Expenditure. Free T4 and Free T3 measures were not available to report in the Lipodystrophy group.

4.3.2. Ethics

The study received a favourable opinion from the Cambridge Central East of England Research Ethics Committee and was funded by and conducted in the NIHR/Wellcome Trust Clinical Research Facility (WTCRF; Cambridge, UK).

4.3.3. Statistical analysis

Multiple correlation analyses were undertaken using SPSS19 (SPSS Inc., Chicago, IL, USA) to identify variables or combinations of variables that correlate ($P < 0.05$) to REE and DXA-measured total body LM.

Once the correlating variables were established, forward stepwise multiple linear regression analysis was performed to relate REE (kJ/min) to FFM (kg), FM (kg) and age in all subjects and to relate LM to FM and height for females and LM to height and bone mineral content in males.

A statistical K-fold cross-validation approach was then undertaken to test the reliability of both the models. The dataset was randomly numbered and split into test datasets and a validation dataset. For the REE validation the analysis was repeated eight times making sure each data point was tested and validated to establish whether the same variables significantly contributed to the prediction of REE, then the standard deviations of the residuals (the individual differences between predicted and measured values) were compared. For LM cross validation the analysis was repeated five times and was also tested on an additional dataset of 19 females and 18 males.

Residuals were derived for each contributing data point and normality was confirmed for the set of all residuals using Shapiro-Wilk test for normality. This allowed the distributions of residuals to be described by their standard deviations, the magnitudes of which were taken as a measure of the precision of the prediction. Furthermore each experimental data point could be defined in terms of the number of standard deviations from the predicted value (Z-score). When investigating the disease groups, REE or LM was predicted as though belonging to the healthy cohort, and an associated Z-score used as a measure of the deviation from the healthy norm.

Although we have not assigned an absolute threshold for defining whether an individual data point is outside of the healthy range, if the Z-score for the patient is 1, then it suggests there is a 32% probability that the observation belongs in the healthy cohort. If the Z-score is 2, then the probability falls to 5%, making it 95% likely that the observation is associated with a disordered group mean.

4.4. Results

4.4.1. Resting energy expenditure

To establish the appropriate variables to include in the prediction of REE we examined the literature and subsequently explored correlations of REE with age, gender, height², bone mass, FFM and FM.

Analysis of variance was carried out to test the effect of ethnicity (white, black and Asian) on REE and LM, and showed that in this group of volunteers there was no effect of ethnicity on REE or LM (REE, F = 0.286, LM, F = 0.921). Stepwise multiple regression analysis was carried out to establish which correlates contributed significantly to the prediction of REE and LM. Those that did not contribute were excluded (Table 4.5).

Table 4.5. Multiple correlations of measured REE (kJ/min) and LM (kg), with demographic measurements. (n = 135, males = 47 and females = 88)

Variable		Age	Gender	Height²	FM	FFM	Bone
REE	Coefficient	-0.133	-0.620	0.675	0.207	0.813	0.740
kJ/min	Sig	0.123	0.000	0.000	0.016	0.000	0.000
LM	Coefficient	0.004	-0.819	0.845	-0.012	1.000	0.805
kg	Sig	0.961	0.000	0.000	0.890	0.000	0.000

REE, Resting Energy Expenditure, LM, Lean Mass.

The variables that contributed the least to the prediction of REE were gender (R^2 = 0.004), height² (R^2= 0.005), and bone mass (R^2 = 0.002). With these removed, age continued to contribute to the overall prediction leaving FM (R^2 = 0.043), FFM (R^2 = 0.660) and age (R^2 = 0.018) in the regression (R^2 = 0.732). The resulting expression derived from the 135 healthy participants is,

REE (kJ/min) = -0.010 (age) + 0.016 (FM kg) + 0.054 (FFM kg) + 1.736.

(Model R^2 =0.732)

4.4.2. REE regression validation

The regression expression for REE above has been subject to K-fold validation. The source data was randomised into 8 groups and regressions repeatedly derived from 7x17 and 1x16 subjects and tested in the remaining group. The coefficients of variation for the resulting 8 estimates of each regression coefficient were: Age 7.3%, FM 12.1%, FFM 2.9%, and Constant 4.9%. The SD of residuals in the test group for the eight regressions ranged from 0.27 to 0.49 kJ/min, compared to 0.36 kJ/min for the whole data set.

4.4.3. Lean mass

The least significant coefficient, age ($P > 0.05$) was taken out of the analysis first. Once this had been removed fat and height² were highly significant contributors in females but height² alone was significant in males. Bone mass was a significant contributor to LM in males when it replaced FM but this was not the case in females. Therefore the two gender specific regression equations for the prediction of LM are as follows:

Male LM (kg) (n = 47) = 5.30 * Bone mass (kg) + 10.66 * Height² (m) + 6.40

Female LM (kg) (n = 88) = 0.20 * Fat (kg) + 14.08 * Height² (m) -2.94

The standard deviations of residuals for these two regressions are respectively 3.90 and 3.85kg. The Model R^2 for males is 0.55, and females is 0.59.

4.4.4. Lean Mass regression validation

As with the REE validation process, the male and female lean mass regressions have undergone K-Fold validation, randomised into 5 groups and the analysis repeated 5 times. The female results indicated the SD of residuals ranged from 3.0 to 4.26kg compared to 3.85 kg from the whole dataset. The male results indicated a range of 2.38kg to 4.83kg compared to 3.90kg from the whole dataset. The data was also tested in independent male and female data sets drawn from the entire control group of another study and its ongoing successor (n = 18 males and 19 females). For the male group, the mean residual in the test group is -1.49kg with SD 3.91kg. The offset of the male mean from zero is predominantly due to a single outlier whose residual was double that of any other subject, yet is not significantly different from zero. For the female group the mean residual is 0.15kg (ns) with SD 2.2kg.

4.4.5. Representation of data: Z Scores.

4.4.5.1. Resting Energy Expenditure

To represent the normative data, the residuals of measured REE - predicted REE were plotted with corresponding Z-scores (Figure 4.1).

Figure

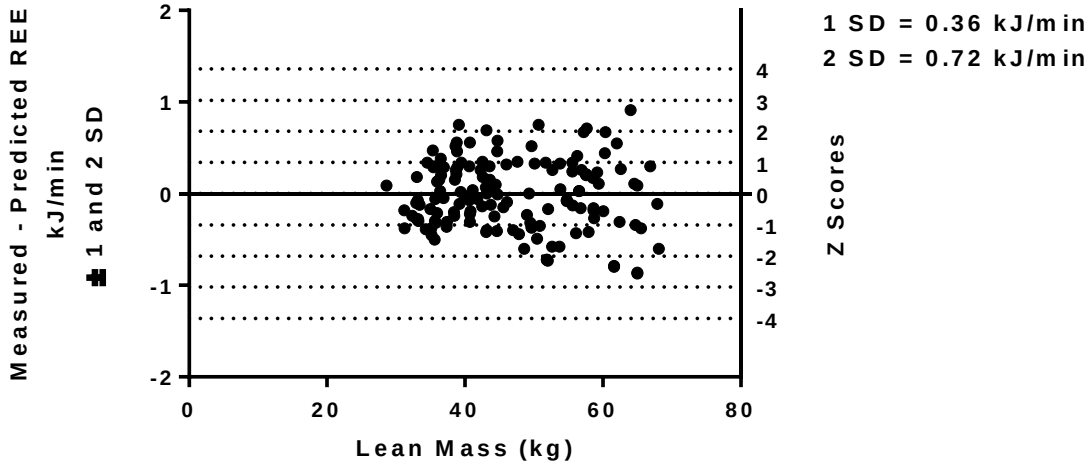

4.1

Figure 4.1. Measured – predicted REE (kJ/min) in healthy controls with 2 SD.

LM, the strongest predictive variable, is used to separate the data points. To assess the utility of this approach in disorder states known to be associated with altered body composition and resting metabolic rate, we characterised patients with RTHα, RTHβ,

thyrotoxicosis and LD [1 30]. Figure 4.2 presents measured REE and LM data from patients with metabolic disorders alongside the healthy volunteer data, demonstrating significant differences between health and the disorder states with the exception of RTHα. After adjusting measured REE by measured lean mass alone, removes the significant difference between the LD patients and the control group but reinstates a significant difference in the RTHα group.

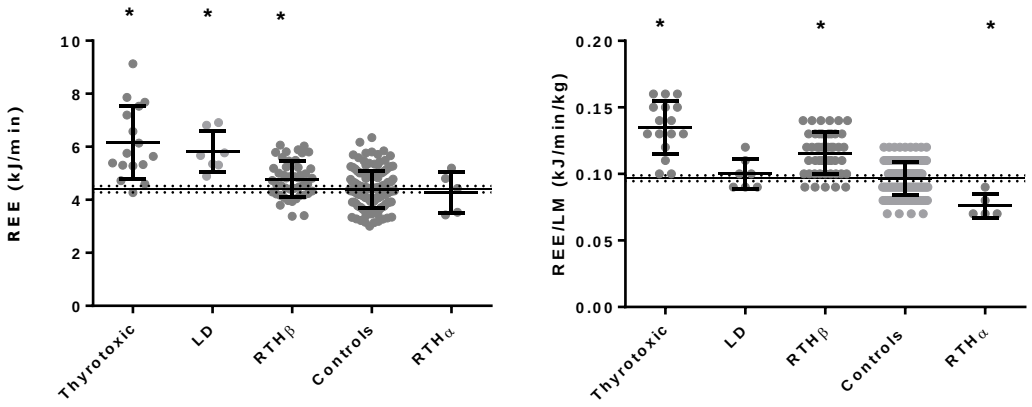

Figure 4.2. Differences in measured REE between metabolic disorders and the healthy cohort and after adjusting REE by LM. * = P < 0.05.

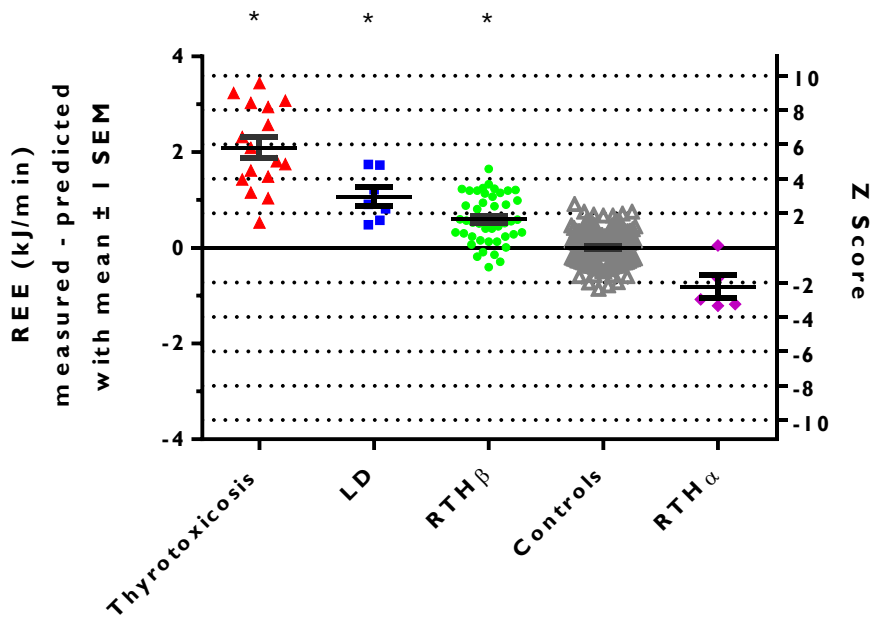

presents the differences in REE between metabolic disorders and healthy controls, taking into account fat, FFM and age in the prediction of REE. Residuals of measured – predicted REE were plotted with corresponding Z scores. RTHβ, LD and thyrotoxic metabolic disease groups manifest significantly elevated REE (mean Z RTHβ: 1.77, LD: 2.97), compared to controls, with the thyrotoxicosis group having the highest REE values with a mean Z score of 5.8 and a range from 1.5 – 9.6. RTHα on the other hand demonstrated low REE with a mean Z score of -2.25 which was not significantly different from controls.

4.4.5.2. Lean Mass

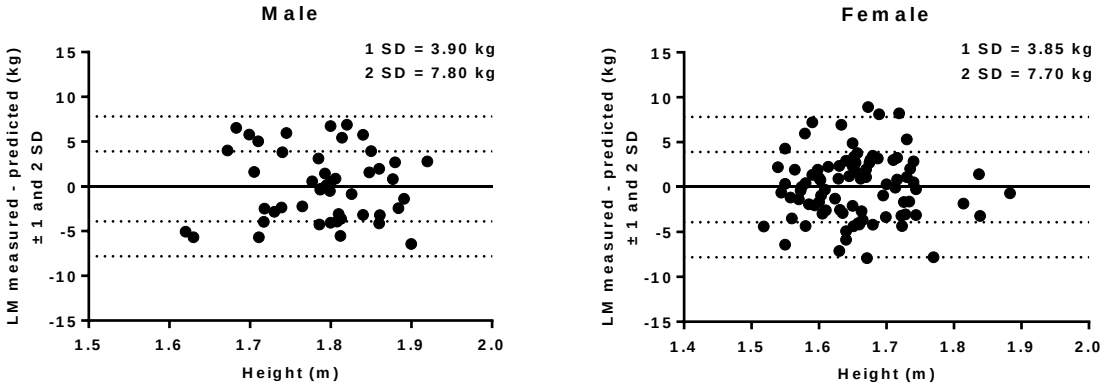

Figure 4.3. Measured and predicted LM in males and females as measured by DXA presented with 1 and 2 SD.

Figure 4.3 shows the variability in LM within the metabolically healthy males and females demonstrated by presenting the residuals of the difference between measured and predicted LM together with Z-scores. Height was used to separate the points.

Figure 4.4 illustrates the difference in measured LM measurements between metabolic disorders and healthy controls and after adjustment by height^2. After adjustment for height^2 alone the RTHβ was no longer significantly different from the healthy controls, however significant differences remain between other metabolic cohorts, specifically LD and RTHα, and the healthy controls.

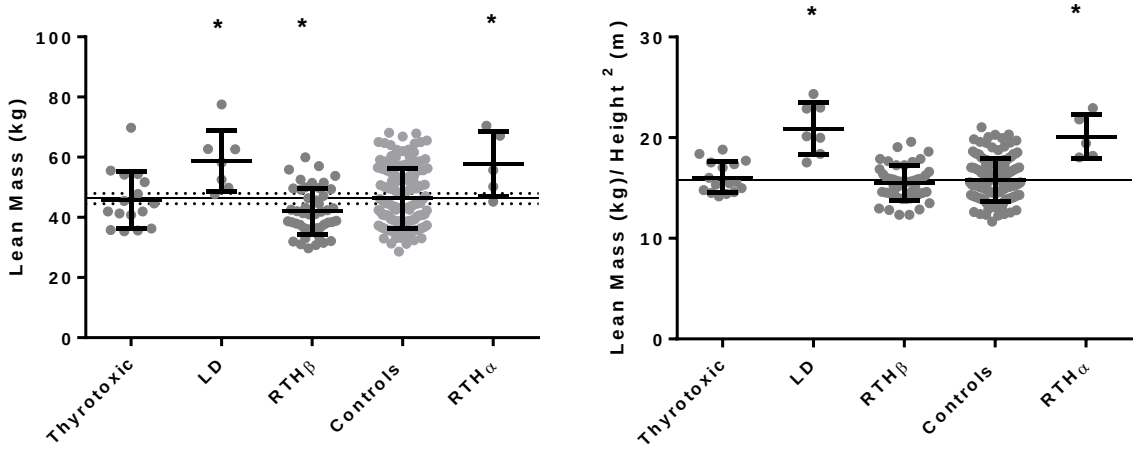

Figure 4.4. Difference in measured lean mass and after adjustment by height^2 between metabolic disorders and healthy controls. * = P < 0.05.

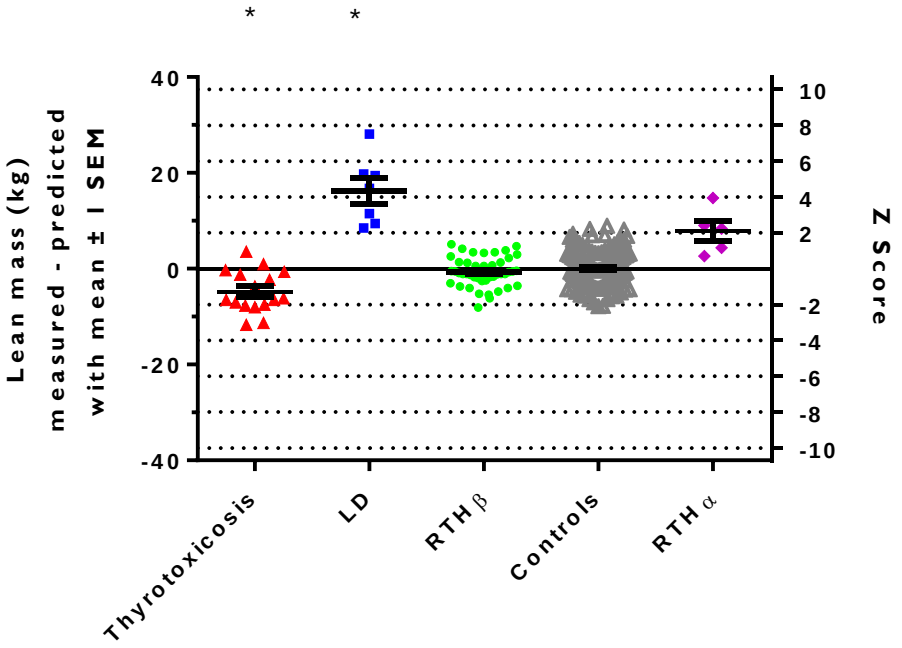

Figure 4.5. Differences between measured and predicted LM (residuals) in metabolic disorders and the healthy cohort with corresponding Z scores. * = P < 0.05.

Figure 4.5 demonstrates the differences between measured and predicted LM, taking into account height^2 and bone mass in males and height^2 and fat mass in the females, compared to the healthy cohort (mean Z Thyrotoxic: -1.23, RTHα: 2.10 and RTHβ: -0.17). The

Thyrotoxic and Lipodystrophy demonstrated significantly different results from the controls, whereas the RTH groups did not. The lipodystrophy data (mean Z: 4.20) illustrates the substantial excess of lean tissue present in this disorder even after adjustment for height and body composition differences.

LM and REE Z-scores may be plotted orthogonally, where they combine to offer a succinct insight into the phenotypes of metabolic disorders.

Figure 4.7 illustrates the relationship between changes in REE and LM in metabolic disorders compared to the healthy group. The lipodystrophic group are characterised by elevated LM and elevated REE with Z scores ranging from 2.2 - 7.3 Z for LM and 1.4 – 4.8 Z for REE. The thyrotoxicosis group also manifest elevated REE (1.5 – 9.6 Z) but, in contrast to the lipodystrophy group, have reduced LM (mean Z = -1.2). RTHα is characterised by low REE (mean Z, -2.3) and high lean mass (mean Z, 2.1), in contrast to the RTHβ cohort with elevated REE and slightly reduced lean mass (mean REE Z = 1.77 and -0.17 for LM).

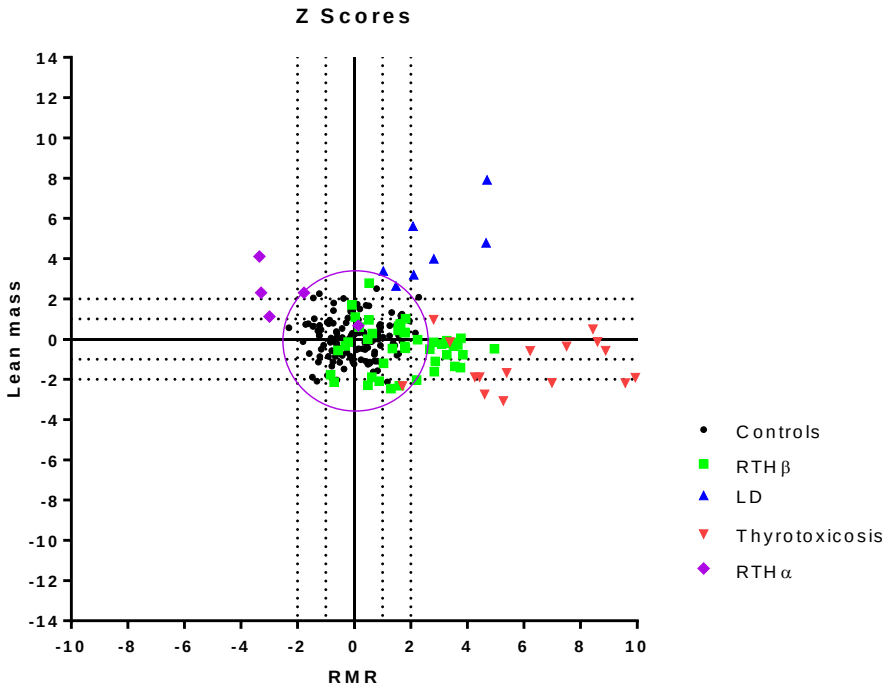

Figure 4.6. Combination of LM and REE Z Scores to illustrate the contribution to metabolic disorders. The circle indicates a Z score of +/- 2 for REE and LM. REE, resting energy expenditure, LM, lean mass.

Figure 4.8 illustrates REE and LM Z scores throughout treatment of an individual RTHα patient. REE Z score was typically low before treatment (pre) with a Z score of -3.4 (a residual of -1.2 kJ/min) improving through treatment to a Z score of -1.4 (a residual of -0.5 kJ/min) but dropping again at the later stages of treatment to -1.9 (a residual of -0.7 kJ/min, corresponding to a LSC < 0.5 kJ/min). Lean mass Z scores replicate the changes in REE Z scores throughout treatment. Lean mass Z commenced pre-treatment at 3.8 (a residual of 14.7 kg) reducing to 2.1 (a residual of 8.3 kg, corresponding to a LSC > 1.13 kg) with treatment towards the end of visit 6.

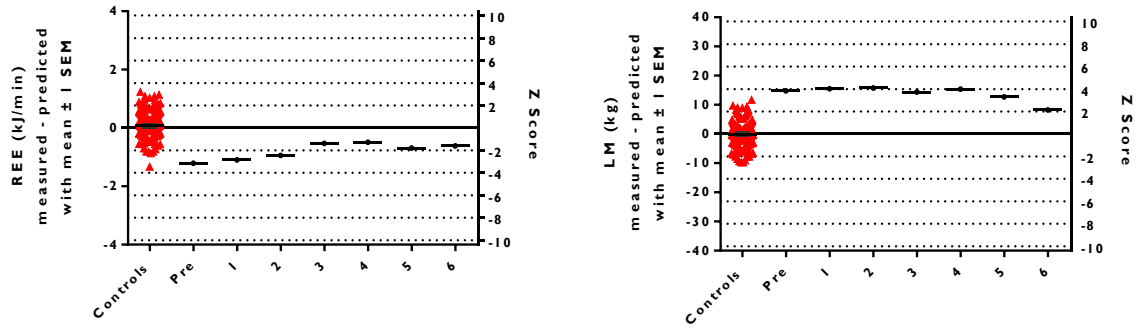

Figure 4.7. Example of the use of the Z score approach to illustrate changes in metabolic parameters in a female RTHα patient at baseline (Pre) and serial visits (1-6) when on thyroxine therapy, in comparison to age and gender-matched controls. REE: 1 Z score = 0.36 kJ/min, LM: 1 Z score = 3.85 kg.

4.5. Discussion

The aim of this work was to develop approaches to describe metabolic phenotypes in terms of the distribution of REE and LM in metabolically healthy people. The novelty of our approach lies in the way in which metabolic and body composition data is represented. Subtracting a predicted value from measured values produces a residual; and dividing this by the standard deviation of residuals in a healthy cohort, we can assign a Z-score. Z-scores are commonly used in the analysis of bone densitometry [31] and on growth charts in order to highlight individuals whose results deviate from the population average [32]. Here, we commend the use of Z scores to highlight individuals and groups of patients with abnormal metabolic rates and/or abnormal LM.

4.5.1. Body composition measurements

The body composition measurements on which this paper relies were undertaken by DXA. This is a widely-available technique which is able to provide quick and well-tolerated estimates of body composition supported by reports of good accuracy and precision [7]. However, it is important consider whether any disorder to which our proposed methodology is applied might generate a bias in the DXA measurements relative to the healthy population. The work of Williams *et al* [33] offers valuable context for this consideration. In the case of our example disorder groups we do not believe bias in DXA estimates to have been a concern. Body composition data in our most extreme phenotype, lipodystrophy, was corroborated by Air Displacement Plethysmography measurements [34].

4.5.2. Resting Energy Expenditure

The results from the REE multiple regression analysis in this study demonstrate a model that predicts REE accurately and with good precision in healthy individuals. The variables which contribute to our predictive equation are FFM, FM and age. These have previously been documented as appropriate covariates [6 35-37]. FFM is recognised as the main predictor of the inter-individual variability in resting energy expenditure. The relationship between FFM and REE differs between men and women when constrained through the origin, as is implicit when REE is expressed per unit FFM. However in preparing this work, we have confirmed that when an intercept is allowed, men and women tend to fall on the same regression line. Moreover, the relationship between REE and FFM is strengthened and therefore allows one regression equation for both genders. There is, however, conflicting

literature regarding the contribution of FM to energy expenditure. In a review, Cunningham [6] suggested that FM contributes to energy expenditure in women, but mostly in obese women. Our study found that FM explained 4.0% of the variance in energy expenditure and when the analysis was broken down by gender there was no significant difference in the variance explained by FM between males and females, even though we had a greater number of females in the cohort. The most commonly used predictive equations for estimating energy expenditure in a clinical setting are Schofield and Henry [3 5]. They include simple measurements such as height and weight, age and gender, regardless of literature that disputes their accuracy and precision, especially when applied to individuals outside the original datasets [38 39]. Weijs, et al. [40] performed a meta-analysis of common REE prediction equations on 48-outpatients and 45-inpatients with conditions including anorexia, overweight, thyroid disease and inflammatory bowel disease, all of which have body compositions and energy expenditures differing from healthy controls [41-45]. They saw errors ranging from 975 to 1782 kJ/d, with at most only 40% of inpatients having an accurately predicted REE when compared to measured REE. Johnstone, et al. [46] demonstrated an average increase in accuracy of 32.9% (240kJ/d) when including body composition (FFM and FM) and anthropometric measurements (skinfold thickness and circumference) compared with the Schofield equation [3].

FFM and FM may explain between 60-85% of the variance in REE [6], leaving at least 15% unaccounted for. Our results demonstrated that FFM and FM combined account for 70%, leaving 30% unexplained. Age, gender, ethnicity and physical activity have been reported to contribute to this variance [36]. In our study we found a significant but small contribution of age to the prediction of REE (2%). Nielsen [35] investigated whether adjusting FFM for extracellular fluid would improve the prediction of REE, but found that this was not the case. Johnstone *et al*, [47] investigated the influence of FFM, FM, age, thyroxine (T4), triiodothyronine (T3) and leptin levels on REE. They concluded that REE was not influenced by age, gender, leptin or T3, although in men 25% of the variance was associated with circulating T4 levels.

4.5.3. Lean Mass

Predictions of FFM or LM are less frequently documented. Previous publications predicting LM have used bioelectrical impedance and skin fold thickness with DXA acting as the reference measurement [48]. The variables chosen for the LM prediction equation in the current study were height^2 and FM for the female group and height^2 and bone mass for the male group. The presence of height^2 in the equation reflects the fat and fat free mass index concept [49 50], which recognises a relationship between body composition and in body size and offers the prospect of discrimination between health and individuals with abnormal fat or fat free mass for their size.

4.5.4. Cross-validation

To test our prediction equations we performed an observational analysis of the coefficients from published studies that have also used FM, FFM and age as variables for prediction of REE (Table 4.6).

Table 4.6. Previously published multiple regression coefficients compared with this current equation.

Regression	Intercept	FFM	FM	Age
Cambridge n = 135	1.736	0.054	0.016	-0.010
Nielson (f) n = 153	2.582 (f)	0.047 (f)	0.023 (f)	-0.014 (f)
(m) n = 100	2.076 (m)	0.045(m)	0.023(m)	-0.015 (m)
Horie n =120	1.629	0.041	-	-
Nelson n = 213	-	0.075	0.012	-
Cunningham n =213	1.076	0.063	-	-

Table 4.6 suggests that our coefficients for FFM, FM and age are similar to those previously published [6 35 51-53]. Of this published work, only Nielson's [35] used DXA for composition measurement; Horrie used bio-impedance [52] while Nelson [51] and Cunningham's [6] papers were based on data previously published by others. When applied to the current dataset, the Nielsen equations produced a residual SD of 0.37 compared to

0.36 produced by our equation. In the light of this sparsity of robust comparative data we performed a K-fold cross-validation analysis on REE and LM models to test their reliability. Comparison of means and standard deviations of residuals in these test groups with those of the training groups suggest that the regressions may be applied beyond the training group with some confidence, though we accept that testing in a larger group would increase this confidence. We would encourage readers who would like to apply our approaches to derive and publish prediction regressions from their own reference cohorts until such time as the published coefficients have converged to a closer consensus than we have presented in Table 4.6 – perhaps when published predictions agree to within 1 pooled SD of their residuals.

4.5.5 Application examples

4.5.5.1. Thyroid disorders

Thyroid conditions such as thyrotoxicosis and Resistance to Thyroid Hormone (RTH) result in altered body composition and energy expenditure. Mitchell *et al* [43] showed that REE is raised in RTHβ and markedly elevated in thyrotoxic patients. In both conditions there was a higher fat to lean mass ratio compared with the healthy controls, though the data suggest that in thyroid disorders the dominant abnormality lies in REE rather than body composition. Our results from the lean mass regression equation suggest that the thyrotoxic group have a slightly reduced LM (Z = -1.23), whereas the RTHβ group have normal LM (Z = -0.17) despite the increased REE.

The RTHα patient displayed a contrasting disassociation in body composition and energy expenditure compared to RTHβ and Thyrotoxicosis. The RTHα subject demonstrated lower REE, as described by Moran *et al* [18 54 55] and increased lean mass.

Our results confirm that REE is higher in a cohort of RTHβ participants and lower in RTHα participants compared to healthy controls; however in patients with thyrotoxicosis, the magnitude of elevation in REE is more substantial. In RTHβ, predominant expression of defective TRβ in the hypothalamus and pituitary mediates resistance to hormone action within the pituitary-thyroid feedback axis, resulting in elevated levels of circulating free thyroxine (T4) and triiodothyronine (T3) with normal or increased levels of TSH [17]. Energy expenditure is raised since some peripheral tissues (e.g. myocardium, skeletal muscle) which

express normal TRα, retain sensitivity to elevated levels of TH [43]. In RTHα, defective TRα expressed in the central nervous system, myocardium and skeletal muscle, inhibits the capability of TRα to respond normally to T3. Such refractoriness to TH actions induces a hypothyroid state in these tissues and low REE response, despite the elevated lean mass. In contrast, both beta and alpha receptor-mediated signalling is intact in conventional thyrotoxicosis, with preserved responsiveness of tissues to elevated TH, resulting in much more markedly increased energy expenditure, despite a reduction in lean body mass [56].

4.5.5.2. Lipodystrophy

Lipodystrophic subjects are characterised by an elevated REE and LM [26]. Importantly, this is not simply a result of a relative reduction in fat mass, which is present in all of these patients, but appears to be a true increase in lean mass. Organomegaly and pseudoacromegaly are features of lipodystrophy (particularly the generalised form) [24], so the increased lean mass probably reflects contributions from several tissues. In healthy men organ tissue will have some contribution to the estimation of lean mass although it has a relatively small mass of approximately 4.4 kg whereas skeletal muscle mass (approx. 32 kg in an average male weighing 84.6 kg) [57] is almost certainly the largest contributing tissue. We show a mean residual increase of lean mass of 16 kg (Z score > 4) relative to our healthy cohort suggesting an increase in lean mass over an above that expected through organ contribution.

When measured REE was presented per kg of LM there was no significant difference between REE in lipodystrophics and healthy controls. Savage *et al* [26] also investigated the increase in REE in the lipodystrophic participants and concluded that the increase in lean mass in lipodystrophy patients accounted for their elevated REE. However we have demonstrated through our Z score approach that this picture changes when other variables that influence REE in a healthy cohort, such as fat mass and age are also accounted for in Lipodystrophy. We have found an elevation in REE with a Z score averaging 2 (range 1.4 – 4.8 kJ/min) relative to our healthy controls (Figure 4.3). As our prediction of REE takes into account the influence of measured FFM, our Z-scores for REE and LM are effectively independent. In doing so, it suggests that there may be a component of the elevation in REE in lipodystrophy beyond that which is associated with FFM alone.

As mentioned in the methods, the lipodystrophic participants had REE measured by room calorimetry rather than the ventilated canopy measurement. In the light of this, we investigated the difference between measurements made using the canopy compared to room calorimetry, on a separate cohort. The results indicated a difference of 0.20 kJ/min between the two methods suggesting that even after accounting for this difference in measurement the lipodystrophic participants would still display an REE Z-score greater than 2 (mean Z score = 2.98).

A limitation of the prediction of lean mass in women is that within the prediction equation fat mass contributes towards the explanation of variance in lean mass. It cannot therefore be distinguished whether the difference between measured and predicted lean mass is soley due to high lean mass but rather may also be due to low fat mass. Further investigations into the prediction of lean mass is warranted.

In summary, we offer expressions for REE and LM in health based on FM, FFM, bone mineral content, age and height^2 measurements. Measurements from individuals with uncommon metabolic disorders were examined in the context of data from healthy subjects and differences to be expressed as a Z-score. This facilitates the representation and differentiation of disease phenotypes. This approach may also aid in the characterisation and potentially evaluation of the treatment in such individuals. Further validation of our regressions on a separate cohort of healthy individuals is desirable, but we believe the Z-score approach to metabolic phenotype description will prove valuable and illuminating in these and other metabolic disorders.

Author Contributions

The authors' responsibilities were as follows: LW – conducted research, analysed data and performed statistical analysis, drafted manuscript and held primary responsibility for the final content; PRB – conducted research, statistical analysis, revision of manuscript and important intellectual contributions; CM, NS, CM, LB, DBS – critical revision of the manuscript and important intellectual contributions, KC – critical revision of the manuscript, important intellectual contributions and supervision; and PRM – study concept and design, critical revision of the manuscript, important intellectual contributions, analysis and the interpretation.

4.6. References

1. Savage DB, Semple RK, Clatworthy MR, et al. Complement abnormalities in acquired lipodystrophy revisited. *J Clin Endocrinol Metab* 2009;94(1):10-6.
2. Psota T, Chen KY. Measuring energy expenditure in clinical populations: rewards and challenges. *European journal of clinical nutrition* 2013;67(5):436-42.
3. Schofield WN. Predicting basal metabolic rate, new standards and review of previous work. *Human nutrition Clinical nutrition* 1985;39 Suppl 1:5-41.
4. Harris JA, Benedict FG. A Biometric Study of Human Basal Metabolism. *Proceedings of the National Academy of Sciences of the United States of America* 1918;4(12):370-3.
5. Henry CJ. Basal metabolic rate studies in humans: measurement and development of new equations. *Public Health Nutr* 2005;8(7A):1133-52.
6. Cunningham JJ. Body composition as a determinant of energy expenditure: a synthetic review and a proposed general prediction equation. *The American journal of clinical nutrition* 1991;54(6):963-9.
7. Withers RT, LaForgia J, Pillans RK, et al. Comparisons of two-, three-, and four-compartment models of body composition analysis in men and women. *J Appl Physiol* 1998;85(1):238-45.
8. Cordero-MacIntyre ZR, Peters W, Libanati CR, et al. Reproducibility of DXA in obese women. *Journal of clinical densitometry : the official journal of the International Society for Clinical Densitometry* 2002;5(1):35-44.
9. Genton L, Karsegard VL, Zawadynski S, et al. Comparison of body weight and composition measured by two different dual energy X-ray absorptiometry devices and three acquisition modes in obese women. *Clin Nutr* 2006;25(3):428-37.
10. Arngrimsson S, Evans EM, Saunders MJ, et al. Validation of body composition estimates in male and female distance runners using estimates from a four-component model. *American journal of human biology : the official journal of the Human Biology Council* 2000;12(3):301-14.
11. Chen Z, Wang Z, Lohman T, et al. Dual-energy X-ray absorptiometry is a valid tool for assessing skeletal muscle mass in older women. *The Journal of nutrition* 2007;137(12):2775-80.
12. Deurenberg-Yap M, Schmidt G, van Staveren WA, et al. Body fat measurement among Singaporean Chinese, Malays and Indians: a comparative study using a four-

compartment model and different two-compartment models. *The British journal of nutrition* 2001;85(4):491-8.

13. Goran MI, Toth MJ, Poehlman ET. Assessment of research-based body composition techniques in healthy elderly men and women using the 4-compartment model as a criterion method. *International journal of obesity and related metabolic disorders : journal of the International Association for the Study of Obesity* 1998;22(2):135-42.
14. Van Der Ploeg GE, Withers RT, Laforgia J. Percent body fat via DEXA: comparison with a four-compartment model. *J Appl Physiol* 2003;94(2):499-506.
15. Visser M, Fuerst T, Lang T, et al. Validity of fan-beam dual-energy X-ray absorptiometry for measuring fat-free mass and leg muscle mass. Health, Aging, and Body Composition Study--Dual-Energy X-ray Absorptiometry and Body Composition Working Group. *J Appl Physiol* 1999;87(4):1513-20.
16. Silva AM, Heymsfield SB, Sardinha LB. Assessing body composition in taller or broader individuals using dual-energy X-ray absorptiometry: a systematic review. *European journal of clinical nutrition* 2013
17. Chatterjee VK, Nagaya T, Madison LD, et al. Thyroid hormone resistance syndrome. Inhibition of normal receptor function by mutant thyroid hormone receptors. *The Journal of clinical investigation* 1991;87(6):1977-84.
18. Moran C, Chatterjee K. Resistance to thyroid hormone due to defective thyroid receptor alpha. *Best practice & research Clinical endocrinology & metabolism* 2015;29(4):647-57.
19. Lafranchi SH, Snyder DB, Sesser DE, et al. Follow-up of newborns with elevated screening T4 concentrations. *The Journal of pediatrics* 2003;143(3):296-301.
20. Chiesa A, Olcese MC, Papendieck P, et al. Variable clinical presentation and outcome in pediatric patients with resistance to thyroid hormone (RTH). *Endocrine* 2012;41(1):130-7.
21. Weiss RE, Refetoff S. Resistance to thyroid hormone. *Reviews in endocrine & metabolic disorders* 2000;1(1-2):97-108.
22. Brent GA. Clinical practice. Graves' disease. *The New England journal of medicine* 2008;358(24):2594-605.
23. Weetman AP. Graves' disease. *The New England journal of medicine* 2000;343(17):1236-48.

24. Garg A. Clinical review#: Lipodystrophies: genetic and acquired body fat disorders. *The Journal of clinical endocrinology and metabolism* 2011;96(11):3313-25.
25. Simha V, Garg A. Lipodystrophy: lessons in lipid and energy metabolism. *Current opinion in lipidology* 2006;17(2):162-9.
26. Savage DB, Murgatroyd PR, Chatterjee VK, et al. Energy expenditure and adaptive responses to an acute hypercaloric fat load in humans with lipodystrophy. *The Journal of clinical endocrinology and metabolism* 2005;90(3):1446-52.
27. Westerterp KR. Obesity and physical activity. *International journal of obesity and related metabolic disorders : journal of the International Association for the Study of Obesity* 1999;23 Suppl 1:59-64.
28. Elia M, Livesey G. Energy expenditure and fuel selection in biological systems: the theory and practice of calculations based on indirect calorimetry and tracer methods. *World review of nutrition and dietetics* 1992;70:68-131.
29. Oldroyd B, Smith AH, Truscott JG. Cross-calibration of GE/Lunar pencil and fan-beam dual energy densitometers--bone mineral density and body composition studies. *European journal of clinical nutrition* 2003;57(8):977-87.
30. Chatterjee VKK. Resistance to Thyroid Hormone. *Hormone research* 1997;48(4):43-46.
31. Ellis KJ, Shypailo RJ, Hardin DS, et al. Z score prediction model for assessment of bone mineral content in pediatric diseases. *Journal of bone and mineral research : the official journal of the American Society for Bone and Mineral Research* 2001;16(9):1658-64.
32. Ogden CL, Kuczmarski RJ, Flegal KM, et al. Centers for Disease Control and Prevention 2000 Growth Charts for the United States: Improvements to the 1977 National Center for Health Statistics Version. *Pediatrics* 2002;109(1):45-60.
33. Williams JE, Wells JC, Wilson CM, et al. Evaluation of Lunar Prodigy dual-energy X-ray absorptiometry for assessing body composition in healthy persons and patients by comparison with the criterion 4-component model. *The American journal of clinical nutrition* 2006;83(5):1047-54.
34. Fields DA, Goran MI, McCrory MA. Body-composition assessment via air-displacement plethysmography in adults and children: a review. *The American journal of clinical nutrition* 2002;75(3):453-67.

35. Nielsen S, Hensrud DD, Romanski S, et al. Body composition and resting energy expenditure in humans: role of fat, fat-free mass and extracellular fluid. *International journal of obesity and related metabolic disorders : journal of the International Association for the Study of Obesity* 2000;24(9):1153-7.
36. Ravussin E, Bogardus C. Relationship of genetics, age, and physical fitness to daily energy expenditure and fuel utilization. *The American journal of clinical nutrition* 1989;49(5 Suppl):968-75.
37. Hunter GR, Weinsier RL, Gower BA, et al. Age-related decrease in resting energy expenditure in sedentary white women: effects of regional differences in lean and fat mass. *The American journal of clinical nutrition* 2001;73(2):333-7.
38. Horgan GW, Stubbs J. Predicting basal metabolic rate in the obese is difficult. *European journal of clinical nutrition* 2003;57(2):335-40.
39. Scalfi L, Marra M, De Filippo E, et al. The prediction of basal metabolic rate in female patients with anorexia nervosa. *International journal of obesity and related metabolic disorders : journal of the International Association for the Study of Obesity* 2001;25(3):359-64.
40. Weijs PJ, Kruizenga HM, van Dijk AE, et al. Validation of predictive equations for resting energy expenditure in adult outpatients and inpatients. *Clin Nutr* 2008;27(1):150-7.
41. El Ghoch M, Alberti M, Capelli C, et al. Resting Energy Expenditure in Anorexia Nervosa: Measured versus Estimated. *Journal of nutrition and metabolism* 2012;2012:652932.
42. Sasaki M, Johtatsu T, Kurihara M, et al. Energy expenditure in Japanese patients with severe or moderate ulcerative colitis. *Journal of clinical biochemistry and nutrition* 2010;47(1):32-6.
43. Mitchell CS, Savage DB, Dufour S, et al. Resistance to thyroid hormone is associated with raised energy expenditure, muscle mitochondrial uncoupling, and hyperphagia. *J Clin Invest* 2010;120(4):1345-54.
44. Herwig A, Ross AW, Nilaweera KN, et al. Hypothalamic thyroid hormone in energy balance regulation. *Obesity facts* 2008;1(2):71-9.
45. Ahmad A, Duerksen DR, Munroe S, et al. An evaluation of resting energy expenditure in hospitalized, severely underweight patients. *Nutrition* 1999;15(5):384-8.

46. Johnstone AM, Rance KA, Murison SD, et al. Additional anthropometric measures may improve the predictability of basal metabolic rate in adult subjects. *European journal of clinical nutrition* 2006;60(12):1437-44.

47. Johnstone AM, Murison SD, Duncan JS, et al. Factors influencing variation in basal metabolic rate include fat-free mass, fat mass, age, and circulating thyroxine but not sex, circulating leptin, or triiodothyronine. *The American journal of clinical nutrition* 2005;82(5):941-8.

48. Stewart AD, Hannan WJ. Prediction of fat and fat-free mass in male athletes using dual X-ray absorptiometry as the reference method. *Journal of sports sciences* 2000;18(4):263-74.

49. Dulloo AG, Jacquet J, Solinas G, et al. Body composition phenotypes in pathways to obesity and the metabolic syndrome. *Int J Obes (Lond)* 2010;34 Suppl 2:S4-17.

50. VanItallie TB, Yang MU, Heymsfield SB, et al. Height-normalized indices of the body's fat-free mass and fat mass: potentially useful indicators of nutritional status. *The American journal of clinical nutrition* 1990;52(6):953-9.

51. Nelson KM, Weinsier RL, Long CL, et al. Prediction of resting energy expenditure from fat-free mass and fat mass. *The American journal of clinical nutrition* 1992;56(5):848-56.

52. Horie LM, Gonzalez MC, Torrinhas RS, et al. New specific equation to estimate resting energy expenditure in severely obese patients. *Obesity (Silver Spring)* 2011;19(5):1090-4.

53. Cunningham JJ. A reanalysis of the factors influencing basal metabolic rate in normal adults. *The American journal of clinical nutrition* 1980;33(11):2372-4.

54. Moran C, Chatterjee K. Resistance to Thyroid Hormone alpha-Emerging Definition of a Disorder of Thyroid Hormone Action. *The Journal of clinical endocrinology and metabolism* 2016;101(7):2636-9.

55. Moran C, Schoenmakers N, Agostini M, et al. An adult female with resistance to thyroid hormone mediated by defective thyroid hormone receptor alpha. *The Journal of clinical endocrinology and metabolism* 2013;98(11):4254-61.

56. Acotto CG, Niepomniszcze H, Mautalen CA. Estimating body fat and lean tissue distribution in hyperthyroidism by dual-energy X-ray absorptiometry. *Journal of clinical densitometry : the official journal of the International Society for Clinical Densitometry* 2002;5(3):305-11.

57. Muller MJ, Langemann D, Gehrke I, et al. Effect of constitution on mass of individual organs and their association with metabolic rate in humans--a detailed view on allometric scaling. *PloS one* 2011;6(7):e22732.

5. An approach to quantifying abnormalities in energy expenditure in paediatric metabolic disease.

5.1. Abstract

Background. The objective of this study was to develop an approach to describing and predicting resting energy expenditure (REE) in a healthy paediatric population in terms of body composition. The predictions were then applied to paediatric Thyroid Hormone (TH) disease patients to explore departures of measured REE from expectations.

Methods. Body composition was measured by dual energy X-ray absorptiometry and REE was assessed by indirect calorimetry in 107 female and 94 male healthy children and adolescents. Prediction equations for REE were derived from the body composition measurements by multiple linear regression. Individual Z scores were calculated as the difference between measured and predicted REE divided by the standard deviation of the regression residuals between measured and predicted REE. The clinical application was demonstrated in Resistance to Thyroid Hormone due to mutations in either thyroid hormone receptor β or α (β female n= 17, male n= 8, α female n=1, male n=1) in which their deviation of REE from the healthy population is expressed as a Z score.

Results. Prediction equations were derived based on the total cohort; LnREE (kJ/min) = 0.006 * Fat mass (kg) + 0.012 * Lean mass (kg) – 0.069 * gender (m = 0, f = 1) + 1.006 (R^2 = 0.754, SD = 0.38 kJ/min), male LnREE = 0.009 * Fat mass (kg) + 0.012 * Lean mass (kg) + 0.991 (R^2 = 0.800, SD of residuals = 0.38 kJ/min), female LnREE = 0.015 * Lean mass (kg) + 0.931 (R^2 = 0.638, SD = 0.38 kJ/min). Average REE Z scores based on exponentiated deltas were for male RTHβ = -0.15 ± 0.84 and female RTHβ = 0.15 ± 1.42. In RTHα, male Z = -0.82 and female Z = -2.16.

Conclusion. This approach describes the differences between individual patients or groups of patients with metabolic disorders to be quantified against a healthy cohort by the simplicity of a Z score. This has the potential to facilitate clinical findings throughout a treatment process.

5.2. Introduction

Predicting resting energy expenditure (REE) has become a more efficient method of assessing nutritional requirements for participants or patients without access to the expertise and facilities to accurately measure it. The most common published equations used in a paediatric setting are Schofield *et al* [1], Henry [2], Harris and Benedict [3] and Molnar *et al* [4]. These equations are based on characteristics such as age, gender, height and weight and are derived from large, often pooled, diverse cohorts [5 6]. As children grow, the proportions of fat and lean mass do not increase at the same rate due to the variability in body composition by age, pubertal and gender [7] and therefore the use of mass as a whole when predicting REE in children may not result in the most accurate predictions of REE. Many studies have reported on the inaccuracies of current REE prediction equations based on traditional height and weight measurements across a variety of ages, ethnicities and disease populations [8-12]. The most recent published equations based on body composition measurements relevant to healthy child age ranges include Muller *et al* (2004) [5] which consists of coefficients from fat-free mass (FFM), fat mass and gender and explains 72% of the variance. However, the population is based on data pooled from separate German databases collected over a period of 18 years and may not be appropriate for other geographical populations or disease groups.

REE accounts for around 65 -75% of total daily energy expenditure in most sedentary individuals and in adults REE is mostly dependent on the amount of fat-free mass or lean mass within the body [13]. In the past there have been discrepancies in estimate of the contribution of other variables such as fat mass, gender and age on REE [14]. However, recent publications support the concept that fat mass does make a contribution to REE, albeit smaller than lean mass [15 16].

In children, the amount of fat, lean and organ mass increase with growth and puberty however the timing of growth and puberty differs substantially within age groups [17]. For this reason, puberty should be adequately controlled for when investigating body composition in pre and pubertal children, however this does not come without difficulty. Assessing the onset of puberty in children has its own limitations. None of the usual methods used to acquire such information can accurately pinpoint the onset of puberty and therefore it is often estimated or general age ranges are used.

Puberty is controlled by the hypothalamic pituitary gonadal axis (HPG). During childhood gonadotropin-releasing hormone (GnRH) secretion, released from the

hypothalamus, is supressed to low concentrations. At the onset of puberty Gonadotropin-releasing hormone (GnRH) secretion is enhanced and released in a pulsatile manner which signals the secretion of luteinising hormone (LH) and follicle-stimulating hormone (FSH) from the pituitary. The secretion of LH and FSH act on the gonads to promote the production of sex steroids and the development of secondary sex characteristics and menstruation in females [18 19].

Typically in girls puberty usually occurs between the ages of 8-12 y and in boys between 9-14y. The first physical sign of puberty in girls is thelarche or age of menarche in girls and testicular development in boys, which are often self-reported using validated questionnaires [20 21] or by physical assessment by paediatricians. However, the accuracy of self-reported techniques are inconclusive [22-24] and physical examination may not be appropriate for research in healthy individuals. Therefore, assessing the biochemical markers of puberty such as LH and FSH may provide sufficient information of pubertal status without the inaccuracies and invasiveness of the alternative methods.

Metabolic disorders are often associated with altered body composition [15]. In adults, metabolic conditions such as thyrotoxicosis, Resistance to Thyroid Hormone (RTH) and lipodystrophy (LD) have previously been shown to differ in both body composition and energy expenditure [15], [25-28], compared to healthy controls (Chapter 4). In children, these conditions are rarely identified, mainly due to lack of early diagnosis.

RTHβ is a genetic disorder due to the mutations in the thyroid hormone receptor β gene, caused by reduced tissue responsiveness to thyroid hormone and its clinical markers are typically elevated serum free TH levels with non-supressed TSH levels (Ferrera 2012). The characteristics of RTHβ are highly heterogeneous with the majority of individuals being asymptomatic in a compensated euthyroid state. Others may demonstrate hyperthyroid symptoms including hyperactivity, weight loss and tachycardia. The large unpredictability of the manifestations makes management of the disorder in childhood difficult [29].

TRα mutations causing RTHα are rare, with 19 patients from 14 families having been reported worldwide, 7 of which were children. The symptoms of RTHα are generally more severe due to a hypothyroid state in TRα expressing tissues. Characteristics include development delay throughout infancy and childhood, learning disabilities and growth retardation [30 31], typical features of uncorrected childhood hypothyroidism.

Once diagnosed, thyroxine therapy can alleviate some of the symptoms and promote normal growth and development in RTHα. Conversely, in RTHβ, treatment with triiodothyroacetic acid (TRIAC)m a TH analogue which acts centrally to reduce hormone levels but is relatively devoid of thyromimetic effects in peripheral tissues, is used to lower heart rate and promote weight gain. Biochemical changes are monitored frequently throughout treatment, however, monitoring whole body consequences of the treatment, in relation to body composition and energy expenditure, in RTH children compared to healthy controls, has not yet been explored.

The aim of this research is to firstly predict energy expenditure in healthy children aged 6-16 years. By adjusting energy expenditure measurements by body composition the second aim is to describe healthy and disordered energy expenditure by the application of a Z score by applying the healthy prediction equations to a cohort of RTH patients.

5.3. Methods

5.3.1. Participants

Two hundred and one healthy male and female children aged between 6 and 16years old (107 females, mean age 11.2 ± 3.0; n = 27 age 6-8, n = 37 age 9-11, n = 29 age 12-14 and n = 14 age 15-16, and 94 males, mean age 12.1 ± 3.2; n = 18 age 6-8, n = 29 age 9-11, n = 22 age 12-14 and n = 25 age 15-16), free from disease and medications took part in the study. After reading the relevant information leaflets and having the study fully explained the children then assented and parents consented to taking part in the study. The children were recruited locally through advertisements and radio and approval was granted by the Cambridge South ethics committee.

5.3.2. Body composition

On arrival and after the consent process, the children underwent some basic observations consisting of blood pressure, temperature and ECG to screen them for any initial abnormalities. Height was measured on a stadiometer and recorded to the nearest millimetre (SECA electronic stadiometer) and weight was measured on electronic scales to the nearest gram (Kern & Sohn GmbH, Germany).

The participants also a whole body dual energy X-ray absorptiometry (DXA) assessment for bone density and body composition (fat mass and lean mass) (GE Lunar Prodigy and iDXA, analysed in version 16, enhanced mode).

During the early phase of the study, the DXA machine at the facility where the measurements were performed underwent an instrument upgrade resulting in seventeen children having DXA scans using an older DXA instrument, the GE Lunar Prodigy. The rest of the cohort had measurements performed on a newer GE Lunar iDXA. To combine the data from the Lunar Prodigy with the iDXA data, 71 participants of the original 201 cohort and 24 participants of a separate study underwent repeated whole-body bone and soft tissue composition measurement on each instrument. Cross-calibration equations were derived and applied to the Prodigy data. All data was analysed using Encore software version 16 in enhanced analysis mode. The additional twenty-four children were consented under a second paediatric study (NRES, 13/EE/0233).

5.3.3. Energy Expenditure

The participants stayed overnight at the clinical research facility (CRF), Cambridge. They were fed an energy balanced meal based on the Schofield predictions for energy intake at their usual dinner time. Usual bedtimes and waking times were also discussed for each participant and adhered to.

Resting energy expenditure (REE) was measured by indirect calorimetry using a ventilated hood 30 min after waking. The participants were asked to remain still and awake with no interactions for 40 min. The calorimeter was calibrated prior to the measurement using 1% CO_2 and 78.1% nitrogen. Gas measurements of the room were measured for the first 10 min as this will be different from the calibration concentrations, then the ventilated hood measurement of the participant followed for 20min with a further 10 min of room gas analysis at the end of the measurement to account for any offsets. The gas measurements were then converted into energy equivalents using calculations by Elia and Livesey [32].

5.3.4. Pubertal assessment

For females the onset of menstruation was recorded if applicable. Immediately following the morning REE measurement the participants gave a blood sample for various metabolic biomarkers, including Luteinising Hormone (LH) and Follicle Stimulating Hormone (FSH), a precursor of the gonadArche stage of the pubertal process.

5.3.5. Statistical analysis

To begin with the cross-calibration equations were derived so that converted body composition data could be used in the REE regression analysis. The differences between Prodigy and iDXA instruments were determined by paired t test and Bland-Altman plots were used to determine the agreement between the instruments. Linear regression was then performed to derive equations for converting Prodigy data to iDXA data for the variables that displayed a significant difference. The level of significance was determined at $P < 0.05$.

Spearmans correlation determined which variables were significantly related to each other and REE. Appropriate variables were then added to a stepwise multiple regression analysis to establish how variables contributed towards the prediction of REE. Preliminary descriptive investigations into the relationship of REE and the other variables demonstrated a skewness in variability with increasing mass and for this reason REE was logged prior to entering the regression models and then anti-logged before undergoing Bland-Altman

analysis. The difference between measured and predicted REE is described as the residual. When an individual residual is divided by the standard deviation of all the gender-specific residuals this represents a cohort Z score. SPSS statistical software (version 22) was used for descriptive statistics, correlations and regression analysis. GraphPad Prism Version 6 was used to generate figures and Bland-Altman analyses.

5.4. Results

5.4.1. Cross-calibration of DXA data

Descriptive statistics of the 95 participants involved in the cross-calibration of the Prodigy data to iDXA data are presented in table 5.1.

Table 5.1 Descriptive statistics of the iDXA-Prodigy cross-calibration analysis

	Females (n= 50)		**Males (n = 45)**	
N = 95 (F=50, M=45)	**Mean ± SD (median)**	**Range**	**Mean ± SD (median)**	**Range**
Age (years)	10.1 ± 2.6 (10.0)	6.0 – 16.0	10.8 ± 2.8 (9.0)	6.0 – 16.0
Height (m)	1.44 ± 15.7	1.15 – 1.77	1.49 ± 19.0	1.02 – 1.87
Mass (DXA, kg)	37.9 ± 12.2	23.8 – 61.5	40.1 ± 15.1	16.2 – 79.9
BMI (kg/m^2)	17.6 ± 2.6	13.8 – 24.7	17.4 ± 3.0	14.0 – 29.1
Fat mass (DXA, kg)	10.5 ± 4.7	4.6 – 23.9	8.9 ± 4.5	2.6 – 26.9

DXA, dual energy X-ray Absorptiometry, BMI; body mass index.

Table 5.2 presents the differences between iDXA and Prodigy whole-body measurements. All the variables were significantly correlated. However there were significant differences between all variables measured on iDXA and Prodigy with the exception of whole-body bone mineral content (BMC) (mean difference -0.01 ± 0.03, P = 0.07).

Table 5.2. Differences between iDXA and Prodigy whole-body bone and soft tissue measurements.

	iDXA	Prodigy	Difference	Sig
BMC (kg)	1.50 ± 0.60	1.51 ± 0.59	-0.01 ± 0.03	0.067
BA cm^2	1.66 ± 0.35	1.64 ± 0.34	0.03 ± 0.04*	0.000
BMD (g/cm^2)	0.88 ± 0.16	0.89 ± 0.16	-0.02 ± 0.02*	0.000
Fat mass (kg)	9.7± 4.7	10.4 ± 4.7	-0.65 ± 0.48*	0.000
Lean mass (kg)	27.7 ± 9.8	26.7 ± 9.6	0.94 ± 0.50*	0.000
Total mass (kg)	38.9 ± 13.6	38.6 ± 13.5	0.29 ± 0.34*	0.000

Bone mineral content; BMC, bone area; BA, bone mineral density; BMD, *P < 0.05

With this in mind, it was therefore appropriate to develop cross-calibration equations to translate the Prodigy DXA measurements to iDXA estimates. Cross-calibration equations are presented in Table 5.3.

Table 5.3. Cross-calibration equations for the translation of Prodigy measurements to iDXA measurements.

	Slope	CI	Intercept	CI
Prodigy BMC (kg)	1.01	1.00 – 1.02	-0.02	-0.04 - -0.01
Prodigy BA (cm^2)	1.03	1.00 – 1.06	-0.02	-0.07 – 0.02
Prodigy BMD (g/cm^2)	1.00	0.97 – 1.02	-0.01	-0.04 – 0.01
Prodigy Fat (kg)	0.98	0.96 – 1.00	-0.43	-0.66 - -0.20
Prodigy Lean (kg)	1.02	1.01 – 1.03	0.34	0.06 – 0.61
Prodigy Total mass (kg)	1.01	1.00 – 1.01	0.10	-0.10 – 0.31

Bone mineral content; BMC, bone area; BA, bone mineral density; BMD

5.4.2. Description of REE in healthy children by regression analysis.

Descriptive statistics for the regression cohort are presented in Table 5.4. There were significant differences between the genders in height, age, DXA fat, lean and bone, and REE but not in weight (equal variances not assumed).

Table 5.4. Descriptive statistics for 201 children included in the multiple regression analysis for the prediction of REE.

	Females n = 107		Males n = 94	
	Mean ± SD	Range	Mean ± SD	Range
Height (m)	1.47 ± 0.17	1.11 – 1.77	1.54 ± 0.20	1.12 – 1.88
Weight (kg)	41.3 ± 13.7	18.2 – 84.4	45.5 ± 15.7	20.0 – 78.6
BMI (kg/m^2)	18.6 ± 3.1	9.9 – 29.2	18.5 ± 2.7	13.9 – 29.1
Age (years)	11.2 ± 3.0	6.2 – 16.97	12.1 ± 3.2	6.1 – 17.01
DXA Fat mass (kg)	12.3 ± 5.6	4.3 – 32.7	10.3 ± 4.4	3.3 – 26.9
DXA Lean mass (kg)	27.8 ± 8.8	13.0 – 49.3	33.6 ± 12.7	16.1 – 62.4
DXA Bone mass (kg)	1.55 ± 0.54	0.70 – 2.95	1.81 ± 0.72	0.81 – 3.43
REE (kJ/min)	3.91 ± 0.63	2.43 – 5.38	4.49 ± 0.87	2.97 – 6.96

BMI; body mass index, REE; resting energy expenditure, ± SD; standard deviation, DXA; dual energy X-ray absorptiometry.

Correlation analysis demonstrated that all of the chosen variables were significantly correlated to REE (Table 5.5). Weight, DXA mass and BMI were excluded from the analysis as they were considered duplicates of other variables such as height, bone, fat and lean mass. Table 5.5 illustrates the variables to be inserted into the regression model.

Table 5.5. Correlation coefficients and significance of REE with potential contributing variables

	Height (m)	Age (years)	DXA mass (kg)	Bone mass (kg)	Fat mass (kg)	Lean mass (kg)	FFM (kg)
REE kJ/min	0.824	0.736	0.844	0.830	0.511	0.866	0.865
Sig	0.000	0.000	0.000	0.000	0.000	0.000	0.000

Correlation coefficient; R, $P < 0.05$, REE; resting energy expenditure, DXA; dual energy X-ray absorptiometry, FFM; fat-free mass.

The first step was to investigate the variables that contribute towards the prediction of REE in the entire dataset. Figure 5.1 supports this notion by demonstrating a similar relationship between REE and LM in males and females.

To present the skewed data so that is appears normally distributed, REE values were logged prior to entering all the regression models. The variables in Table 5.5 were entered into a stepwise multiple regression model. This resulted in three models of significant variables; lean mass, lean mass and gender and lean mass, gender and fat mass (Table 5.6).

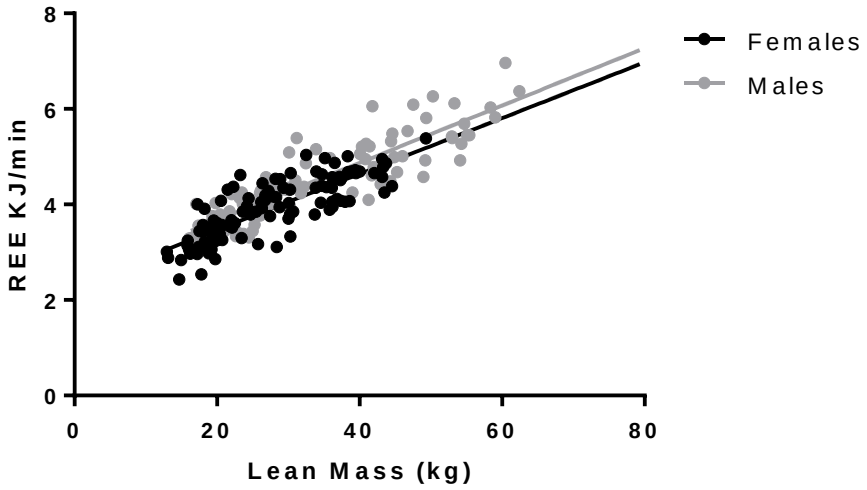

Figure 5.1. Comparison of male and female lean mass linear regression with REE. Linear regression lines have been extended for visualisation purposes.

Lean and fat mass were entered into the regression model without gender, out of curiosity, (model 2) and the same was done for total mass (model 3).

Table 5.6. Regression coefficients for the prediction of REE in 201 male (male = 0) and female (female = 1) healthy controls.

Model	Variables	LnSlope ± SE	95% CI	R^2
Model 1	Lean mass (kg)	0.012 ± 0.001	0.011 – 0.014	0.754
	Gender (kg)	-0.069 ± 0.015	-0.098 – -0.040	
	Fat mass (kg)	0.006 ± 0.002	0.003 – 0.009	
	Intercept (kJ/min)	1.006 ± 0.023	0.961 – 1.052	
Model 2	Lean mass (kg)	0.014 ± 0.001	0.012 – 0.015	0.728
	Fat mass (kg)	0.003 ± 0.002	0.000 – 0.006	
	Intercept	0.957 ± 0.022	0.915 – 1.000	
Model 3	Total mass (kg)	0.011 ± 0.000	0.010 – 0.012	0.693
	Intercept	0.953 ± 0.023	0.907 – 0.998	

Ln, loge, SE, standard error, CI, confident intervals, R^2 adjusted R^2 representing the fit of the model.

Gender presented as the second highest significant coefficient, following lean mass, in model 1 of the stepwise regression (Table 5.6). This justifies exploring the analysis separately by gender. Age did not significantly contribute towards the prediction of REE and was therefore excluded by stepwise regression. Figure 5.2 illustrates gender based differences between body composition variables, fat and lean mass.

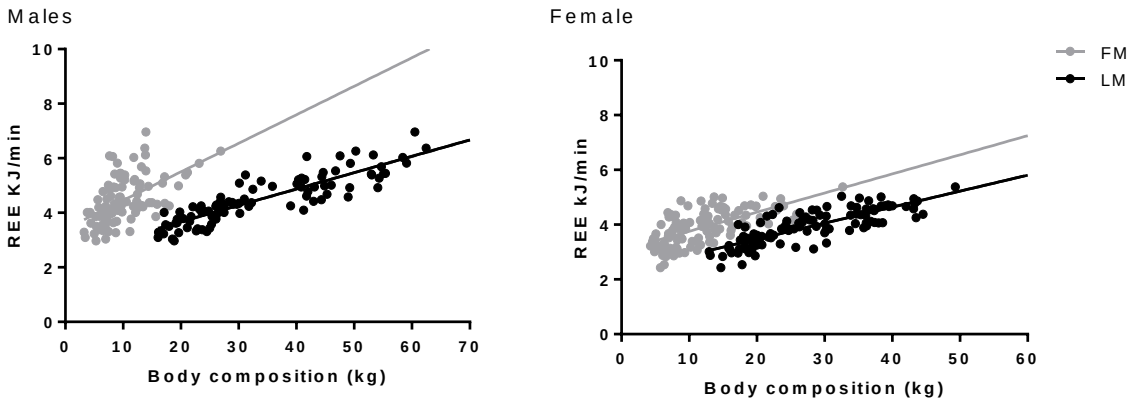

Figure 5.2. Illustration of the relationship fat and lean mass present with resting energy expenditure in males and females. Linear regression lines have been extended for visualisation purposes.

Stepwise multiple regression for the female group demonstrated that only lean mass remained a contributing variables towards the prediction of REE (model 4, Table 5.7). For the males DXA mass explained the most amount of variance in REE (model 7), however, as demonstrated in Figure 5.2, the fat and lean components of body mass demonstrate different relationships with REE between the genders and therefore lean, fat and bone mass contributions were explored separately, excluding DXA mass from the analysis. The resulting regression analysis for the males produced two models, model 8 containing only DXA lean mass and model 9 containing both DXA lean and fat mass. Out of interest, fat and lean mass were entered into the female regression (model 5) and DXA mass was entered (model 6), however, it made little difference to the regression output. As with the genders combined, age was removed during stepwise regression as its contribution remained insignificant.

Table 5.7. Stepwise regression coefficients for the prediction of REE in females and males.

	Model	Variable	LnSlope ± SE	LnIntercept ± SE	R^2
Females	4	Lean mass	0.015 ± 0.001	0.931 ± 0.032	0.638
	5	Lean mass	0.014 ± 0.002	0.932 ± 0.032	0.639
		Fat mass	0.003 ± 0.002		
	6	DXA mass	0.009 ± 0.001	0.961 ± 0.032	0.611
Males	7	DXA mass	0.011 ± 0.001	0.988 ± 0.027	0.801
	8	Lean mass	0.013 ± 0.001	1.041 ± 0.027	0.764
	9	Lean mass	0.012 ± 0.001	0.991 ± 0.028	0.800
		Fat mass	0.009 ± 0.002		

Ln, loge, SE, standard error, R^2 adjusted R^2 representing the fit of the model, DXA, dual energy X-ray absorptiometry.

5.4.3. Prediction of REE in healthy children

The coefficients of the variables from model 1 in Table 5.6 were applied to the whole dataset. The resulting predictions were then exponentiated and the difference between measured and predicted REE, residuals, were calculated as 0.06 kJ/min and the standard deviation of that difference was 0.38 kJ/min (Z score).

The regression coefficients from models 4 and 9 were then applied separately to the male and female datasets as gender was found to be a significant contributor to the prediction of REE. The predictions were also exponentiated and the difference between measured and predicted REE was calculated. For the males the mean and standard deviation of the residuals was 0.00 and 0.38 kJ/min. For the females, the mean and standard deviation of the residuals were 0.04 and 0.38 kJ/min. The range of Z scores for females were -2.04 to 2.70 and males were -2.28 to 3.34. Atypical Z scores in this cohort can therefore be defined as greater than -2.0 and 2.0.

The variations between the measured REE and the predicted models in the whole dataset and separately by gender are presented by Bland-Altman plots in Figure 5.3. For all the models, the prediction of REE was significantly correlated to measured REE (combined R; 0.873, males; 0.910 and females, 0.822).

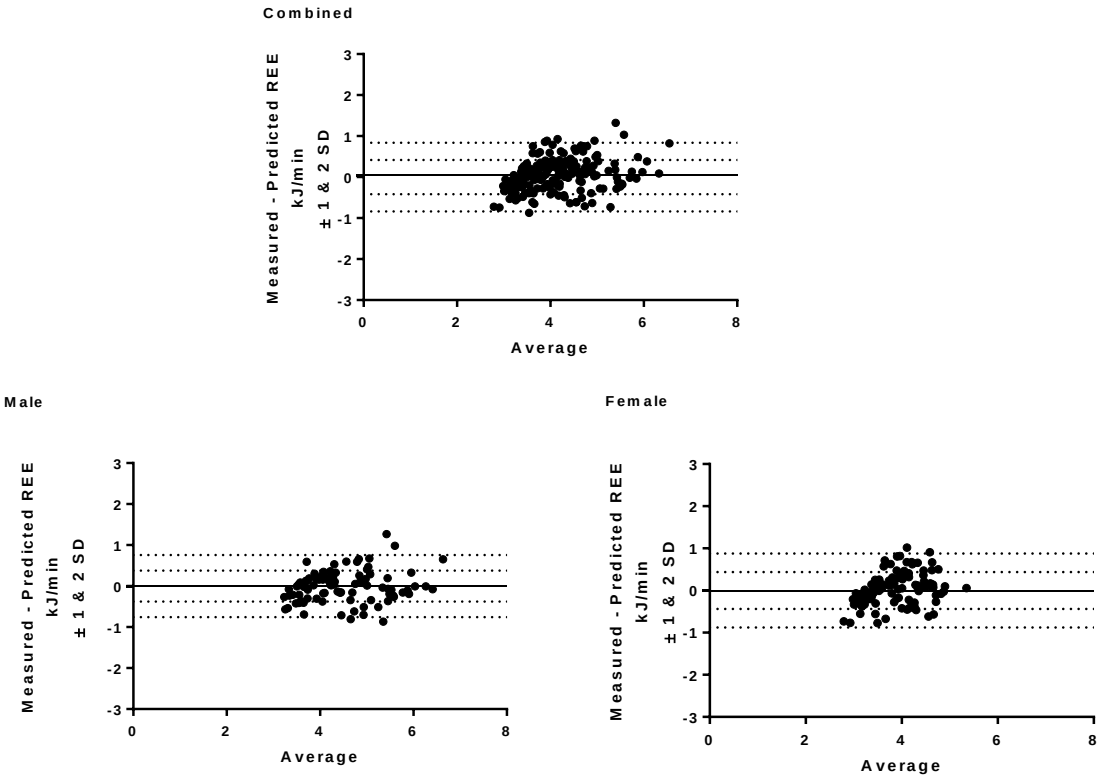

Figure 5.3. The variation between measured and predicted REE based on reversed lnREE models derived on the entire dataset, the males or females only.

5.4.4. Pubertal contributions

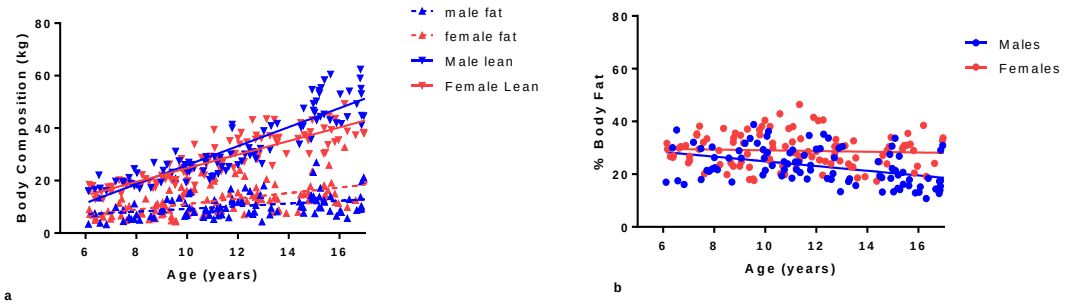

Figure 5.4. The relationship between body composition (fat and lean mass (a) and percent body fat (b)) and age in males and females.

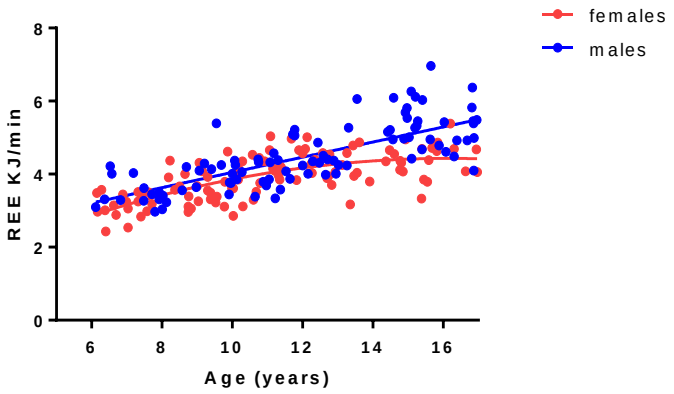

Figure 5.5. The relationship between age and REE in males and females using non-linear quadratic polynomial regression.

Figures 5.4 and 5.5 illustrate the relationship that both body composition and age have with REE. With increasing age, the rate of change between age, lean and fat mass differs with gender (Figure 5.4). Fat and lean mass values increase with growth (a), although percent fat in the males decreases with age (b). In REE (Figure 5.5), the relationship in the males is similar to that of body composition, however in the females the relationship becomes non-linear at around 12-14 years, suggesting a pubertal effect on REE, rather than age alone.

One hundred and twenty four of the original cohort (64 males and 60 females) provided blood samples for the assessment of pubertal contribution, by LH and FSH, towards the prediction of REE. The cohort was first studied without separating by gender and then gender was studied separately as with the regression analysis above. LH and FSH was significantly correlated to REE in both males and females. However, in the stepwise regression,

LH and FSH failed to add any contribution to the prediction of REE when the cohort was studied as a whole and separately by gender. Lean mass remained the most significant contributor in the whole cohort (R^2 0.740), with DXA mass leading as the most significant in the males (R^2, 0.835) and height in the females (R^2, 0.562).

5.4.5. Clinical Application

Table 5.9. Characteristics of RTHβ n = 25 and RTHα n =2 patients.

	RTHβ		RTHα	
	Female n=17	Male n=8	Female n=1	Male n=1
Age	10.6 ± 3.8	10.7 ± 2.9	5.8	15.5
TSH	3.4 ± 1.07	3.3 ± 1.07	1.04	2.07
FT4	46.1 ± 30.2	51.7 ± 30.2	5.7	8.4
FT3	17.8 ± 7.67	19.1 ± 7.67	6.9	9.1
Total mass (kg)	39.8 ± 21.9	27.5 ± 8.7	22.7	49.2
Fat mass (kg)	13.6 ± 12.5	3.7 ± 2.8	4.6	8.4
Lean mass (kg)	24.8 ± 9.4	22.7 ± 6.6	17.5	39.1
REE kJ/min	3.86 ± 1.06	3.62 ± 0.55	2.40	3.98

Mean ± standard deviation, RTH; resistance to thyroid hormone, TSH; thyroid stimulating hormone, REE; resting energy expenditure. Normal reference ranges are based on age and range from 9.01 - 22.7 for FT4 and 2.63 – 7.6 for FT3.

Table 5.9 demonstrates the characteristics of the RTH patient groups and Figure 5.6 illustrates the raw REE measurements between groups. In this form RTHβ present on average a lower REE compared to controls and RTHα demonstrating the lowest REE value, however statistically these were not significantly different from the controls.

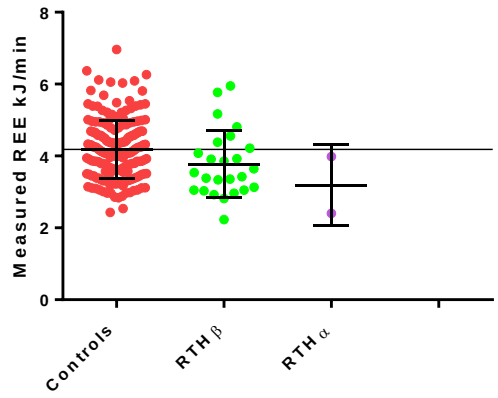

Figure 5.6. Differences between measured REE between controls and disease groups. Solid line represents the mean REE in control group (4.185 kJ/min).

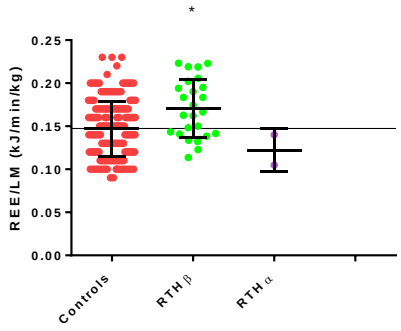

Figure 5.7. Differences between measured REE adjusted for lean mass between control and disease groups. Control mean presented by solid line (0.15 kJ/min/kg). *P < 0.05.

When REE is simply adjusted for lean mass (Figure 5.7), the RTHβ group now display a significantly increased REE compared to the controls and increased compared to the RTHα groups. Within the RTHα group the male now exhibits much lower REE compared to the female.

When the gender specific linear regression equations (models 4 and 9) which adjust for lean mass in the females but lean and fat mass in the males, were applied to patients with known metabolic disorders prior to treatment it is possible to see yet another difference between the healthy controls and the patient groups.

Figure 5.8 illustrates RTHβ and RTHα against gender matched healthy controls. The male and female RTHβ group display similar differences in measured and predicted REE. There was no statistical difference in REE between the male and female RTHβ patients and the healthy controls (males; mean difference, -0.06 ± 0.32 kJ/min, Z score -0.15 ± 0.84, females; mean difference 0.08 kJ/min ± 0.63, Z score 0.20 ± 1.65). The RTHα patients displayed a lower energy expenditure for both the male and the female participants (female difference -0.90 kJ/min Z score -2.00, male difference -0.31 kJ/min, Z score -0.81) but due to the sample size statistical significance could not be determined.

Figure 5.9 demonstrates the multiple regression method being utilised in tracking changes in REE in an RTHα patient with thyroxine treatment against age and gender matched controls. Z scores are presented alongside the differences between measured and predicted REE. The Z score is determined by applying the SD of the difference in healthy male (0.38) and female (0.38) controls to the difference in measured and predicted REE in disordered metabolism. Figure 5.9 illustrates the change in REE with thyroxine treatment in a male RTHα patient. At pre-treatment at the age of 15 REE was lower than the age and gender matched control group (mean difference -0.31 kJ/min, Z score, -0.81) returning to normal at the age of 16 (Z score, -0.03) showing lowest metabolic rate at 17 years (Z score, -0.51) compared to their pre-treatment Z score. Figure 5.9 also shows the serial measurement in a female RTHα patient starting at the age of 5, prior to treatment. REE, at baseline, is at the lowest range of the healthy controls (Z score, -2.37). As thyroxine treatment progresses, REE rises with values at ages of 7 and 8 being closest to the mean of the healthy controls (Z score, -0.23 and -0.75 respectively), then declining at age of 8 (Z score, -1.50) and rising again following increases in thyroxine dosage, at the age of 10 (Z Score, -0.74).

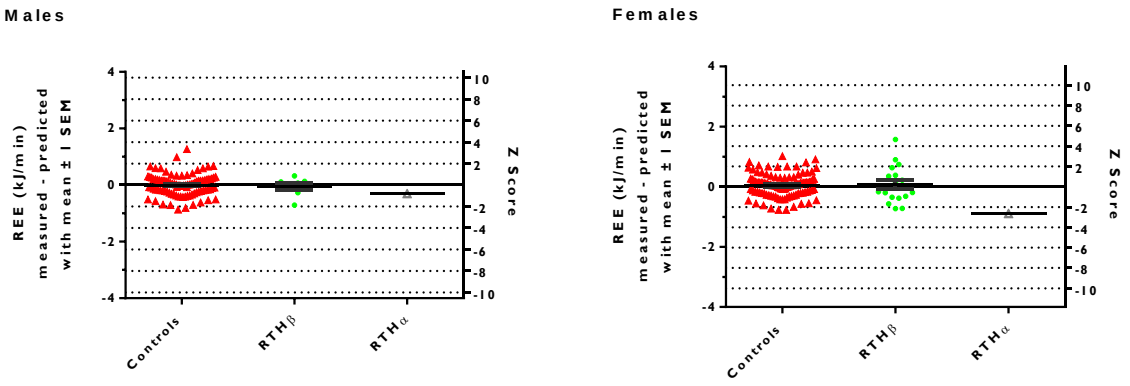

Figure 5.8. Representation of disordered metabolism in males and females against healthy controls. The residuals of measured and predicted REE have been plotted with the right y-axis corresponding to a Z score.

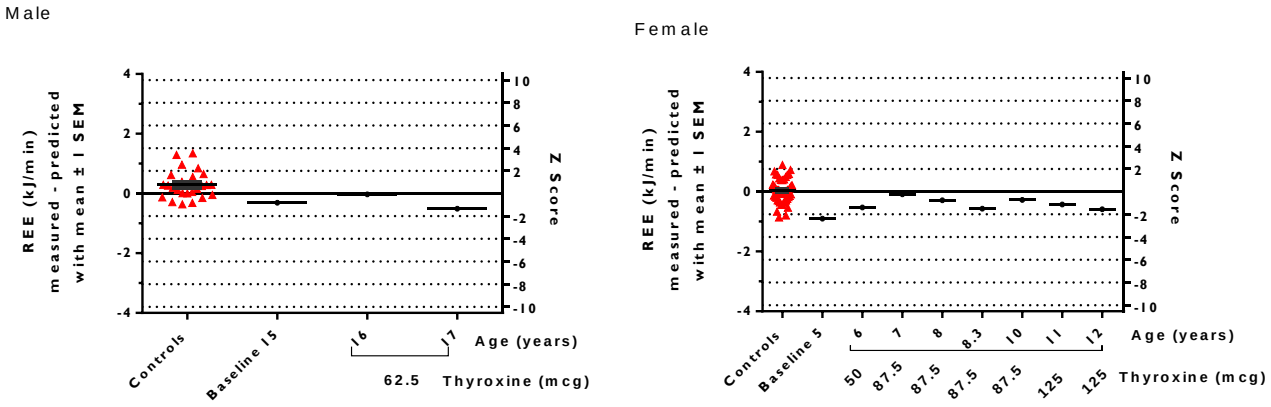

Figure 5.9. Illustration of individual RTHα patients resting energy expenditure response to treatment over the years in comparison to an age and gender matched healthy control group. REE residuals are plotted (left axis) with the right y-axis demonstrating the corresponding Z score.

5.5. Discussion

The aim of this study was to first describe resting energy expenditure (REE) in healthy children and adolescents. Predictions of REE were then developed in healthy children based on body composition measurements and then applied to paediatric cohorts and individuals with disordered metabolism to describe their differences in energy expenditure and body compositions compared to a healthy cohort. The novelty of the concept lies in the derivation and application of a Z score by subtracting a predicted value from a measured value, giving a residual, and dividing this by the standard deviation of residuals in the healthy comparable cohort in which the prediction equation was derived. This has previously been demonstrated in an adult population (chapter 4), but its application to a paediatric population in REE has not yet been explored.

Frequently in research where data collection spans many years an institution may face an instrument upgrade or replacement with a newer model. During the time course of this research the DXA scanner used for the measurement of body composition (GE Lunar Prodigy) was replaced with a newer model (GE Lunar iDXA) which had undergone significant improvements both in its technical specifications and the subsequent precision of data acquisition [33] (Chapter 3). Testing the precision and accuracy is recommended when replacing a system with either an upgrade of the same model or a different model [34]. Furthermore, if there are significant differences between the instruments then cross-calibration equations relevant to the population being studied should be derived and applied to the existing data so that all the data within a cohort is comparable [34].

In the current study, significant differences were found between the two instruments in whole body bone masses and body composition therefore cross-calibration equations were derived. Before the research question could be addressed, the derived equations were applied to all Prodigy data in both the healthy cohort and patient cohort so that it could all be in a comparable condition.

Typically, REE prediction equations have been derived based on particular populations of interest; children, obese, elderly, or disease groups [8-12]. Their purposes have been either for assessing nutritional requirements or for explaining changes in body composition such as weight loss or gain. This study proposes the use of prediction equations, not for the purpose of accurately predicting REE in metabolically disordered groups, but to describe and illustrate their deviation from a healthy population.

The analysis began with the description of REE in healthy children and adolescents. Firstly, the cohort was investigated without the separation of genders. This revealed a similar relationship between lean mass and REE in the males and females. When the relevant variables were entered into the stepwise regression analysis to generate a prediction of REE, lean mass was indeed the most significant contributor. The model that could explain the greatest amount variation in the prediction of REE was based on lean mass, gender and fat mass explaining 75.4 % of the variation in REE. Goran *et al* [35] and Muller *et al* [5] have also used these variables as determinants of REE explaining 63% and 72% of the variation in REE in healthy non-obese children.

Gender significantly contributed to the prediction of REE. To explore this further gender was removed from the regression which left fat and lean mass explaining 72.8% highlighting that the majority of the variance was explained by body composition, but an extra 2 % could be attributed to gender differences. When the analysis was subsequently separated by gender, lean mass remained the strongest and only significant variable in the females. In light of this, total body mass, the sum of lean, fat and bone mass, was entered into the regression to establish whether it explained as much variance as lean mass alone. The results demonstrated that DXA mass explained 61 % compared to 63.8 % explained by lean mass. This was possibly because of the highly significant correlation between lean and fat mass in the females and what is being presented within lean mass is the contribution of both variables. In the males both fat mass and lean mass came through as strong predictors. These variables were also less correlated to each other than demonstrated in the females. DXA mass was also entered into the regression for the males, which resulted in the same amount of variance being explained as fat and lean mass combined. The significance of keeping lean and fat mass in the prediction, rather than total mass, is that it highlights that the variance is explained by lean and fat mass with no additional contribution of bone mass.

Of the studies that have derived REE equations in healthy children, few have chosen to analyse the genders separately, instead gender has been added to an equation as a contributing variant as seen in model 1. However, as the results in the current study have demonstrated, different variables have differing contributions to REE between the genders.

We have demonstrated that there are gender differences in body composition and REE across the age range of 6 to 16 years. Levels of fat mass increase at a greater rate in females compared to males, lean mass increases linearly with age, although the gradient of the

increase is less in females than in males and around the ages of 12-14 years tapers off. These gender differences are associated with gender specific increases in growth hormones such insulin-like growth factor 1 (IGF-1), gonadotrophin and sex steroids [7], which in turn alter energy metabolism during the pubertal phase of life.

Previously published prediction equations have shown to differ in accuracy based on pubertal stage [36]. Lazzer *et al* [37] proposed two REE prediction equations in obese children based on body mass or body composition. Their body composition equation was determined by the variables; FFM, FM, gender and pubertal stage using Tanner and Marshall scales (R^2 0.70) [38 39]. The inclusion of pubertal stage in relation to REE by Lazzer *et al* reiterates the importance of using pubertal status rather than chronological age when investigating children with atypical body composition or REE. Lazzer studied children with mild to severe obesity, discussing that children with higher levels of fat mass may influence pubertal development due to hormonal mechanisms within adipose tissue and boys often display delayed pubertal development by mechanisms that are less clear. In the current study, the clinical biomarkers, LH and FSH, were used as markers of puberty. LH and FSH are gonadotrophins, whose rate of secretion rises as pubertal progresses [40]. Clinically, there is no defined value for LH and FSH representing the onset of puberty, however there is some published literature indicating normal reference ranges based on age ranges in males and females [41].

In this study, LH and FSH values were entered into the regression analysis on the 124 participants who provided blood samples alongside their metabolic measurements. The pubertal markers in this instance did not significantly contribute to the prediction of REE, Few studies have investigated the influence of puberty on REE in healthy children. Rodriguez *et al* [42] also found no significant contribution of puberty, by Tanner scales, to the prediction of REE in healthy obese and non-obese children and adolescents.

Despite the evidence suggesting pubertal status does not account of any of the variation, the lack of contribution may be down to the way that puberty is assessed. This is the first study, to our knowledge, that has combined biochemical markers to the traditional body composition variables in the hope of further expressing REE in growing children. Hormones such as LH and FSH act in a pulsatile manner [18] making an accurate assessment difficult in a spot measurement. Although investigations into the triggers of puberty remain elusive, further investigations into alternative biochemical markers and their contribution to REE should be explored. McNeilly *et al* [43] investigated whether urinary LH and FSH could

differentiate between pre and post pubertal children in comparison to self-assessment by Tanner scale. Their results demonstrated that LH:FSH ratios were higher in pubertal children than pre pubertal children, although differences were not significant in the females. Additionally, Soeborg *et al* [44] documented that biochemical levels of sex steroids; 4-androstenedione (Adione), testosterone, and androgen, were found to significantly increase with each genital stage in males and testosterone increased with each breast stage in females. Importantly, these metabolite concentrations increased markedly with the onset of puberty (clinically assessed rather than self-assessed). Further investigation into the relationship between these sex hormones (in addition to LH and FSH) and REE would be valuable.

The aim of generating the prediction equations was to apply them in the context of metabolic disorders. The gender specific prediction equations were applied to patients with disorders of thyroid hormone action to describe the magnitude of the difference in REE compared to a healthy population. Chapter 4 describes this approach in adults [15], where thyrotoxicosis, lipodystrophy and RTHβ all displayed the elevated energy expenditure Z scores. Energy expenditure in children with TH disorders is less well documented because of the rarity of the disease and diagnosis in childhood. The results of the current study demonstrate differences in REE in two disorders, RTHβ and RTHα. In RTHβ, the males exhibit a normal albeit slightly decreased REE with a mean Z score of -0.15 and the females display normal REE with a Z score of 0.21. These results are consistent with the known variability of the RTHβ phenotype. Some patients present as asymptomatic whilst others exhibit hyperthyroid symptoms suggesting the degree of peripheral tissue resistance varies [25 45]. Mitchell *et al* [25] found that in both adults and children REE was substantially increased with values 20 % above that of predicted REE in children, based on previously published equations [3 4].

In the RTHα patients low REE Z scores were documented, but with clear differences between the male and female. The male patient demonstrated a Z score of -0.81 with a Z score of -2.37 in the female patient. These Z scores correlate with the hypothyroid phenotype of the disorder and are in agreement with previously published case reports [30 46]. This includes the description of another adolescent male RTHα patient with decreased REE but within a normal range [30] and two additional female RTHα patients with hypothyroid features in whom REE or body composition was not measured [47 48].

The concept of applying a healthy prediction equation serially in individual, metabolically disordered, patients has also been demonstrated in this study. As a patient with hypothyroid features is treated with thyroid hormone, one would expect an improvement in thyroid status and therefore an improvement in their REE. By tracking or monitoring a patients REE Z score over time, provides an indirect indication of whether thyroxine therapy is effective. The advantage of presenting patient data using a Z score, rather than in a raw format, is that their REE has been adjusted for changes in body composition and also enables comparison with healthy controls.

Several limitations of this study should be considered. First, the prediction equations should be validated against an independent healthy paediatric subject cohort [49]. Ideally this would have been undertaken prior to its clinical application, however, due to the numbers of participants required per dataset this has not been possible within this time frame. Further work is in progress to validate the prediction equations. Second, the dataset used to derive the equations was lacking in sample size in some age groups. To apply the equations with confidence in an age range of 6-16y a larger, more consistent sample size needs to be generated. Lastly, reiterating the need for a larger sample size, more studies into a method for accurately describing pubertal status and its effect on REE are warranted.

In summary, gender differences in body composition and energy expenditure have been described in a cohort of healthy children and adolescents aged 6-16 years. REE was predicted in the healthy cohort by equations generated using gender-specific body composition measurements. REE measurements from patients with rare disorders of TH action have been made and calculated in the context of healthy age and gender matched counterparts using a Z score approach. This approach may facilitate the phenotyping of a metabolic disorder, aid in the interpretation of REE in metabolic disease and assist in the evaluation of patient therapy over time.

5.6. References

1. Schofield WN. Predicting basal metabolic rate, new standards and review of previous work. *Human nutrition Clinical nutrition* 1985;39 Suppl 1:5-41.
2. Henry CJ. Basal metabolic rate studies in humans: measurement and development of new equations. *Public Health Nutr* 2005;8(7A):1133-52.
3. Harris JA, Benedict FG. A Biometric Study of Human Basal Metabolism. *Proceedings of the National Academy of Sciences of the United States of America* 1918;4(12):370-3.
4. Molnar D, Jeges S, Erhardt E, et al. Measured and predicted resting metabolic rate in obese and nonobese adolescents. *The Journal of pediatrics* 1995;127(4):571-7.
5. Muller MJ, Bosy-Westphal A, Klaus S, et al. World Health Organization equations have shortcomings for predicting resting energy expenditure in persons from a modern, affluent population: generation of a new reference standard from a retrospective analysis of a German database of resting energy expenditure. *The American journal of clinical nutrition* 2004;80(5):1379-90.
6. Herrmann SD, McMurray RG, Kim Y, et al. The influence of physical characteristics on the resting energy expenditure of youth: A meta-analysis. *American journal of human biology : the official journal of the Human Biology Council* 2017;29(3)
7. Bitar A, Vernet J, Coudert J, et al. Longitudinal changes in body composition, physical capacities and energy expenditure in boys and girls during the onset of puberty. *Eur J Nutr* 2000;39(4):157-63.
8. Sijtsma A, Corpeleijn E, Sauer PJ. Energy requirements for maintenance and growth in 3- to 4-year-olds may be overestimated by existing equations. *Journal of pediatric gastroenterology and nutrition* 2014;58(5):642-6.
9. Lawrence JC, Lee HM, Kim JH, et al. Variability in results from predicted resting energy needs as compared to measured resting energy expenditure in Korean children. *Nutr Res* 2009;29(11):777-83.
10. Carpenter A, Ng VL, Chapman K, et al. Predictive Equations Are Inaccurate in the Estimation of the Resting Energy Expenditure of Children With End-Stage Liver Disease. *JPEN Journal of parenteral and enteral nutrition* 2017;41(3):507-11.
11. Hill RJ, Cleghorn GJ, Withers GD, et al. Resting energy expenditure in children with inflammatory bowel disease. *Journal of pediatric gastroenterology and nutrition* 2007;45(3):342-6.

12. Hofsteenge GH, Chinapaw MJ, Delemarre-van de Waal HA, et al. Validation of predictive equations for resting energy expenditure in obese adolescents. *The American journal of clinical nutrition* 2010;91(5):1244-54.
13. Crabtree NJ, Shaw NJ, Boivin CM, et al. Pediatric in vivo cross-calibration between the GE Lunar Prodigy and DPX-L bone densitometers. *Osteoporosis international : a journal established as result of cooperation between the European Foundation for Osteoporosis and the National Osteoporosis Foundation of the USA* 2005;16(12):2157-67.
14. Cunningham JJ. Body composition as a determinant of energy expenditure: a synthetic review and a proposed general prediction equation. *The American journal of clinical nutrition* 1991;54(6):963-9.
15. Watson LP, Raymond-Barker P, Moran C, et al. An approach to quantifying abnormalities in energy expenditure and lean mass in metabolic disease. *European journal of clinical nutrition* 2014;68(2):234-40.
16. Molnar D, Schutz Y. The effect of obesity, age, puberty and gender on resting metabolic rate in children and adolescents. *European journal of pediatrics* 1997;156(5):376-81.
17. Willemsen RH, Dunger DB. Normal Variation in Pubertal Timing: Genetic Determinants in Relation to Growth and Adiposity. *Endocr Dev* 2016;29:17-35.
18. Abreu AP, Kaiser UB. Pubertal development and regulation. *Lancet Diabetes Endocrinol* 2016;4(3):254-64.
19. Pinyerd B, Zipf WB. Puberty-timing is everything! *J Pediatr Nurs* 2005;20(2):75-82.
20. Tanner J. Growth at adolescence: with a general consideration of the effects of hereditary and environmental factors upon growth and maturation from birth to maturity. Oxford: Blackwell Scientific Publications 1962.
21. Taylor SJ, Whincup PH, Hindmarsh PC, et al. Performance of a new pubertal self-assessment questionnaire: a preliminary study. *Paediatr Perinat Epidemiol* 2001;15(1):88-94.
22. Desmangles JC, Lappe JM, Lipaczewski G, et al. Accuracy of pubertal Tanner staging self-reporting. *Journal of pediatric endocrinology & metabolism : JPEM* 2006;19(3):213-21.
23. Chavarro JE, Watkins DJ, Afeiche MC, et al. Validity of Self-Assessed Sexual Maturation Against Physician Assessments and Hormone Levels. *The Journal of pediatrics* 2017
24. Rasmussen AR, Wohlfahrt-Veje C, Tefre de Renzy-Martin K, et al. Validity of self-assessment of pubertal maturation. *Pediatrics* 2015;135(1):86-93.

25. Mitchell CS, Savage DB, Dufour S, et al. Resistance to thyroid hormone is associated with raised energy expenditure, muscle mitochondrial uncoupling, and hyperphagia. *The Journal of clinical investigation* 2010;120(4):1345-54.
26. Moran C, Schoenmakers N, Agostini M, et al. An adult female with resistance to thyroid hormone mediated by defective thyroid hormone receptor alpha. *The Journal of clinical endocrinology and metabolism* 2013;98(11):4254-61.
27. Ajluni N, Meral R, Neidert AH, et al. Spectrum of disease associated with partial lipodystrophy: lessons from a trial cohort. *Clin Endocrinol (Oxf)* 2017;86(5):698-707.
28. Huang-Doran I, Sleigh A, Rochford JJ, et al. Lipodystrophy: metabolic insights from a rare disorder. *The Journal of endocrinology* 2010;207(3):245-55.
29. Chiesa A, Olcese MC, Papendieck P, et al. Variable clinical presentation and outcome in pediatric patients with resistance to thyroid hormone (RTH). *Endocrine* 2012;41(1):130-7.
30. Moran C, Agostini M, McGowan A, et al. Contrasting phenotypes in Resistance to Thyroid Hormone alpha correlate with divergent properties of thyroid hormone receptor alpha1 mutant proteins. *Thyroid : official journal of the American Thyroid Association* 2017
31. Bochukova E, Schoenmakers N, Agostini M, et al. A mutation in the thyroid hormone receptor alpha gene. *The New England journal of medicine* 2012;366(3):243-9.
32. Elia M, Livesey G. Energy expenditure and fuel selection in biological systems: the theory and practice of calculations based on indirect calorimetry and tracer methods. *World review of nutrition and dietetics* 1992;70:68-131.
33. Toombs RJ, Ducher G, Shepherd JA, et al. The impact of recent technological advances on the trueness and precision of DXA to assess body composition. *Obesity (Silver Spring)* 2012;20(1):30-9.
34. Shepherd JA, Lu Y, Wilson K, et al. Cross-calibration and minimum precision standards for dual-energy X-ray absorptiometry: the 2005 ISCD Official Positions. *Journal of clinical densitometry : the official journal of the International Society for Clinical Densitometry* 2006;9(1):31-6.
35. Goran MI, Kaskoun M, Johnson R. Determinants of resting energy expenditure in young children. *The Journal of pediatrics* 1994;125(3):362-7.

36. Bandini LG, Morelli JA, Must A, et al. Accuracy of standardized equations for predicting metabolic rate in premenarcheal girls. *The American journal of clinical nutrition* 1995;62(4):711-4.

37. Lazzer S, Patrizi A, De Col A, et al. Prediction of basal metabolic rate in obese children and adolescents considering pubertal stages and anthropometric characteristics or body composition. *European journal of clinical nutrition* 2014;68(6):695-9.

38. Marshall WA, Tanner JM. Variations in the pattern of pubertal changes in boys. *Arch Dis Child* 1970;45(239):13-23.

39. Marshall WA, Tanner JM. Variations in pattern of pubertal changes in girls. *Arch Dis Child* 1969;44(235):291-303.

40. Mundy LK, Simmons JG, Allen NB, et al. Study protocol: the Childhood to Adolescence Transition Study (CATS). *BMC pediatrics* 2013;13:160.

41. Soldin SJ, Morales A, Albalos F, et al. Pediatric reference ranges on the Abbott IMx for FSH, LH, prolactin, TSH, T4, T3, free T4, free T3, T-uptake, IgE, and ferritin. *Clinical biochemistry* 1995;28(6):603-6.

42. Rodriguez G, Moreno LA, Sarria A, et al. Determinants of resting energy expenditure in obese and non-obese children and adolescents. *J Physiol Biochem* 2002;58(1):9-15.

43. McNeilly JD, Mason A, Khanna S, et al. Urinary gonadotrophins: a useful non-invasive marker of activation of the hypothalamic pituitary-gonadal axis. *Int J Pediatr Endocrinol* 2012;2012(1):10.

44. Soeborg T, Frederiksen H, Mouritsen A, et al. Sex, age, pubertal development and use of oral contraceptives in relation to serum concentrations of DHEA, DHEAS, 17alpha-hydroxyprogesterone, Delta4-androstenedione, testosterone and their ratios in children, adolescents and young adults. *Clinica chimica acta; international journal of clinical chemistry* 2014;437:6-13.

45. Moran C, Chatterjee K. Resistance to Thyroid Hormone alpha-Emerging Definition of a Disorder of Thyroid Hormone Action. *The Journal of clinical endocrinology and metabolism* 2016;101(7):2636-9.

46. Moran C, Chatterjee K. Resistance to thyroid hormone due to defective thyroid receptor alpha. *Best practice & research Clinical endocrinology & metabolism* 2015;29(4):647-57.

47. van Mullem AA, Chrysis D, Eythimiadou A, et al. Clinical phenotype of a new type of thyroid hormone resistance caused by a mutation of the TRalpha1 receptor: consequences of

LT4 treatment. *The Journal of clinical endocrinology and metabolism* 2013;98(7):3029-38.

48. van Gucht AL, Meima ME, Zwaveling-Soonawala N, et al. Resistance to Thyroid Hormone Alpha in an 18-Month-Old Girl: Clinical, Therapeutic, and Molecular Characteristics. *Thyroid : official journal of the American Thyroid Association* 2016;26(3):338-46.
49. Ivanescu AE, Li P, George B, et al. The importance of prediction model validation and assessment in obesity and nutrition research. *Int J Obes (Lond)* 2016;40(6):887-94.

6. General Discussion

The objective of this thesis was to develop a new approach to describe resting energy expenditure (REE) and body composition in healthy adults and children. With this approach, normative resting energy expenditure and body composition are defined by the assignment of Z-scores derived from studying the difference between measured and predicted REE and lean mass (LM) in a healthy population. Z-scores are then applied to measurements of REE and LM in patients with metabolic disorders in order to characterise their deviation from a healthy population.

6.1. Measurement of body composition by DXA

Throughout the studies described in this thesis, body composition in adults and children was assessed by Dual-energy X-ray Absorptiometry (DXA), a method that is a well-established in the literature. During the course of these studies, the DXA instrument was upgraded from a GE Lunar Prodigy to a GE Lunar iDXA, which prompted the investigation (Chapter 3) into the precision and accuracy of DXA for the measurement of regional and whole-body bone and body composition in adults. This was achieved by first establishing the precision of the iDXA by performing repeated measurements, then comparing iDXA and Prodigy measurements to enable the development of cross-calibration equations in order that a combined dataset could be used. Finally, the accuracy of fat mass measurements performed on the iDXA were evaluated against fat mass derived from a 4-component (4-C) model.

In an adult population, the iDXA demonstrated excellent precision of bone and body composition measurements in all regions, with the exception of arm fat mass, which was consistent with previously published literature [1-4]. The improved precision of the iDXA over that previously reported for the Prodigy [5], especially in body composition measurements, is largely attributed to the improvements in hardware within the instrument, such as the new x-ray filter and detector, which enhance bone edge detection. The advantage of improved precision is that clinically, when performing repeat scans at follow-up appointments, smaller biological changes in body composition can be detected. This is of significant benefit when studying individual patients or small disease cohorts.

Significant differences between the Prodigy and the iDXA were found to be present in all regions of bone and body composition with the exception of the hip. Based on these findings, cross-calibration equations were developed, specific to the healthy adult

population being studied (Chapter 3). As significant differences between whole-body composition measurements from the two instruments were also observed in children, separate cross-calibration equations were developed for a paediatric population (Chapter 5).

Investigations into the accuracy of DXA fat mass measurements compared to a 4-C model revealed a positive bias across DXA instruments. This bias was accentuated in the latest versions of the software, demonstrating the largest inaccuracies at the highest fat masses. The clinical implications of this include poor validity of DXA fat mass measurements in patients with large quantities of adipose tissue, such as patients with obesity. A limitation of this study was the lack of participants with high fat mass; further insights into the behaviour of DXA and 4-C in this cohort will be valuable. Knowledge of the strengths and limitations of body composition measurements from DXA instruments, or measurements made by any other method, is imperative when interpreting data from participants that present with atypical proportions of fat and lean mass, such as those observed in clinical populations.

6.2. Prediction of REE and lean mass in healthy adults

Chapter 4 investigates the development of multiple regression equations to predict healthy resting energy expenditure (REE) and lean mass (LM) in adults; these equations are extended to paediatrics in chapter 5. Gender did not significantly contribute to the explanation of the variance in predictions of REE in adults, therefore one equation consisting of the significant variables, age (years), fat mass (FM) (kg) and fat-free mass (FFM) (kg), was derived for both genders; this explained 73% of the variance in REE. However, gender did significantly contribute towards the variance in the prediction of lean mass in adults, therefore two gender-specific equations were derived based on the significant variables. In males, the significant variables were bone mineral content and height^2, whereas fat mass and height^2 were the significant variables in females. These equations explained 55% and 59% of the variance in lean mass in males and females, respectively.

Predicting REE in a healthy cohort is not a novel concept; predicted REE is often used to predict energy intake. There are many publications of REE predictions based on large, amalgamated datasets of healthy participants. However, several of these publications state that their REE predictions are inaccurate when applied to cohorts outside the demographics of their dataset [6-8]. For this reason, it is common for cohort-specific prediction equations to be derived, such as in obesity [9 10] or childhood [11-13]. Differences between prediction

equations are often due to differences in the measurement conditions and methods, such as the use of height and weight versus bioelectrical impedance analysis and DXA, or dissimilarities in the characteristics and demographics of the sample, such as age, ethnicity or geographical location.

Using normative data acquired from the studies conducted for this thesis, the differences between measured REE and predictions of REE in a healthy cohort by the most commonly used equations (Schofield [14], Henry [15] and Harris-Benedict [16]) and our newly developed prediction equations can be illustrated in adults and children (Figure 6.1).

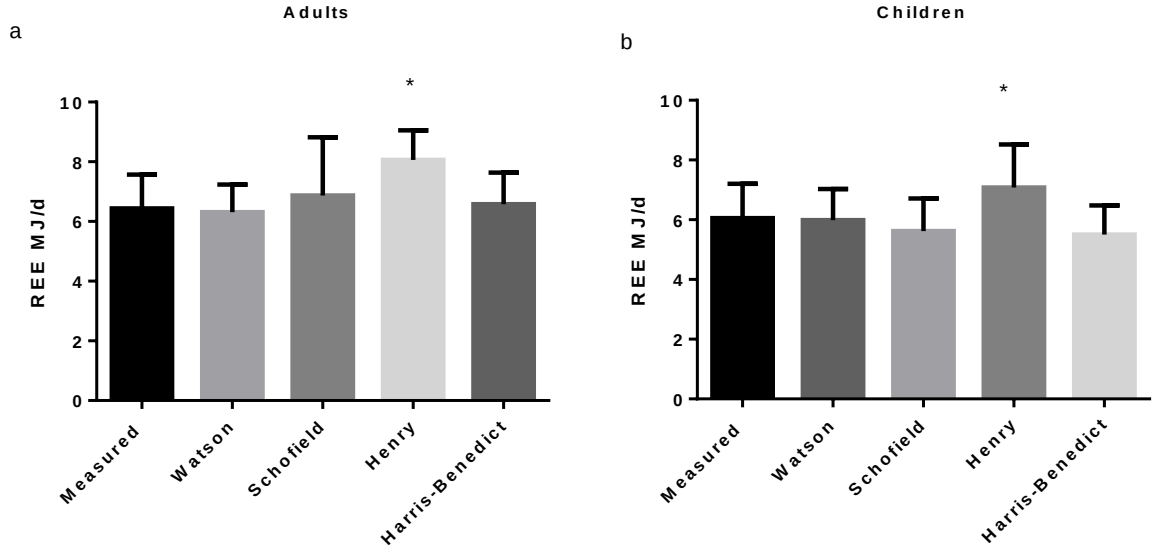

Figure 6.1. Measured and predicted REE in healthy adults (a) and children (b). Data are mean ± SE. "Watson" REE equations are derived within this thesis for adults and children (chapter 4 and 5).

Significant differences were found between Henry [15] and both our measured and predicted REE. This emphasizes the variation in prediction equations across healthy cohorts. Within a disease cohort, the severity of the disease can vary substantially between patients. It is, therefore, not always appropriate to derive a prediction equation for a specific disease group, especially when the disease cohorts are small. Using the concept being presented in this thesis, the use of a Z-score describes how close an REE or lean mass measurement is to the expected value, based on healthy participants. By applying this approach to individual patients or disease conditions, specifically thyroid hormone (TH) disorders and lipodystrophy, the degree by which these conditions deviate from a normal population can

be illustrated. More importantly, the change within an individual patient over a course of treatment can also be quantified.

6.2.1. Clinical Application

6.2.1.1. RTHβ

In adult RTHβ patients, average Z-scores were 1.77 for REE and -0.17 for lean mass. The increased REE is a manifestation of the elevated levels of circulating thyroid hormones, which are characteristic of the condition. The lower lean mass Z-score is most likely to be linked to clinical features of RTHβ such as muscle weakness caused by hormone sensitivity in TRα-expressing peripheral tissue. However, the RTHβ condition is a diverse disorder, with many patients displaying typical scores of REE and lean mass, emphasising the complexity of the condition and suggesting that within this condition it is possible for the body to continue to regulate energy expenditure and body composition.

6.2.1.2. RTHα

Five adult RTHα patients, two females and three males, were identified for the application of the healthy prediction equations. We found these RTHα patients to have low REE (mean Z-score of -2.3) and high LM (mean Z-score of 2.1), in contrast to the RTHβ cohort. The average REE Z-score was lower in the females (-2.6) compared to the males (-2.0). However, the LM Z-score was higher in the females (3.2) than the males (1.4). Larger sample sizes will be required in order to conclude whether a true gender difference exists. The REE results are in accordance with clinically reported hypothyroid features of the condition [17]. High LM has not been reported previously, but it is a common feature across the five RTHα patients investigated. The increased LM may be linked to the resistant TRα receptor in skeletal muscle over-compensating, resulting in an increase in protein deposition. Alternatively, as previously reported in lipodystrophy [18], it could be related to muscle hypertrophy.

6.2.1.3. Thyrotoxicosis

In the thyrotoxic group, the average Z-score for REE was the highest of the three conditions, at 5.8. In contrast, the average Z-score for lean mass was the lowest, at -1.2, revealing the greatest dissociation between REE and LM across the three conditions. The elevated REE Z-score reflects the metabolic effects of the thyroid hormone excess associated with Graves' disease. The reduced LM reflects the catabolic state of the disorder, leading to weight loss and muscle weakness. Again, the severity of the disorder varied between the

seven patients studied, with REE Z-score ranging from 1.5 to 9.6, but despite this, there is a clear separation between healthy controls and thyrotoxicosis.

6.2.1.4. Lipodystrophy

Typically, lipodystrophy (LD) patients are characterised by an elevated REE and LM [18 19]. In chapter 4 we confirm an increased REE and LM in LD with an REE Z score of 2.97 and a lean mass Z score of 4.2. However, the Z scores demonstrate a disproportionate increase in REE and LM. The increased LM may explain a proportion of the elevated REE reported in the LD group. When measured REE was adjusted for measured LM, no significant difference was evident between LD and healthy controls, as reported in a previous study [19]. However, this assumes that LM is the only influence on REE and that the relationship between REE and LM has no intercept. Reporting REE based on predictions using multiple regression analysis derived from healthy controls, not only quantifies the difference in REE and LM between LD and healthy but is also independent of body composition influences and the presence of an intercept. Therefore it suggests that there are components of the elevation in REE and lean mass that are still unaccounted for. Organomegaly is a common feature of LD and may account for some of the increased LM present in the LD group. Another mechanism involved in the presence of increased LM may be due to the spillover effects of hyperinsulinemia on IGF-I receptors [20]. However the exact mechanisms involved in increased muscle mass in LD is not fully understood and requires further investigation. The increase in REE independent of LM may be explained by increased fat oxidation due to the consumption of dietary fat within the meals provided. Although meals were standardised across all studies within this thesis (30-35% fat), this may induce levels of dietary fat greater than is typical for an individual. Excess dietary fat has been previously reported to increase total energy expenditure in LD patients due to the impairment in their ability to store fat subcutaneously [19]. Further studies into the oxidation and storage of dietary fat in LD would prove valuable.

A key benefit of the Z-score approach is its suitability for serial application in individual patients, which is often necessary in rare conditions where sample sizes are very small. Such serial Z-score measurements have highlighted REE and lean mass as strong markers of abnormal metabolism which respond to thyroxine treatment as expected for other parameters. Therefore, it may be possible to use REE and lean mass as markers of treatment response over time, which could inform clinical practice. When applied to the four

metabolic conditions described, the trend throughout the analysis was a dissociation between REE and LM, in contrast to the normative data.

6.3. Predicting REE in paediatrics

Chapter 5 replicated the Z-score approach from chapter 4 in a cohort of healthy paediatric subjects. First, cross-calibration equations were derived from a paediatric healthy cohort and applied to body composition and bone data obtained from the Prodigy DXA within the dataset. As demonstrated in the adult population in chapter 3, significant differences were observed between measurements from the two DXA instruments in the paediatric cohort.

In contrast to the adult population, REE prediction equations were found to differ significantly by gender in the paediatric cohort. In the boys, LM and fat mass explain 80% of the variance in REE, whereas in girls, only LM contributed significantly, explaining 60% of the variance. The separation of the equations by gender in paediatrics but not in adults indicates gender-specific differences in energy expenditure that are mediated by growth. During puberty, body mass increases in both boys and girls; however, the increases in proportions of fat and LM differ by gender. The increase in body mass in boys is primarily due to an increase in LM, as body fat percentage appears to reduce with age. In girls, on the other hand, both fat mass and LM increase with linear growth, yet fat mass does not contribute to the variation in REE in girls; this may be because both fat mass and LM are so highly correlated.

6.3.1. Pubertal contributions to REE

The effect of puberty on REE in boys and girls was explored by investigating the influence of luteinising hormone (LH) and follicle-stimulating hormone (FSH), biochemical markers of puberty, combined with body composition. In boys, LH stimulates testosterone production and FSH supports sperm maturation. In girls, LH and FSH stimulate ovarian production of oestrogen, progesterone and testosterone [21].

Of the 201 paediatric participants studied, 124 gave blood samples which were analysed for sex hormone levels. The analysis demonstrated that LH and FSH, as pubertal markers, did not contribute towards the prediction of REE in this subset of participants. The reason for this may have been due to the difficulty in capturing a reliable hormone level in a fasted, morning, spot measurement due to the pulsatile manner of its secretion [22].

Assessment at night during the initial phase of puberty has been suggested, along with 24 hour assessment of LH and FSH as puberty advances [23]. Additionally, in girls, before the onset of puberty, the pre-ovulatory surge required for ovulation may also raise plasma LH to levels that could be mistaken for pubertal levels [24]. Since LH and FSH act on the production of testosterone in boys and oestrogen, progesterone and testosterone in girls, further investigations into these and other sex steroid hormones as indicators of pubertal status may help to explain the variance in REE within and between genders.

Most pubertal literature relies on self-assessment of pubertal status based on Tanner stages, or physical assessments performed by clinicians and compared to Tanner stages. These methods have their limitations, such as the intrusiveness of a physical examination and the inaccuracy of self-assessments compared to physical assessments. Therefore, the addition of biochemical markers for estimating stages of puberty is an ideal for supporting existing methods.

6.3.2. Clinical applications

6.3.2.1. RTHβ

Twenty five RTHβ children were studied: eight boys and seventeen girls. The mean Z-score in the boys was -0.15, ranging from -1.9 to 0.8, and in girls, the mean Z-score was 0.20 with a range from -1.9 to 4.1. The mean Z-scores differ between boys and girls, with boys displaying lower REE and a smaller range of values whilst girls exhibit higher REE and a greater range of Z-scores compared to the healthy controls. However, in both groups these Z-scores are not different from those observed in the healthy controls; in contrast, the adult RTHβ cohort exhibited elevated Z-scores for REE.

The difference in REE results for two overlapping paediatric RTHβ cohorts, that reported by Mitchell et al. [25] (n=13) and the cohort described in chapter 5 (n=25), warrants discussion. Mitchell predicted REE using Schofield equations, demonstrating a significantly high ratio between measured and predicted REE of 118%. When I applied Schofield equations to predict REE in the RTHβ cohort reported in chapter 5 their ratio between measured and predicted REE was lower at 112%, indicating that my RTHβ sample had slightly lower REE. To investigate the contribution of choice of prediction equation to the difference in findings, I applied the Schofield equation also to the healthy control cohort in chapter 5 and found their ratio between measured and predicted REE was 109%. This suggests that the Schofield equations slightly under-predict REE, and this will also contribute

to the high ratio between measured and predicted REE in the RTHβ cohort reported by Mitchell et al. [25]. A large difference between the two healthy child cohorts, Schofield and the healthy control cohort in chapter 5, is the sample size and the multiple populations within the Schofield cohort. Schofield's healthy cohort consisted of 7173 European and North American children, an amalgamation of data from 114 published studies totalling 7173 data points. By contrast, my healthy child cohort in chapter 5 comprised 201 measurements from a solely UK population [15]. Studies that have applied Schofield's equations have reported a mix of over estimation and underestimation of REE in children depending on their nationality [15]. This emphasizes the extent to which the population from which the prediction expressions are developed may influence the accuracy of predictions when applied in other populations. When employing prediction expressions it is important that they are developed in a population comparable with that in which they are to be applied. Aside from a population difference, it is also not clear how controlled the measurements of REE were within the Schofield cohort as it consists of data from previously published studies including group mean values [15]. Therefore measurement techniques and instrument error may well also contribute towards the differences in the predictions of REE.

6.3.2.2. RTHα

RTHα is a rare thyroid hormone (TH) disorder with only fourteen cases having been identified world-wide to date, five of which are in children. In this thesis, two children are studied, one boy and one girl. Both RTHα children demonstrated low REE Z-scores at the pre-treatment stage, with the girl demonstrating a much lower REE Z-score than the boy (-2.4 compared to -0.8 respectively). As with the RTHβ patients, we are presented with a gender difference; however, there is a large age gap between these patients, with the boy being diagnosed at the age of 15 years compared to just under 6 years in the girl. In contrast to the RTHβ patients, the RTHα children are consistent with the RTHα adults, showing lower REE compared to controls and lower REE Z-scores in the female patients compared to the males. As for RTHβ, further studies involving higher numbers of participants are necessary in order for reliable conclusions to be drawn.

The Z-score is a useful tool for distinguishing between the two RTH mutations and supporting the other clinical diagnostic parameters used to identify a patient with this disorder. In addition to its use in the study of a disease cohort as a whole, the Z-score approach can also be applied to individual patients to monitor their response to treatment

over time, with regard to the effect of TH on REE. An increase in an REE Z-score approaching the mean of the control group could reflect an improvement with TH therapy, whereas a drop in REE could indicate a need for a change in thyroxine dose. Figure 8 of chapter 5 illustrates this in a male patient where, as a result of the decrease in REE at the age of 17 years, dosage of thyroxine therapy was increased.

6.4. Summary, conclusions and future work

In summary, the work of this thesis has demonstrated the unique role of the use of Z-scores to quantify the differences between healthy and disordered REE and body composition. The generation of equations to predict REE in healthy adults and children and lean mass in adults has allowed the description of disordered metabolism relative to a prediction of normal REE or LM based on body composition. Presentation of the Z-scores on an individual basis can assist in the evaluation of the patient's disorder and treatment progress.

The main findings of the thesis are as follows:

- DXA is a precise method for the measurement of body composition, but its accuracy compared to a 4-C model should be explored further in patients with high fat masses.
- Newly-derived equations accurately predict REE and LM in European healthy adults.
- Application of the prediction equations and Z-scores to adults with metabolic disorders indicates increased REE in thyrotoxicosis, lipodystrophy and RTHβ patients but reduced REE in RTHα subjects. Reduced LM is described in RTHβ and thyrotoxicosis, whereas this is elevated in lipodystrophy and RTHα.
- In children and adolescents, two gender-specific prediction equations were derived from a healthy cohort. When applied to RTHβ patients, REE was not different from healthy controls, but RTHα patients exhibited decreased REE.
- Z-scores can describe an individual patient's progress during treatment.

Further research will be undertaken to validate the paediatric prediction equations on a separate cohort of healthy children ranging from 6 – 16 years of age. Future work will also include the exploration of body composition measurements by DXA compared to a 4-C model in children and adolescents.

In addition to validating the existing equations, further exploration of pubertal contributions to body composition and energy expenditure will be undertaken by using other measures to assess pubertal stage. It would also be interesting to explore the application of serial Z-scores in further RTH cases and in other disorders in which the relationship between body composition and energy expenditure is atypical.

6.5. References

1. Hind K, Oldroyd B, Truscott JG. In vivo precision of the GE Lunar iDXA densitometer for the measurement of total body composition and fat distribution in adults. *European journal of clinical nutrition* 2011;65(1):140-2.
2. Hind K, Oldroyd B, Truscott JG. In vivo precision of the GE Lunar iDXA densitometer for the measurement of total-body, lumbar spine, and femoral bone mineral density in adults. *Journal of clinical densitometry : the official journal of the International Society for Clinical Densitometry* 2010;13(4):413-7.
3. Rothney MP, Martin FP, Xia Y, et al. Precision of GE Lunar iDXA for the measurement of total and regional body composition in nonobese adults. *Journal of clinical densitometry : the official journal of the International Society for Clinical Densitometry* 2012;15(4):399-404.
4. Kaminsky LA, Ozemek C, Williams KL, et al. Precision of total and regional body fat estimates from dual-energy X-ray absorptiometer measurements. *The journal of nutrition, health & aging* 2014;18(6):591-4.
5. Oldroyd B, Smith AH, Truscott JG. Cross-calibration of GE/Lunar pencil and fan-beam dual energy densitometers--bone mineral density and body composition studies. *European journal of clinical nutrition* 2003;57(8):977-87.
6. Song T, Venkataraman K, Gluckman P, et al. Validation of prediction equations for resting energy expenditure in Singaporean Chinese men. *Obes Res Clin Pract* 2014;8(3):e201-98.
7. Wahrlich V, Teixeira TM, Anjos LA. Validity of a population-specific BMR predictive equation for adults from an urban tropical setting. *Clin Nutr* 2016
8. Muller MJ, Bosy-Westphal A, Klaus S, et al. World Health Organization equations have shortcomings for predicting resting energy expenditure in persons from a modern, affluent population: generation of a new reference standard from a retrospective analysis of a German database of resting energy expenditure. *The American journal of clinical nutrition* 2004;80(5):1379-90.
9. Lazzer S, Patrizi A, De Col A, et al. Prediction of basal metabolic rate in obese children and adolescents considering pubertal stages and anthropometric characteristics or body composition. *European journal of clinical nutrition* 2014;68(6):695-9.
10. Ivanescu AE, Li P, George B, et al. The importance of prediction model validation and assessment in obesity and nutrition research. *Int J Obes (Lond)* 2016;40(6):887-94.

11. Molnar D, Schutz Y. The effect of obesity, age, puberty and gender on resting metabolic rate in children and adolescents. *European journal of pediatrics* 1997;156(5):376-81.
12. Rodriguez G, Moreno LA, Sarria A, et al. Determinants of resting energy expenditure in obese and non-obese children and adolescents. *J Physiol Biochem* 2002;58(1):9-15.
13. Schmelzle H, Schroder C, Armbrust S, et al. Resting energy expenditure in obese children aged 4 to 15 years: measured versus predicted data. *Acta Paediatr* 2004;93(6):739-46.
14. Schofield WN. Predicting basal metabolic rate, new standards and review of previous work. *Human nutrition Clinical nutrition* 1985;39 Suppl 1:5-41.
15. Henry CJ. Basal metabolic rate studies in humans: measurement and development of new equations. *Public Health Nutr* 2005;8(7A):1133-52.
16. Harris JA, Benedict FG. A Biometric Study of Human Basal Metabolism. *Proceedings of the National Academy of Sciences of the United States of America* 1918;4(12):370-3.
17. Bochukova E, Schoenmakers N, Agostini M, et al. A mutation in the thyroid hormone receptor alpha gene. *The New England journal of medicine* 2012;366(3):243-9.
18. Ji H, Weatherall P, Adams-Huet B, et al. Increased skeletal muscle volume in women with familial partial lipodystrophy, Dunnigan variety. *The Journal of clinical endocrinology and metabolism* 2013;98(8):E1410-3.
19. Savage DB, Murgatroyd PR, Chatterjee VK, et al. Energy expenditure and adaptive responses to an acute hypercaloric fat load in humans with lipodystrophy. *The Journal of clinical endocrinology and metabolism* 2005;90(3):1446-52.
20. Pan DA, Lillioja S, Kriketos AD, et al. Skeletal muscle triglyceride levels are inversely related to insulin action. *Diabetes* 1997;46(6):983-8.
21. Pinyerd B, Zipf WB. Puberty-timing is everything! *J Pediatr Nurs* 2005;20(2):75-82.
22. Abreu AP, Kaiser UB. Pubertal development and regulation. *Lancet Diabetes Endocrinol* 2016;4(3):254-64.
23. Choi JH, Yoo HW. Control of puberty: genetics, endocrinology, and environment. *Curr Opin Endocrinol Diabetes Obes* 2013;20(1):62-8.
24. Plant TM. Neuroendocrine control of the onset of puberty. *Frontiers in neuroendocrinology* 2015;38:73-88.
25. Mitchell CS, Savage DB, Dufour S, et al. Resistance to thyroid hormone is associated with raised energy expenditure, muscle mitochondrial uncoupling, and hyperphagia. *The Journal of clinical investigation* 2010;120(4):1345-54.

European Journal of Clinical Nutrition (2014) 68, 234–240

www.nature.com/ejcn

OPEN

ORIGINAL ARTICLE

An approach to quantifying abnormalities in energy expenditure and lean mass in metabolic disease

LPE Watson[1], P Raymond-Barker[1], C Moran[2], N Schoenmakers[2], C Mitchell[2], L Bluck[1,3], VK Chatterjee[2], DB Savage[2] and PR Murgatroyd[1,2]

BACKGROUND/OBJECTIVES: The objective of this study was to develop approaches to expressing resting energy expenditure (REE) and lean body mass (LM) phenotypes of metabolic disorders in terms of *Z*-scores relative to their predicted healthy values.
SUBJECTS/METHODS: Body composition and REE were measured in 135 healthy participants. Prediction equations for LM and REE were obtained from linear regression and the range of normality by the standard deviation of residuals. Application is demonstrated in patients from three metabolic disorder groups (lipodystrophy, $n = 7$; thyrotoxicosis, $n = 16$; and resistance to thyroid hormone (RTH), $n = 46$) in which altered REE and/or LM were characterised by departure from the predicted healthy values, expressed as a *Z*-score.
RESULTS: REE (kJ/min) $= -0.010 \times$ age (years) $+ 0.016 \times$ FM (kg) $+ 0.054 \times$ fat-free mass (kg) $+ 1.736$ ($R^2 = 0.732$, RSD $= 0.36$ kJ/min). LM (kg) $= 5.30 \times$ bone mineral content (kg) $+ 10.66 \times$ height^2 (m) $+ 6.40$ (male). LM (kg) $= 0.20 \times$ fat (kg) $+ 14.08 \times$ height^2 (m) $- 2.93$ (female). (male $R^2 = 0.55$, RSD $= 3.90$ kg; female $R^2 = 0.59$, RSD $= 3.85$ kg). We found average *Z*-scores for REE and LM of 1.77 kJ/min and -0.17 kg in the RTH group, 5.82 kJ/min and -1.23 kg in the thyrotoxic group and 2.97 kJ/min and 4.20 kg in the LD group.
CONCLUSION: This approach enables comparison of data from individuals with metabolic disorders with those of healthy individuals, describing their departure from the healthy mean by a *Z*-score.

European Journal of Clinical Nutrition (2014) **68,** 234–240; doi:10.1038/ejcn.2013.237; published online 27 November 2013

Keywords: resting energy expenditure; lean mass; body composition; *Z*-score; metabolic disease

INTRODUCTION

Many metabolic disorders such as thyroid disease or lipodystrophy (LD) are associated with changes in body composition, energy expenditure or both.[1,2] In describing the phenotypes of such conditions, it is often desirable to describe the extent to which body composition or energy metabolism deviates from that of healthy individuals, but this is not always straight forward. Comparisons against standard predictions of energy expenditure[3–5] may be compromised by atypical body composition, whereas comparisons based on body composition proxies such as body mass index (BMI) may not reveal unusual relationships between fat and lean masses.

Commonly used predictions of resting energy expenditure (REE) may be troublesome owing to their dependence on age and gender, as well as body mass and height.[6] Their piecewise linear nature can lead to substantial differences between predicted REE just above and below the intersection of adjacent regression ranges. The use of fat-free mass (FFM = lean body mass (LM) + bone mineral content (BMC) in kg) as a predictor of REE is more accurate and is widely accepted[6] and, when allowed an intercept, is disassociated from gender differences in body composition.

Against this background, we have set out an approach to characterise REE and LM in metabolic disorders by reference to measurements in a metabolically healthy cohort. It utilises the accurate and precise measurements of body composition that are now widely available using dual-energy X-ray absorptiometry (DXA).[7–16] The key to our approach has been the description of variability in the difference between measurements and predictions when applied to healthy individuals. This allows us to state with confidence where an individual data point observed in a metabolic disorder lies relative to the healthy range, and so to discuss whether a disorder presents with altered REE or body composition phenotype, or indeed both.

Three conditions (resistance to thyroid hormone (RTH), thyrotoxicosis and LD) in which abnormal energy expenditure and/or increased lean body mass (LM) have been previously documented provide ideal examples to illustrate our method. RTH is a rare genetic condition, with an incidence of 1 in 40 000,[17,18] that is characterised by elevated circulating thyroid hormones (THs) together with central (hypothalamopituitary) and variable peripheral tissue refractoriness to thyroid hormones. More than 90% of affected individuals with RTH have an identified mutation in the *THRB* gene.[19] Thyrotoxicosis (or hyperthyroidism, by which it is known interchangeably) is due to excess TH secretion from the thyroid gland. Most commonly (50–80% of cases), thyrotoxicosis is caused by Graves' disease, which affects $\sim 0.5\%$ of the population,[20] and is due to autoantibodies causing excess TH production by stimulating the thyroid-stimulating hormone (TSH) receptor in the thyroid gland.[21] LD can be either genetic or acquired[22] and is characterised by reduced adipocyte storage capacity and loss of adipose tissue with significantly increased LM,

[1]NIHR/Wellcome Trust Clinical Research Facility, Addenbrooke's Hospital, Cambridge, UK; [2]University of Cambridge Metabolic Research Laboratories, Wellcome Trust-MRC Institute of Metabolic Science, Addenbrookes Hospital, Cambridge, UK and [3]MRC-Human Nutrition Research, Elsie Widdowson Laboratory, Cambridge, UK. Correspondence: LPE Watson, NIHR/Wellcome Trust Clinical Research Facility, Box 127, Addenbrooke's Hospital, Cambridge CB2 0QQ, UK.
E-mail: lpew2@medschl.cam.ac.uk
Received 28 May 2013; revised 25 September 2013; accepted 27 September 2013; published online 27 November 2013

contributing to metabolic complications such as insulin resistance and diabetes mellitus.[23] We have extensive data in these disorders, which are of particular interest to us, and so have invoked them here for demonstration, although we believe our approach is more generally applicable.

SUBJECTS AND METHODS

Healthy volunteers were recruited by local advertisement in the East Anglian region of the United Kingdom. We recruited 135 male and female non-smokers, aged between 17 and 65 years who had no known medical conditions, were not taking any medications or supplements likely to influence energy expenditure or body composition and who did not normally exercise for over an hour a day. Volunteers were from different ethnic backgrounds (126 Caucasian, 2 Black, 6 Asian, and 1 Hispanic). All participants provided written, informed consent.

Volunteers from the metabolic disorder groups (LD, $n = 7$; thyrotoxicosis, $n = 16$; and RTH, $n = 46$) were recruited following referral to Addenbrooke's Hospital and provided written informed consent to participation in their studies. Participants were non-smoking, not on any β-blockers or antiarrhythmic treatment and had no current or past history of eating disorder. All patients with RTH had a mutation identified in the *THRB* gene. Thyrotoxic patients were identified based on thyroid function tests suggestive of thyroxicosis (serum TSH < 0.03 mU/l, free thyroxine (T4) > 22.5 pmol/l) and had Graves' disease, as evidenced by elevated anti-TSH receptor antibody titres. Details on the recruitment of the lipodystrophic participants have been documented previously.[24]

Healthy participants and metabolically disordered participants were asked to refrain from strenuous physical activity, alcohol and caffeine for 24 h before their visit. Each participant arrived at the NIHR/Wellcome Trust Clinical Research Facility in Cambridge at 1400 hours on day 0 and remained until 1200 hours on day 1. After informed consent and medical examination on day 0, height, weight and body composition were measured. Body composition (fat mass, lean mass and bone mineral density) was assessed by DXA (GE Lunar Prodigy GE Healthcare, Madison, WI, USA; software version 12.2). At 1800 hours, a standardised dinner was served. The energy content of the meal was 1/3 of a participant's daily requirements estimated from predicted resting metabolic rate[3] multiplied by an activity factor of 1.35.[25] Meal composition was 30–35% fat, 12–15% protein and 50–55% carbohydrate by energy. The participant retired to bed at 2300 hours and was woken the next morning at 0700 hours. REE was measured between 0700 and 0800 hours by ventilated canopy respiratory gas exchange (GEM; GEMNutrition, Daresbury, UK). Measurements were recorded at 30 s intervals over 20 min. The LD participants' REE was measured by indirect room calorimetry for 60 min and has been described previously.[24] All participants were asked to remain awake and still, without any interactions, for the duration of the measurement. Energy expenditure was calculated from the macronutrient respiratory quotients and energy equivalents of oxygen published by Elia and Livesey.[26] Following the REE measurement, fasting blood samples were taken for renal and liver function tests, plasma glucose and thyroid function (free triiodothyronine (T3), T4 and TSH). Urinary metanephrines were also measured.

Body composition and REE measurements were performed in all healthy and metabolically disordered volunteers and are summarised in Supplementary Table 1, Table 1 and Table 2.

Ethics

The study received a favourable opinion from the Cambridge Central East of England Research Ethics Committee and was funded by and conducted in the NIHR/Wellcome Trust Clinical Research Facility (WTCRF, Cambridge, UK).

Statistical analysis

Multiple correlation analyses were undertaken using SPSS19 (SPSS Inc., Chicago, IL, USA) to identify variables or combinations of variables that correlate ($P < 0.05$) to REE and DXA-measured total body LM.

Once the correlating variables were established, forward stepwise multiple linear regression analysis was performed to relate REE (kJ/min) to FFM (kg), FM (kg) and age in all subjects and to relate LM to FM and height for female subjects and LM to height and BMC in male subjects.

Table 2. Characteristics of the lipodystrophy group

Variable	*Male* (n = 2) *Mean ± s.d.*	*Female* (n = 5) *Mean ± s.d.*
Age (years)	34.2 ± 23.5	48.8 ± 13.2
Height (m)	1.75 ± 0.13	1.64 ± 0.05
Weight (kg)	78.8 ± 13.0	66.2 ± 6.9
BMI (kg/m^2)	25.8 ± 0.3	24.5 ± 2.4
FM (kg)	5.6 ± 2.9	9.3 ± 6.8
LM (kg)	70.0 ± 10.5	54.2 ± 6.2
FFM (kg)	73.3 ± 10.1	56.9 ± 6.0
BMC (kg)	3.2 ± 0.4	2.7 ± 0.6
REE (kJ/min)	6.3 ± 0.9	5.6 ± 0.7
TSH (mU/l)	1.2 ± 0.1	0.7 ± 0.4
Plasma glucose (mmol/l)	10.4 ± 3.3	6.9 ± 4.5

Abbreviations: BMC, bone mineral content; BMI, body mass index; FFM, fat-free mass; FM, fat mass; LM, lean mass; REE, resting energy expenditure; TSH, thyroid-stimulating hormone. Free T4 and free T3 measures were not available to report in the lipodystrophy group.

Table 1. Characteristics of the RTH and thyrotoxic groups

Variable	*RTH* (n = 46)		*Thyrotoxicosis* (n = 16)	
	Male (n = 12) *Mean ± s.d.*	*Female* (n = 34) *Mean ± s.d.*	*Male* (n = 6) *Mean ± s.d.*	*Female* (n = 10) *Mean ± s.d.*
Age (years)	38.1 ± 16.8	39.4 ± 13.6	40.7 ± 14.4	45.8 ± 14.2
Height (m)	1.74 ± 0.1	1.61 ± 0.1	1.76 ± 0.1	1.63 ± 0.1
Weight (kg)	72.8 ± 10.4	71.7 ± 14.4	74.1 ± 18.8	64.5 ± 9.4
BMI (kg/m^2)	24.1 ± 3.8	27.6 ± 5.1	23.81 ± 3.6	24.2 ± 3.4
FM (kg)	18.2 ± 8.2	29.7 ± 10.0	20.9 ± 10.6	26.4 ± 7.6
LM (kg)	51.7 ± 4.8	38.6 ± 5.2	50.6 ± 9.6	35.6 ± 5.7
FFM (kg)	54.1 ± 5.1	40.9 ± 5.5	53.1 ± 10.1	38.1 ± 5.8
BMC (kg)	2.4 ± 0.5	2.3 ± 0.4	3.0 ± 0.6	2.5 ± 0.3
REE (kJ/min)	5.2 ± 0.6	4.6 ± 0.7	7.2 ± 1.4	5.5 ± 0.9
TSH (mU/l)	2.2 ± 0.7	3.8 ± 3.4	< 0.03 ± 0.9	< 0.03 ± 0.0
Free T4 (pmol/l)	29.5 ± 5.1	35.1 ± 13.1	47.2 ± 41.5	43.3 ± 19.6
Free T3 (pmol/l)	10.5 ± 1.6	12.7 ± 4.3	22.4 ± 11.1	24.3 ± 11.3
Plasma glucose (mmol/l)	4.7 ± 0.8	5.0 ± 0.5	5.5 ± 0.3	4.9 ± 0.4

Abbreviations: BMC, bone mineral content; BMI, body mass index; FFM, fat-free mass; FM, fat mass; LM, lean mass; REE, resting energy expenditure; RTH, resistance to thyroid hormone; T3, triiodothyronine; T4, thyroxine; TSH, thyroid-stimulating hormone.

A *K*-fold cross-validation approach was then undertaken to test the reliability of both the models. The data set was randomly numbered and split into test data sets and a validation data set. For the REE validation, the analysis was repeated eight times making sure each data point was tested and validated to establish whether the same variables significantly contributed to the prediction of REE, and then the standard deviations of the residuals (the individual differences between predicted and measured values) were compared. For LM cross-validation, the analysis was repeated five times and was also tested on an additional data set of 19 female subjects and 18 male subjects.

Residuals were derived for each contributing data point and normality was confirmed for the set of all residuals using Shapiro–Wilk test for normality. This allowed the distributions of residuals to be described by their standard deviations, the magnitudes of which were taken as a measure of the precision of the prediction. Furthermore, each experimental data point could be defined in terms of the number of standard deviations from the predicted value (*Z*-score). When investigating the disease groups, REE or LM was predicted as though belonging to the healthy cohort, and an associated *Z*-score used as a measure of the deviation from the healthy norm.

RESULTS

Resting energy expenditure

To establish the appropriate variables to include in the prediction of REE, we examined the literature and subsequently explored correlations of REE with age, gender, height^2, bone mass, FFM and FM.

Analysis of variance was carried out to test the effect of ethnicity (white, black and Asian) on REE and LM, and showed that in this group of volunteers there was no effect of ethnicity on REE or LM (REE, $F = 0.286$, LM, $F = 0.921$). Stepwise multiple regression analysis was carried out to establish which correlates contributed significantly to the prediction of REE and LM. Those that did not contribute were excluded (Table 3).

The variables that contributed the least to the prediction of REE were gender ($R^2 = 0.004$), height^2 ($R^2 = 0.005$) and bone mass ($R^2 = 0.002$). With these removed, age continued to contribute to the overall prediction leaving FM ($R^2 = 0.043$), FFM ($R^2 = 0.660$) and age ($R^2 = 0.018$) in the regression ($R^2 = 0.732$). The resulting expression derived from the 135 healthy participants is

$$\mathrm{REE(kJ/min)} = -0.010(\mathrm{age}) + 0.016(\mathrm{FM(kg)}) + 0.054(\mathrm{FFM(kg)}) + 1.736$$

REE regression validation

The regression expression for REE above has been subject to *K*-fold validation. The source data was randomised into eight groups and regressions repeatedly derived from 7×17 and 1×16 subjects and tested in the remaining group. The coefficients of variation for the resulting eight estimates of each regression coefficient were: age 7.3%, FM 12.1%, FFM 2.9% and constant 4.9%. The standard deviation of residuals in the test group for the eight regressions ranged from 0.27 to 0.49 kJ/min compared with 0.36 kJ/min for the whole data set.

Lean mass

The least significant coefficient, age ($P > 0.05$), was taken out of the analysis first. Once this had been removed fat and height^2 were highly significant contributors in female subjects but height^2 alone was significant in male subjects. Bone mass was a significant contributor to LM in male subjects when it replaced FM but this was not the case in female subjects. Therefore, the two gender-specific regression equations for the prediction of LM are as follows:

Male LM (kg) ($n = 47$) $= 5.30 \times$ bone mass (kg) $+ 10.66 \times$ height^2 (m) $+ 6.40$

Female LM (kg) ($n = 88$) $= 0.20 \times$ fat (kg) $+ 14.08 \times$ height^2 (m) $- 2.94$

The standard deviations of residuals for these two regressions are, respectively, 3.90 and 3.85 kg.

Lean mass regression validation

As with the REE validation process, the male and female lean mass regressions have undergone *K*-fold validation, randomised into five groups and the analysis repeated five times. The female results indicated that the standard deviation of residuals ranged from 3.0 to 4.26 kg compared with 3.85 kg from the whole data set. The male results indicated a range of 2.38–4.83 kg compared with 3.90 kg from the whole data set. The data were also tested in independent male and female data sets drawn from the entire control group of another study and its ongoing successor ($n = 18$ males and 19 females). For the male group, the mean residual in the test group is -1.49 kg with s.d. 3.91 kg. The offset of the male mean from zero is predominantly due to a single outlier whose residual was double that of any other subject, yet is not significantly different from zero. For the female group, the mean residual is 0.15 kg (NS) with s.d. 2.2 kg.

Representation of data: *Z*-scores

Resting energy expenditure. To represent the normative data, the residuals of measured REE − predicted REE were plotted with corresponding *Z*-scores (Figure 1). LM, the strongest predictive variable, is used to separate the data points. To assess the utility of this approach in disorder states known to be associated with altered body composition and resting metabolic rate, we characterised patients with RTH, thyrotoxicosis and LD.[1,27] When data from patients with metabolic disorders is represented alongside the healthy volunteer data, clear differences between health and the disorder states emerge (Figure 2). As expected, all the metabolic disease groups manifest elevated REE (mean *Z* RTH: 1.77; LD: 2.97) with the thyrotoxicosis group having the highest REE values with a mean *Z*-score of 5.8 and a range from 1.5 to 9.6.

Lean mass. Supplementary Figure 1 shows the variability in LM within the metabolically healthy male and female subjects. The residuals of the difference between measured and predicted

Table 3. Multiple correlations of measured REE (kJ/min) and LM (kg), with demographic measurements

	Variable	*Age (years)*	*Gender*	*Height^2*	*FM*	*FFM*	*Bone*
REE	Coefficient	−0.133	−0.620	0.675	0.207	0.813	0.740
kJ/min	Sig	0.123	0.000	0.000	0.016	0.000	0.000
LM	Coefficient	0.004	−0.819	0.845	−0.012	1.000	0.805
kg	Sig	0.961	0.000	0.000	0.890	0.000	0.000

Abbreviations: FFM, fat-free mass; FM, fat mass; LM, lean mass; REE, resting energy expenditure. $N = 135$, males $= 47$ and females $= 88$.

LM are again presented together with *Z*-scores. Height was used to separate the points. Figure 2 also demonstrates how metabolic disorders may be characterised by comparison with healthy subject data. The differences between LM in thyrotoxicosis and RTH can be compared with that of the healthy cohort (mean *Z* thyrotoxic: −1.23; RTH: −0.17). The LD data (mean *Z*: 4.20) illustrates the substantial excess of lean tissue present in this disorder.

LM and REE *Z*-scores may be plotted orthogonally, where they combine to offer a succinct insight into the phenotypes of metabolic disorders. Figure 3 illustrates the relationship between changes in REE and LM in metabolic disorders compared with the healthy group. The lipodystrophic group are characterised by elevated LM and elevated REE with *Z*-scores ranging from 2.2 to 7.3 *Z* for LM and 1.4 to 4.8 *Z* for REE. The thyrotoxicosis group also manifest elevated REE (1.5–9.6 *Z*) but, in contrast to the LD group, have reduced LM (mean $Z = -1.2$).

DISCUSSION

The aim of this work was to develop approaches to the description of metabolic phenotypes in terms of the distribution of REE and LM in metabolically healthy people. The novelty of our approach lies in the way in which metabolic and body composition data is represented. Subtracting a predicted value from measured values produces a residual; and dividing this by the standard deviation of residuals in a healthy cohort, we can assign a *Z*-score. *Z*-scores are commonly used in the analysis of bone densitometry[28] and on growth charts to highlight individuals whose results deviate from the population average.[29] Here, we commend the use of *Z*-scores to highlight individuals and groups of patients with abnormal metabolic rates and/or abnormal LM.

Body composition measurements

The body composition measurements on which this paper relies were undertaken by DXA. This is a widely available technique that is able to provide quick and well-tolerated estimates of body composition supported by reports of good accuracy and precision.[7] However, it is important to consider whether any disorder to which our proposed methodology is applied might generate a bias in the DXA measurements relative to the healthy population. The work of Williams *et al.*[30] offers valuable context for this consideration. In the case of our example disorder groups, we do not believe bias in DXA estimates to have been a concern. Body composition data in our most extreme phenotype, LD, was corroborated by air displacement plethysmography measurements.[31]

Resting energy expenditure

The results from the REE multiple regression analysis in this study demonstrate a model that predicts REE accurately and with good precision in healthy individuals. The variables that contribute to

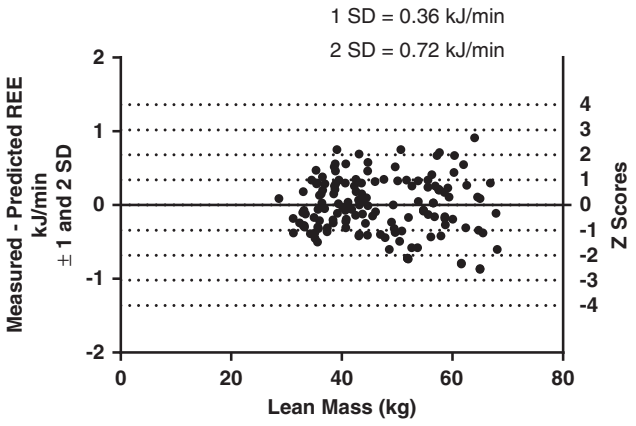

Figure 1. Measured − predicted REE (kJ/min) in healthy controls with 2 s.d.

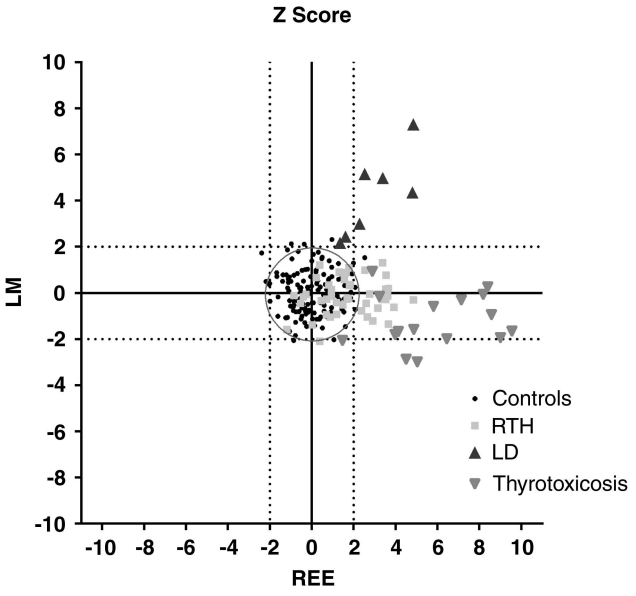

Figure 3. Combination of LM and REE *Z*-scores to illustrate the contribution to metabolic disorders. The circle indicates a *Z*-score of ±2 for REE and LM.

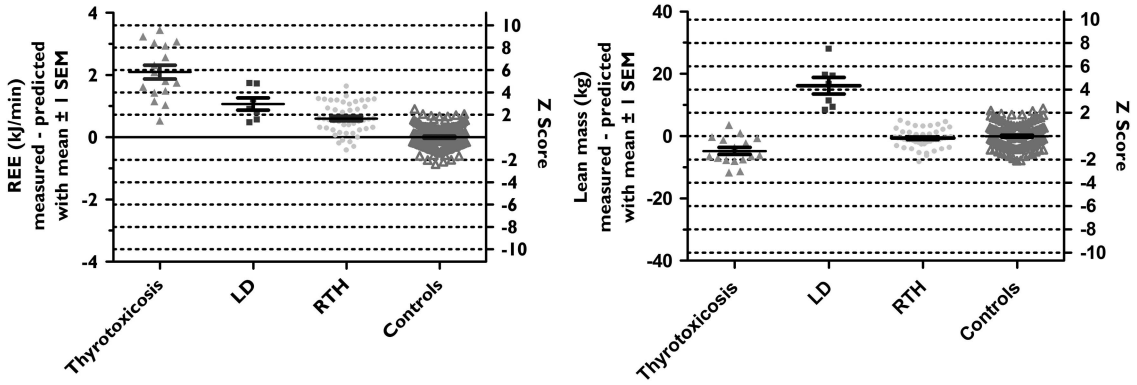

Figure 2. Differences between measured and predicted REE and LM in metabolic disorders and the healthy cohort.

our predictive equation are FFM, FM and age. These have previously been documented as appropriate covariates.[6,32–34] FFM is recognised as the main predictor of the interindividual variability in resting energy expenditure. The relationship between FFM and REE differs between men and women when constrained through the origin, as is implicit when REE is expressed per unit FFM. However, in preparing this work, we have confirmed that when an intercept is allowed, men and women tend to fall on the same regression line. Moreover, the relationship between REE and FFM is strengthened and therefore allows one regression equation for both genders. There is, however, conflicting literature regarding the contribution of FM to energy expenditure. In a review, Cunningham[6] suggested that FM contributes to energy expenditure in women, but mostly in obese women. Our study found that FM explained 4.0% of the variance in energy expenditure and when the analysis was broken down by gender there was no significant difference in the variance explained by FM between male and female subjects, even though we had a greater number of female subjects in the cohort. The most commonly used predictive equations for estimating energy expenditure in a clinical setting are Schofield and Henry.[3,5] They include simple measurements such as height and weight, age and gender, regardless of literature that disputes their accuracy and precision, especially when applied to individuals outside the original data sets.[35,36] Weijs *et al.*[37] performed a meta-analysis of common REE prediction equations on 48 outpatients and 45 in-patients with conditions including anorexia, overweight, thyroid disease and inflammatory bowel disease, all of which have body compositions and energy expenditures differing from healthy controls.[38–42] They saw errors ranging from 975 to 1782 kJ per day, with at most only 40% of in-patients having an accurately predicted REE when compared with measured REE. Johnstone *et al.*[43] demonstrated an average increase in accuracy of 32.9% (240 kJ per day) when including body composition (FFM and FM) and anthropometric measurements (skinfold thickness and circumference) compared with the Schofield equation.[3]

FFM and FM may explain between 60 and 85% of the variance in REE,[6] leaving at least 15% unaccounted for. Our results demonstrated that FFM and FM combined account for 70%, leaving 30% unexplained. Age, gender, ethnicity and physical activity have been reported to contribute to this variance.[33] In our study, we found a significant but small contribution of age to the prediction of REE (2%). Nielsen *et al.*[32] investigated whether adjusting FFM for extracellular fluid would improve the prediction of REE, but found that this was not the case. Johnstone *et al.*[44] investigated the influence of FFM, FM, age, T4, T3 and leptin levels on REE. They concluded that REE was not influenced by age, gender, leptin or T3, although in men 25% of the variance was associated with circulating T4 levels.

Lean mass

Predictions of FFM or LM are less frequently documented. Previous publications predicting LM have used bioelectrical impedance and skinfold thickness with DXA acting as the reference measurement.[45] The variables chosen for the LM prediction equation in the current study were height^2 and FM for the female group and height^2 and bone mass for the male group. The presence of height^2 in the equation reflects the fat and FFM index concept,[46,47] which recognises a relationship between body composition and in body size and offers the prospect of discrimination between health and individuals with abnormal fat or FFM for their size.

Cross-validation

To test our prediction equations, we performed an observational analysis of the coefficients from published studies that have also used FM, FFM and age as variables for prediction of REE (Supplementary Table 2). Supplementary Table 2 suggests that our coefficients for FFM, FM and age are similar to those published previously.[6,32,48–50] Of this published work, only Nielson's[32] used DXA for composition measurement; Horrie used bioimpedance,[49] whereas Nelson *et al.*'s[48] and Cunningham's[6] papers were based on data previously published by others. When applied to the current data set, the Nielsen equations produced a residual standard deviation of 0.37 compared with 0.36 produced by our equation. In the light of this sparsity of robust comparative data, we performed a *K*-fold cross-validation analysis on REE and LM models to test their reliability. Comparison of means and standard deviations of residuals in these test groups with those of the training groups suggests that the regressions may be applied beyond the training group with some confidence, although we accept that testing in a larger group would increase this confidence. We would encourage readers who would like to apply our approaches to derive and publish prediction regressions from their own reference cohorts until such time as the published coefficients have converged to a closer consensus than we have presented in Supplementary Table 2—perhaps when published predictions agree to within 1 pooled standard deviation of their residuals.

Application examples

Thyroid disorders. Thyroid conditions such as thyrotoxicosis and RTH result in altered body composition and a raised energy expenditure. Mitchell *et al.*[40] showed that REE is raised in RTH and markedly elevated in thyrotoxic patients. In both conditions there was a higher fat-to-lean mass ratio compared with the healthy controls, although the data suggest that in thyroid disorders the dominant abnormality lies in REE rather than body composition. Our results from the lean mass regression equation suggest that the thyrotoxic group have reduced LM ($Z = -1.23$), whereas the RTH group have normal LM ($Z = -0.17$) despite the increased REE.

Our results confirm that REE is higher in a cohort of RTH subjects compared with healthy controls; however, in patients with thyrotoxicosis, the magnitude of elevation in REE is more substantial. In RTH, predominant expression of defective thyroid receptor-β in the hypothalamus and pituitary mediates resistance to hormone action within the pituitary–thyroid feedback axis, resulting in elevated levels of circulating free T4 and T3 with normal or increased levels of TSH.[51] Energy expenditure is raised as some peripheral tissues (e.g. myocardium, skeletal muscle) that express normal thyroid receptor-α retain sensitivity to elevated levels of TH.[40] In contrast, both β- and α-receptor-mediated signalling is intact in conventional thyrotoxicosis, with preserved responsiveness of tissues to elevated TH, resulting in markedly increased energy expenditure, despite a reduction in LM.[52]

Lipodystrophy. Lipodystrophic subjects are characterised by an elevated REE and LM.[24] Importantly, this is not simply a result of a relative reduction in fat mass, which is present in all of these patients, but appears to be a true increase in lean mass. Although organomegaly and pseudoacromegaly are features of LD (particularly the generalised form),[22] the increased lean mass probably reflects contributions from several tissues. Organ tissue will have some contribution to the estimation of lean mass, although it has a relatively small mass of approximately 4.4 kg,[34] whereas skeletal muscle mass is almost certainly the largest contributing tissue. We show a mean residual increase of lean mass of 16 kg (Z-score > 4) relative to our healthy cohort, suggesting an increase in lean mass over an above that expected through organ contribution. Savage *et al.*[24] investigated the increase in REE in the lipodystrophic participants and concluded that the increase in lean mass in LD patients accounted for their elevated REE. When REE was presented per kg of LM, there was no significant difference

between REE in lipodystrophics and healthy matched controls. However, this picture changes when the relationship between REE and LM is allowed an intercept, and changes further when fat mass contributes to the model. We have found an elevation in REE with a *Z*-score averaging 2 (range 1.4–4.8 kJ/min) relative to our healthy controls (Figure 2). As our prediction of REE takes into account the influence of measured FFM, our approach arguably removes any coupling between departures from the norm in REE and FFM, so our *Z*-scores are effectively independent. In doing so, it suggests that there may be a component of the elevation in REE in LD beyond that which is associated with FFM alone.

As mentioned in the methods, the lipodystrophic participants had REE measured by room calorimetry rather than the ventilated canopy measurement. In the light of this, we investigated the difference between measurements made using the canopy compared with room calorimetry, on a separate cohort. The results indicated a difference of 0.20 kJ/min between the two methods, suggesting that even after accounting for this difference in measurement the lipodystrophic participants would still display an REE *Z*-score >2 (mean *Z*: 2.98 kJ/min).

In summary, we offer expressions for REE and LM in health based on FM, FFM, BMC, age and height^2 measurements. Measurements from individuals with uncommon metabolic disorders were examined in the context of data from healthy subjects and differences to be expressed as a *Z*-score. This facilitates the representation and differentiation of disease phenotypes. This approach may also aid in the characterisation and potentially evaluation of the treatment in such individuals. Further validation of our regressions on a separate cohort of healthy individuals is desirable, but we believe the *Z*-score approach to metabolic phenotype description will prove valuable and illuminating in these and other metabolic disorders.

CONFLICT OF INTEREST

The authors declare no conflict of interest.

ACKNOWLEDGEMENTS

We thank Elizabeth Blower for assistance in data collection, and all the staff of the NIHR/Wellcome Trust Clinical Research Facility Cambridge for their assistance with the clinical studies. We particularly thank the volunteers who contributed their time and measurements to our research. This study was supported by the NIHR/Wellcome Trust Clinical Research Facility. DBS (078986/Z/06/Z), VKC (095564/Z/11/Z) and NS (100585/Z/12/Z) are supported by the Wellcome Trust, the Medical Research Council Centre for Obesity and Related Disorders, NIHR Cambridge Biomedical Research Centre. LB is supported by the UK Medical Research Council programme number MC_UP_A090_1005.

AUTHOR CONTRIBUTIONS

The authors' responsibilities were as follows: LW—conducted research, analysed data and performed statistical analysis, drafted of manuscript, primary responsibility for the final content; PRB—conducted research, statistical analysis, revision of the manuscript and important intellectual contributions; CM, NS, CM, LB, DBS—critical revision of the manuscript and important intellectual contributions, KC—critical revision of the manuscript, important intellectual contributions and supervision; and PRM—study concept and design, critical revision of the manuscript, important intellectual contributions, analysis and interpretation. All authors read and approved the final manuscript. LB's contribution formed part of the Medical Research Council programme number SPT60.

REFERENCES

1 Savage DB, Semple RK, Clatworthy MR, Lyons PA, Morgan BP, Cochran EK *et al.* Complement abnormalities in acquired lipodystrophy revisited. *J Clin Endocrinol Metab* 2009; **94**: 10–16.
2 Psota T, Chen KY. Measuring energy expenditure in clinical populations: rewards and challenges. *Eur J Clin Nutr* 2013; **67**: 436–442.
3 Schofield WN. Predicting basal metabolic rate, new standards and review of previous work. *Hum Nutr Clin Nutr* 1985; **39**(Suppl 1): 5–41.
4 Harris JA, Benedict FG. A biometric study of human basal metabolism. *Proc Natl Acad Sci USA* 1918; **4**: 370–373.
5 Henry CJ. Basal metabolic rate studies in humans: measurement and development of new equations. *Public Health Nutr* 2005; **8**: 1133–1152.
6 Cunningham JJ. Body composition as a determinant of energy expenditure: a synthetic review and a proposed general prediction equation. *Am J Clin Nutr* 1991; **54**: 963–969.
7 Withers RT, LaForgia J, Pillans RK, Shipp NJ, Chatterton BE, Schultz CG *et al.* Comparisons of two-, three-, and four-compartment models of body composition analysis in men and women. *J Appl Physiol* 1998; **85**: 238–245.
8 Cordero-MacIntyre ZR, Peters W, Libanati CR, Espana RC, Abila SO, Howell WH *et al.* Reproducibility of DXA in obese women. *J Clin Densitometry* 2002; **5**: 35–44.
9 Genton L, Karsegard VL, Zawadynski S, Kyle UG, Pichard C, Golay A *et al.* Comparison of body weight and composition measured by two different dual energy X-ray absorptiometry devices and three acquisition modes in obese women. *Clin Nutr* 2006; **25**: 428–437.
10 Arngrimsson S, Evans EM, Saunders MJ, Ogburn III CL, Lewis RD, Cureton KJ. Validation of body composition estimates in male and female distance runners using estimates from a four-component model. *Am J Hum Biol* 2000; **12**: 301–314.
11 Chen Z, Wang Z, Lohman T, Heymsfield SB, Outwater E, Nicholas JS *et al.* Dual-energy X-ray absorptiometry is a valid tool for assessing skeletal muscle mass in older women. *J Nutr* 2007; **137**: 2775–2780.
12 Deurenberg-Yap M, Schmidt G, van Staveren WA, Hautvast JG, Deurenberg P. Body fat measurement among Singaporean Chinese, Malays and Indians: a comparative study using a four-compartment model and different two-compartment models. *Br J Nutr* 2001; **85**: 491–498.
13 Goran MI, Toth MJ, Poehlman ET. Assessment of research-based body composition techniques in healthy elderly men and women using the 4-compartment model as a criterion method. *Int J Obes Relat Metab Disord* 1998; **22**: 135–142.
14 Van Der Ploeg GE, Withers RT, Laforgia J. Percent body fat via DEXA: comparison with a four-compartment model. *J Appl Physiol* 2003; **94**: 499–506.
15 Visser M, Fuerst T, Lang T, Salamone L, Harris TB. Validity of fan-beam dual-energy X-ray absorptiometry for measuring fat-free mass and leg muscle mass. Health, Aging, and Body Composition Study—Dual-Energy X-ray Absorptiometry and Body Composition Working Group. *J Appl Physiol* 1999; **87**: 1513–1520.
16 Silva AM, Heymsfield SB, Sardinha LB. Assessing body composition in taller or broader individuals using dual-energy X-ray absorptiometry: a systematic review. *Eur J Clin Nutr* 2013; **67**: 1012–1021.
17 Lafranchi SH, Snyder DB, Sesser DE, Skeels MR, Singh N, Brent GA *et al.* Follow-up of newborns with elevated screening T4 concentrations. *J Pediatr* 2003; **143**: 296–301.
18 Chiesa A, Olcese MC, Papendieck P, Martinez A, Vieites A, Bengolea S *et al.* Variable clinical presentation and outcome in pediatric patients with resistance to thyroid hormone (RTH). *Endocrine* 2012; **41**: 130–137.
19 Weiss RE, Refetoff S. Resistance to thyroid hormone. *Rev Endocr Metab Disord* 2000; **1**: 97–108.
20 Brent GA. Clinical practice. Graves' disease. *N Engl J Med* 2008; **358**: 2594–2605.
21 Weetman AP. Graves' disease. *N Engl J Med* 2000; **343**: 1236–1248.
22 Garg A. Clinical review#: Lipodystrophies: genetic and acquired body fat disorders. *J Clin Endocrinol Metab* 2011; **96**: 3313–3325.
23 Simha V, Garg A. Lipodystrophy: lessons in lipid and energy metabolism. *Curr Opin Lipidol* 2006; **17**: 162–169.
24 Savage DB, Murgatroyd PR, Chatterjee VK, O'Rahilly S. Energy expenditure and adaptive responses to an acute hypercaloric fat load in humans with lipodystrophy. *J Clin Endocrinol Metab* 2005; **90**: 1446–1452.
25 Westerterp KR. Obesity and physical activity. *Int J Obes Relat Metab Disord* 1999; **23**(Suppl 1): 59–64.
26 Elia M, Livesey G. Energy expenditure and fuel selection in biological systems: the theory and practice of calculations based on indirect calorimetry and tracer methods. *World Rev Nutr Diet* 1992; **70**: 68–131.
27 Chatterjee VKK. Resistance to thyroid hormone. *Hormone Res* 1997; **48**: 43–46.
28 Ellis KJ, Shypailo RJ, Hardin DS, Perez MD, Motil KJ, Wong WW *et al. Z* score prediction model for assessment of bone mineral content in pediatric diseases. *J Bone Miner Res* 2001; **16**: 1658–1664.
29 Ogden CL, Kuczmarski RJ, Flegal KM, Mei Z, Guo S, Wei R *et al.* Centers for Disease Control and Prevention 2000 Growth Charts for the United States: Improvements to the 1977 National Center for Health Statistics Version. *Pediatrics* 2002; **109**: 45–60.
30 Williams JE, Wells JC, Wilson CM, Haroun D, Lucas A, Fewtrell MS. Evaluation of Lunar Prodigy dual-energy X-ray absorptiometry for assessing body composition in healthy persons and patients by comparison with the criterion 4-component model. *Am J Clin Nutr* 2006; **83**: 1047–1054.

31 Fields DA, Goran MI, McCrory MA. Body-composition assessment via air-displacement plethysmography in adults and children: a review. *Am J Clin Nutr* 2002; **75**: 453–467.
32 Nielsen S, Hensrud DD, Romanski S, Levine JA, Burguera B, Jensen MD. Body composition and resting energy expenditure in humans: role of fat, fat-free mass and extracellular fluid. *Int J Obes Relat Metab Disord* 2000; **24**: 1153–1157.
33 Ravussin E, Bogardus C. Relationship of genetics, age, and physical fitness to daily energy expenditure and fuel utilization. *Am J Clin Nutr* 1989; **49**(Suppl): 968–975.
34 Hunter GR, Weinsier RL, Gower BA, Wetzstein C. Age-related decrease in resting energy expenditure in sedentary white women: effects of regional differences in lean and fat mass. *Am J Clin Nutr* 2001; **73**: 333–337.
35 Horgan GW, Stubbs J. Predicting basal metabolic rate in the obese is difficult. *Eur J Clin Nutr* 2003; **57**: 335–340.
36 Scalfi L, Marra M, De Filippo E, Caso G, Pasanisi F, Contaldo F. The prediction of basal metabolic rate in female patients with anorexia nervosa. *Int J Obes Relat Metab Disord* 2001; **25**: 359–364.
37 Weijs PJ, Kruizenga HM, van Dijk AE, van der Meij BS, Langius JA, Knol DL *et al.* Validation of predictive equations for resting energy expenditure in adult outpatients and inpatients. *Clin Nutr* 2008; **27**: 150–157.
38 El Ghoch M, Alberti M, Capelli C, Calugi S, Dalle Grave R. Resting energy expenditure in anorexia nervosa: measured versus estimated. *J Nutr Metab* 2012; **2012**: 652932.
39 Sasaki M, Johtatsu T, Kurihara M, Iwakawa H, Tanaka T, Bamba S *et al.* Energy expenditure in Japanese patients with severe or moderate ulcerative colitis. *J Clin Biochem Nutr* 2010; **47**: 32–36.
40 Mitchell CS, Savage DB, Dufour S, Schoenmakers N, Murgatroyd P, Befroy D *et al.* Resistance to thyroid hormone is associated with raised energy expenditure, muscle mitochondrial uncoupling, and hyperphagia. *J Clin Invest* 2010; **120**: 1345–1354.
41 Herwig A, Ross AW, Nilaweera KN, Morgan PJ, Barrett P. Hypothalamic thyroid hormone in energy balance regulation. *Obes Facts* 2008; **1**: 71–79.
42 Ahmad A, Duerksen DR, Munroe S, Bistrian BR. An evaluation of resting energy expenditure in hospitalized, severely underweight patients. *Nutrition* 1999; **15**: 384–388.
43 Johnstone AM, Rance KA, Murison SD, Duncan JS, Speakman JR. Additional anthropometric measures may improve the predictability of basal metabolic rate in adult subjects. *Eur J Clin Nutr* 2006; **60**: 1437–1444.
44 Johnstone AM, Murison SD, Duncan JS, Rance KA, Speakman JR. Factors influencing variation in basal metabolic rate include fat-free mass, fat mass, age, and circulating thyroxine but not sex, circulating leptin, or triiodothyronine. *Am J Clin Nutr* 2005; **82**: 941–948.
45 Stewart AD, Hannan WJ. Prediction of fat and fat-free mass in male athletes using dual X-ray absorptiometry as the reference method. *J Sports Sci* 2000; **18**: 263–274.
46 Dulloo AG, Jacquet J, Solinas G, Montani JP, Schutz Y. Body composition phenotypes in pathways to obesity and the metabolic syndrome. *Int J Obes (Lond)* 2010; **34**(Suppl 2): S4–S17.
47 VanItallie TB, Yang MU, Heymsfield SB, Funk RC, Boileau RA. Height-normalized indices of the body's fat-free mass and fat mass: potentially useful indicators of nutritional status. *Am J Clin Nutr* 1990; **52**: 953–959.
48 Nelson KM, Weinsier RL, Long CL, Schutz Y. Prediction of resting energy expenditure from fat-free mass and fat mass. *Am J Clin Nutr* 1992; **56**: 848–856.
49 Horie LM, Gonzalez MC, Torrinhas RS, Cecconello I, Waitzberg DL. New specific equation to estimate resting energy expenditure in severely obese patients. *Obesity (Silver Spring, MD)* 2011; **19**: 1090–1094.
50 Cunningham JJ. A reanalysis of the factors influencing basal metabolic rate in normal adults. *Am J Clin Nutr* 1980; **33**: 2372–2374.
51 Chatterjee VK, Nagaya T, Madison LD, Datta S, Rentoumis A, Jameson JL. Thyroid hormone resistance syndrome. Inhibition of normal receptor function by mutant thyroid hormone receptors. *J Clin Invest* 1991; **87**: 1977–1984.
52 Acotto CG, Niepomniszcze H, Mautalen CA. Estimating body fat and lean tissue distribution in hyperthyroidism by dual-energy X-ray absorptiometry. *J Clin Densitometry* 2002; **5**: 305–311.

Supplementary Information accompanies this paper on European Journal of Clinical Nutrition website (http://www.nature.com/ejcn)

Journal of Clinical Densitometry: Assessment & Management of Musculoskeletal Health, vol. 20, no. 4, 498–506, 2017

1094-6950/20:498–506/$36.00
https://doi.org/10.1016/j.jocd.2017.06.029

Original Article

An Investigation Into the Differences in Bone Density and Body Composition Measurements Between 2 GE Lunar Densitometers and Their Comparison to a 4-Component Model

Laura P. E. Watson,[*,1] *Michelle C. Venables,*[2] *and Peter R. Murgatroyd*[1]

[1]*NIHR/Wellcome Trust Clinical Research Facility, Addenbrooke's Hospital, Cambridge, UK; and* [2]*MRC-Elsie Widdowson Laboratory, Cambridge, UK*

Abstract

We describe a study to assess the precision of the GE Lunar iDXA and the agreement between the iDXA and GE Lunar Prodigy densitometers for the measurement of regional- and total-body bone and body composition in normal to obese healthy adults. We compare the whole-body fat mass by dual-energy X-ray absorptiometry (DXA) to measurements by a 4-component (4-C) model. Sixty-nine participants, aged 37 ± 12 yr, with a body mass index of 26.2 ± 5.1 kg/cm^2, were measured once on the Prodigy and twice on the iDXA. The 4-C model estimated fat mass from body mass, total body water by deuterium dilution, body volume by air displacement plethysmography, and bone mass by DXA. Agreements between measurements made on the 2 instruments and by the 4-C model were analyzed by Bland-Altman and linear regression analyses. Where appropriate, translational cross-calibration equations were derived. Differences between DXA software versions were investigated. iDXA precision was less than 2% of the measured value for all regional- and whole-body bone and body composition measurements with the exception of arm fat mass (2.28%). We found significant differences between iDXA and Prodigy ($p < 0.05$) whole-body and regional bone, fat mass (FM), and lean mass, with the exception of hip bone mass, area and density, and spine area. Compared to iDXA, Prodigy overestimated FM and underestimated lean mass. However, compared to 4-C, iDXA showed a smaller bias and narrower limits of agreement than Prodigy. No significant differences between software versions in FM estimations existed. Our results demonstrate excellent iDXA precision. However, significant differences exist between the 2 GE Lunar instruments, Prodigy and iDXA measurement values. A divergence from the reference 4-C observations remains in FM estimations made by DXA even following the recent advances in technology. Further studies are particularly warranted in individuals with large FM contents.

Key Words: Accuracy; DXA; fat mass; 4-component model; total body water.

Received 03/3/17; Revised 06/23/17; Accepted 06/27/17.

Author contributions: The authors' responsibilities were as follows: LPEW—study concept and design, conduct of the research, analysis and interpretation of data, drafting of the manuscript, and primary responsibility for the final content; MCV—critical revision of the manuscript and important intellectual contributions; PRM—critical revision of the manuscript and important intellectual contributions. All authors read and approved the final manuscript.

*Address correspondence to: Laura Watson, MSc, NIHR/Wellcome Trust Clinical Research Facility, Addenbrooke's Hospital, Box 127, Cambridge, UK. E-mail: lpew2@medschl.cam.ac.uk

Introduction

Dual-energy X-ray absorptiometry (DXA) is widely used for bone density measurements within the clinical environment. Within the research community, there is perhaps more emphasis on body composition measurement, driven by the increasing prevalence of obesity. In both contexts, the ability to detect changes in measurements is arguably of more interest than the absolute value of the measurement so that an apparent change in bone or fat mass (FM) should not be generated and interpreted falsely.

DXA instruments have improved over time, most evidently in reduced scan times. As the technology has matured, the focus of development has shifted to image quality, which has improved through advances in detector design, yielding a higher pixel density. The major benefits of this technology are better discrimination of bone edges and better imaging of soft tissue, particularly in the thoracic region *(1)*. Both translate to improved repeated measures precision *(2,3)*. These benefits come at the cost of a new instrument, compounded by the complexities of managing the migration from old to new, which involves performing cross-calibration assessments to identify any differences between instruments and to account for them using translational regression equations *(4)*.

The iDXA is the latest densitometer to come from GE Lunar, a development of the GE Lunar Prodigy and Prodigy Advance. A new detector and X-ray filter (producing different energy spectra) provide improved resolution and image quality by better bone edge detection *(1)*. This also suggests there may be improved soft tissue algorithms within the software compared to previous instruments. Repeated measures precision describes the variability between 2 measurements caused by the instrument itself, by repositioning and by operator error, and so sets the threshold for discriminating the biological change between the 2 measurements *(5)*. Several authors have documented the iDXA's enhanced precision for repeated measures compared with previous models *(2,3,6)*.

Here we report an investigation that extends the previously reported work. The primary purpose of the present study was to evaluate the precision and accuracy of the iDXA. Secondly, we aim to produce translational regression equations for relating scans between the Lunar Prodigy and the iDXA. Further, we have determined the accuracy of iDXA-measured FM measurement by comparison with a 4-component model (4-C) *(7)*. The 4-C model is widely accepted as a reference against which the accuracy of other body composition methodologies is evaluated.

Materials and Methods

Participants

Sixty-nine healthy men (n = 33) and women (n = 36) were recruited for the purposes of the present study. Two participants were excluded from the hip analysis, one for poor positioning and one for an artificial joint. One participant was excluded from the total body water (TBW) analysis because of an insufficient sample volume. The demographic data of the cohort are presented in Table 1. All participants were made aware of the risks associated with the measurements and provided informed consent in writing. The participants were healthy, free from disease, and nonsmoking; they were excluded if they were pregnant or receiving any metabolism-influencing medications. The study was approved by the Cambridge Central Ethics Committee.

Each participant arrived at NIHR/Wellcome Trust Clinical Research Facility, Addenbrooke's biomedical campus, Cambridge, at noon on the day of their visit to undertake 3 procedures: total-body water determination using deuterium dilution, DXA, and body volume determination using air displacement plethysmography (ADP). The participants wore light, metal-free clothing and refrained from food and drink for 30 min before and during the measurements.

Protocol

Deuterium Dilution

A baseline saliva sample was obtained from the participants shortly after arrival. Height and weight were then measured. Height was measured on a stadiometer and recorded to the nearest millimeter (SECA 242 digital stadiometer; Seca, Hamburg, Germany). Weight was measured on electronic scales to the nearest gram (Kern & Sohn GmbH, Balingen, Germany). The participant then consumed a dose of 70 mg/kg body mass of ^2H_2O (99.8%; CK

Table 1
Descriptive Data of the Participants

	Males (n = 33)		Females (n = 36)	
	Mean ± SD	Range	Mean ± SD	Range
Age (yr)	38.0 ± 12.0	19.9–65.1	37.8 ± 12.7	19.2–57.9
Height (m)	1.80 ± 0.08	1.62–2.01	1.66 ± 6.7	1.53–1.83
Mass (kg)[a]	81.0 ± 12.0	54.1–106.9	73.9 ± 18.1	49.1–129.6
BMI (kg/m^2)	25.3 ± 3.2	20.2–34.2	27.0 ± 6.3	18.4–47.5
Fat mass (kg) (4-C)	16.8 ± 8.1	4.1–33.4	28.0 ± 14.4	9.57–71.5
% Fat (4-C)	20.1 ± 8.0	5.3–34.4	36.0 ± 9.5	18.5–55.1

Note: 4-C model: n = 68; hip analysis: n = 67; scan mode: standard, n = 65, thick, n = 4.
Abbr: 4-C, 4-component; BMI, body mass index; SD, standard deviation.
[a]Air displacement plethysmography mass.

Isotopes Ltd., Ibstock, Leicestershire, UK) *(8)*. Further 1 ml saliva samples were collected at 3, 4, and 5 h post dose. Food and drink were withheld for 30 min before the collection of each saliva sample. The saliva samples were frozen at –20°C until later analysis using dual inlet isotope ratio mass spectrometry (Isoprime, GV Instruments, Wythenshawe, UK).

DXA

Each participant was scanned twice on the iDXA (EnCore software version 16 [enhanced analysis]; GE Healthcare Lunar, Maddison, WI), with repositioning in between scans, and once on the GE Lunar Prodigy (EnCore software version 12.3). The Prodigy data (basic analysis) were reanalyzed on the iDXA using software version 16 to provide enhanced Prodigy analysis. All 3 scans were performed on the same day by the same operator. The sites scanned were the hip (left femur) and the lumbar spine (L2–L4) for bone mass, area and density, and whole body for both whole-body bone mass, area and density, and body composition. Calibration block quality assurance and encapsulated spine phantom quality control scans were performed on each instrument at the start of each scanning day.

The scans were performed by 3 trained operators who performed scans according to the manufacturer positioning and scanning protocols (precision for each operator, represented by the percent coefficient of variance (% CV) of repeated scans, ranged from 0.7% to 1.5% for the lumbar spine and from 0.5% to 1.0% for the total hip, below the recommended 1.9% for the lumbar spine and 1.8% for the total hip by the International Society of Clinical Densitometry (ISCD) *(4)*). Subsequent analysis of all scans was carried out by a single operator to ensure consistency throughout the study.

ADP

The participants were asked to pass urine before the ADP procedure (BODPOD®; Cosmed Srl, Rome, Italy). Tight-fitting swim wear and a swimming cap were worn to minimize air trapped in clothing and hair. Lung volume was estimated by the BODPOD software to provide a net body volume estimate. The weight obtained during the ADP procedure was used as the body mass value for the 4-C analysis.

Analysis and Calculations

TBW Plateau Method. TBW was calculated according to the method of the International Atomic Energy Agency *(8)*. In brief, aliquots of 0.2 ml, drawn from the saliva samples, were placed in 3.7-ml glass bottles with rubber septa (nonevacuated vials; Labco Ltd, Lampeter, UK) and equilibrated with hydrogen in the presence of a platinum catalyst. Data were drift corrected offline and all measurements were made relative to the Vienna standard mean ocean water using laboratory standards traceable to the international standard.

^2H_2O dilution space was determined using the following equation *(9)*:

$$^2H_2O\,(kg)) = \left[\frac{D \times T \times (Ed - Et)}{d \times (Es - Ep)}\right] \Big/ 1000$$

where D is the amount of oral dosing solution, in gram, administered to the subject; T is the amount of deionized tap water used to dilute the enriched isotope dose, in gram; and d is the amount of enriched isotope dose in gram.

Ed is enrichment of the diluted dose d in T; Et is the enrichment of the tap water diluent; Es is the mean enrichment of saliva samples at 3, 4, and 5 h; and Ep is the enrichment of the pre dose sample.

TBW (in kilogram) was then calculated by reducing ^2H_2O dilution space values by 4% to account for the exchange of deuterium with nonaqueous hydrogen *(10)*.

4-Component (4-C) Model. FM (in kilogram) using the 4-C model was calculated using the following equation of Fuller et al *(7)*:

$$FM = 2.747 \times BV - 0.710 \times TBW - 1.460 \times BMC - 2.050 \times BW$$

where BV is body volume, determined using ADP; TBW is total body water, determined using deuterium dilution; bone mineral content (BMC) is whole-body BMC, determined using DXA; and BW is the body weight, determined during the ADP procedure.

Statistical Analysis

Descriptive data are reported as mean ± (standard deviation [SD]) unless otherwise stated.

Precision of the iDXA was expressed as the root mean square standard deviation (RMS-SD) and % CV according to ISCD recommendations. The least significant change was calculated (2.77 × RMS-SD) to establish the smallest change between repeated scans, which could be identified with 95% confidence intervals as originating from the participant rather than instrument and positioning variability *(5)*.

Paired sample t tests were performed to determine the difference between instruments.

Bland-Altman analysis was performed to determine the association and the agreement between the 2 instruments and between each instrument and 4-C-derived FM. Where appropriate, linear regression analysis was used to derive cross-calibration equations between Prodigy data using enhanced analysis mode and iDXA data. It should be noted that enhanced analysis mode is only available on Lunar Prodigy Advanced and iDXA instruments running software versions 15 and 16. If an earlier version of the Lunar Prodigy instrument is being used, refer to supplementary data where we have given whole-body and regional bone and body composition cross-calibration regression equations

to translate from Lunar Prodigy measurements analyzed in basic mode to Lunar iDXA measurements.

Repeated measures ANOVA was applied to test for the significance in fat measurements. *Post hoc* comparisons with Bonferroni correction were applied to discover the significance between methods (4-C, iDXA, Prodigy enhanced, and Prodigy basic). iDXA values were calculated as the mean of 2 iDXA measurements.

GraphPad Prism (Version 6.00 for Windows; GraphPad Software, San Diego, CA) was used to generate Bland-Altman analyses, and IBM SPSS (IBM SPSS Statistics for Windows, Version 21.0; IBM Corp., Armonk, NY) was used for all other statistical analyses.

Significance was assumed for $p < 0.05$ for all statistical tests.

Results

iDXA Precision

The precision error for repeated iDXA scans is shown in Table 2. Precision error, when represented by % CV, was less than 2% for all measures, with the exception of arm FM (2.28%). A greater precision was demonstrated for lean mass (LM) than for FM.

iDXA FM Accuracy

iDXA-measured FM and 4-C-derived FM are highly correlated ($r^2 = 0.99, p < 0.05$) with a slope of 0.892 and an intercept of 3.39. However, there is a significant difference between iDXA-measured FM and 4-C-derived FM (mean difference [SD], –0.936 [1.83], $p < 0.05$) with wide limits of agreements (–4.53 to 2.65). It can be seen in Fig. 1 that there is a significant positive proportional bias and systematic bias. Furthermore, at an average FM of 32.12 kg, the iDXA shifted from overmeasuring to undermeasuring FM compared to 4-C-derived FM.

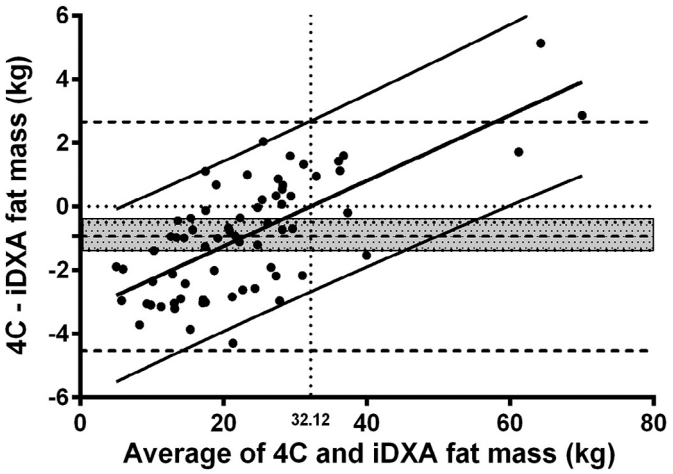

Fig. 1. Bland-Altman plot of iDXA and 4-component model-derived fat mass (n = 68). The solid black linear regression line demonstrates systematic bias, the hashed gray box corresponds to the 95% confidence interval of the systematic bias, the dashed lines represent the limits of agreements, and the vertical dotted lines present the crossover of over- to undermeasuring fat mass at 32.12 kg.

iDXA vs Prodigy

There were significant differences in whole-body mass and spine bone mass between iDXA- and Prodigy enhanced

Table 2
Precision Variables of 2 iDXA Whole-Body and Regional Body Composition Measurements

Region	Variables	Mean ± SD	Mean difference	RMS-SD	% CV	LSC
Hip	BMC (g)	36.0 ± 7.6	-0.1	0.5	1.1	1.3
	Area (cm^2)	33.2 ± 4.0	0.4	0.3	0.6	0.8
	BMD (g/cm^2)	1.08 ± 0.16	0.00	0.01	0.72	0.03
Spine	BMC (g)	58.7 ± 12.1	-0.4	0.7	0.9	2.0
	Area (cm^2)	46.6 ± 0.3	0.0	0.4	0.5	1.2
	BMD (g/cm^2)	1.25 ± 0.01	-0.01	0.01	0.74	0.04
Whole body	BMC (kg)	2.8 ± 0.6	0.0	0.0	0.4	0.0
Arms	Fat mass (kg)	2.3 ± 1.1	0.0	0.0	2.3	0.2
	Lean mass (kg)	5.6 ± 1.8	0.0	0.1	1.2	0.3
Legs	Fat mass (kg)	8.4 ± 4.5	-0.1	0.2	1.3	0.5
	Lean mass (kg)	18.2 ± 4.0	-0.1	0.2	0.7	0.5
Trunk	Fat mass (kg)	6.1 ± 6.5	-0.0	0.3	1.6	0.7
	Lean mass (kg)	24.0 ± 4.7	0.1	0.3	0.9	0.8
Whole body	Fat mass (kg)	23.6 ± 11.5	-0.1	0.3	0.9	0.7
	Lean mass (kg)	51.0 ± 10.4	0.1	0.3	0.4	0.8

Abbr: % CV, percent coefficient of variance; BMC, bone mineral content; BMD, bone mineral density; LSC, least significant change; RMS-SD, root mean square standard deviation; SD, standard deviation.

Table 3
Whole-Body and Regional iDXA and Prodigy Enhanced Bone Density Measurements

Region	Variables	iDXA	Prodigy enhanced	Bias	LOA
Whole body	BMC (kg)	2.8 ± 0.6	2.8 ± 0.6	0.0 ± 0.0*	−0.1 to 0.1
	Area (cm^2)	2255.1 ± 234.3	2219.4 ± 236.9	35.8 ± 51.0*	−64.2 to 135.7
	BMD (g/cm^2)	1.24 ± 0.15	1.25 ± 0.16	−0.01 ± 0.02*	−0.06 to 0.04
Hip	BMC (g)	36.0 ± 7.6	36.1 ± 7.6	−0.1 ± 1.2	−2.3 to 2.2
	Area (cm^2)	33.2 ± 4.0	33.2 ± 3.9	0.1 ± 0.9	−1.6 to 1.8
	BMD (g/cm^2)	1.08 ± 0.16	1.08 ± 0.15	0.00 ± 0.02	−0.04 to 0.04
Spine	BMC (g)	58.7 ± 12.1	59.2 ± 12.3	−0.4 ± 1.2*	−2.8 to 1.9
	Area (cm^2)	46.6 ± 5.6	46.6 ± 5.6	0.0 ± 0.8	−1.5 to 1.5
	BMD (g/cm^2)	1.25 ± 0.15	1.26 ± 0.15	−0.01 ± 0.02*	−0.05 to 0.04

Note: Mean ± standard deviation.
Abbr: BMC, bone mineral content; BMD, bone mineral density; LOA, limits of agreement.
*$p < 0.05$.

measurements; these differences were not seen in any hip measurements (Table 3).

The comparison of body composition measurements between the instruments reveals significant differences in FM and LM across all regions (Table 4).

Differences in whole-body and regional bone and body composition measurements between Prodigy basic mode and iDXA enhanced mode analyses are presented in supplementary Table S1. The relevant cross-calibration regression equations can be found in supplementary Tables S2 and S3.

Figure 2 illustrates the agreement between instruments in FM and LM by Bland-Altman analysis. Compared to iDXA, Prodigy overestimates FM (mean difference −1.29 kg) and underestimates LM (mean difference 1.18 kg).

Because of the observed differences between instruments (Tables 3 and 4), linear regression cross-calibration equations were derived where appropriate and can be seen in Table 5.

Prodigy Accuracy

Prodigy enhanced FM and 4-C-derived FM are highly correlated ($r^2 = 0.993$), with a slope of 0.883 and an intercept of 4.80. As observed with the iDXA (Fig. 1), there is a significant difference between Prodigy enhanced FM and 4-C FM (mean difference [SD] −2.16 [2.05] kg). There are also wider limits of agreement (−6.17 to 1.86) and a more negative systematic bias compared with the iDXA (Fig. 3B and C).

Four Method Comparison

The measurement of FM was significantly affected by method ($F(3, 201) = 41.057$, $p < 0.05$). There was a significant difference between 4-C-derived FM and iDXA (mean difference −0.936, $p = 0.000$), Prodigy enhanced (−2.157, $p = 0.000$) and Prodigy basic (−1.720, $p = 0.000$) FM. However, there was no significant difference between Prodigy basic and Prodigy enhanced FM measurements (0.437, $p = 0.275$).

Table 4
Whole-Body and Regional iDXA and Prodigy Enhanced Body Composition Measurements

Region	Variables	iDXA	Prodigy enhanced	Bias	LOA
Whole body	Fat mass (kg)	23.6 ± 11.6	24.9 ± 11.7	−1.3 ± 0.6*	−2.5 to 0.1
	Lean mass (kg)	51.0 ± 10.4	49.9 ± 10.1	1.1 ± 0.6*	0.0–2.2
Arm	Fat mass (kg)	2.3 ± 1.1	2.5 ± 1.2	−0.3 ± 0.2*	−0.6 to 0.1
	Lean mass (kg)	5.6 ± 1.8	5.4 ± 1.8	0.2 ± 0.3*	−0.5 to 0.9
Leg	Fat mass (kg)	8.4 ± 4.5	8.9 ± 4.5	−0.5 ± 0.3*	−1.1 to 0.1
	Lean mass (kg)	18.2 ± 4.0	17.8 ± 3.9	0.5 ± 0.6*	−0.8 to 1.7
Trunk	Fat mass (kg)	12.1 ± 6.5	12.6 ± 6.4	−0.5 ± 0.4	−1.3 to 0.4
	Lean mass (kg)	24.0 ± 4.7	23.6 ± 4.4	0.4 ± 0.7*	−1.0 to 1.8

Note: Mean ± standard deviation.
Abbr: LOA, limits of agreement.
*$p < 0.05$.

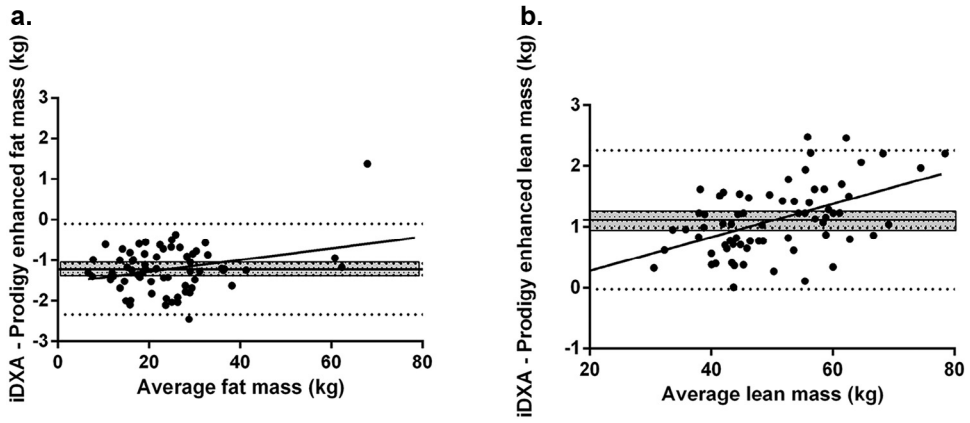

Fig. 2. Bland-Altman analysis of the agreement between iDXA- and Prodigy-measured whole-body fat mass (**A**) and lean mass (**B**). The solid black line corresponds to the systematic bias, the hashed gray box corresponds to the 95% confidence interval of the systematic bias, and the vertical dotted lines represent the limits of agreements.

Table 5
Cross-Calibration Equations (Prodigy Enhanced to iDXA)

	Variable	Slope	95% CI	Intercept	95% CI	r^2
Whole body	BMC (g)	1.003*	0.983–1.023	0.017	–0.041 to 0.074	0.993
	BA (cm^2)	0.966*	0.914–1.017	112.0	–3.543 to 227.6	0.953
	BMD (g/cm^2)	0.965*	0.928–1.001	0.035	–0.011 to 0.081	0.976
	Fat mass (kg)	0.991*	0.978–1.005	–1.016*	–1.393 to –0.639	0.997
	Lean mass (kg)	1.029	1.013–1.045	–0.262	–1.058 to 0.535	0.996
Spine	BMC (g)	0.978*	0.954–1.001	0.877	–0.537 to 2.290	0.990
	BA (cm^2)	0.990*	0.956–1.023	0.505	–1.045 to 2.055	0.981
	BMD (g/cm^2)	0.986	0.950–1.022	0.008	–0.038 to 0.054	0.978
Regional	Arm fat mass (kg)	0.962*	0.923–1.001	–0.155*	–0.262 to – 0.048	0.973
	Arm lean mass (kg)	0.972*	0.927–1.016	0.350*	0.097–0.603	0.966
	Leg fat mass (kg)	0.989*	0.973–1.005	–0.444*	–0.604 to –0.284	0.996
	Leg lean mass (kg)	1.024*	0.985–1.063	0.036	–0.673–0.746	0.976
	Trunk fat mass (kg)	1.010*	0.995–1.026	–0.591*	–0.811– – 0.372	0.996
	Trunk lean mass (kg)	1.042*	1.003–1.080	–0.576	–1.494–0.341	0.978

Note: Adjusted r^2 indicates model variance.
Abbr: BA, bone area; BMC, bone mineral content; BMD, bone mineral density; CI, confidence interval.
*$p < 0.05$.

Figure 3 does show that iDXA limits of agreement with 4-C (–4.78 to 2.63) are narrower compared with Prodigy in basic mode (–5.56 to 2.12), which in turn are narrower than the Prodigy enhanced mode (–6.17 to 1.86).

Discussion

The aim of the present study was 2-fold: firstly, to determine the precision and accuracy of the GE Lunar iDXA, and secondly, to determine if cross-calibration equations are necessary to relate data from the GE Lunar Prodigy to the iDXA densitometers. The differences between software versions for the Prodigy were also investigated.

When introducing a new DXA instrument, the ISCD recommend that a cross-calibration of at least 30 participants, representative of the facility's patient population, should be performed. Participants should be scanned twice on the new system and once on the old, on those anatomical sites most commonly measured *(4)*. We compared the iDXA and Prodigy densitometers for regional and whole-body bone mineral densities, BMCs, and bone areas, and, reflecting our interest in body composition, for LM and FM. Where cross-calibration equations were deemed necessary, they were derived using linear regression.

iDXA Precision

Precision of the iDXA was assessed by % CV of repeated bone and body composition measurements. We found excellent precision in whole-body and regional bone

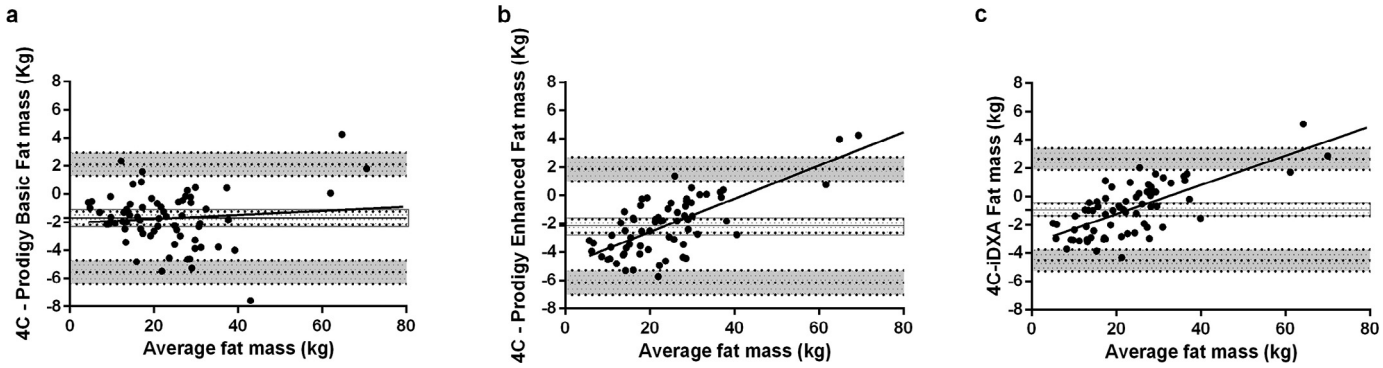

Fig. 3. Demonstration of the difference and progression between the 4-component model and Prodigy basic analysis (**A**), Prodigy Enhanced (**B**), and iDXA (**C**) with 95% limits of agreement. The solid black line corresponds to the systematic bias, the hashed gray box corresponds to the 95% confidence interval of the systematic bias, and the vertical dotted lines represent the limits of agreements with corresponding 95% confidence interval represented by gray boxes.

density with all values below 2%. This was also observed for whole-body and regional body composition measurements with the exception of arm FM, which had a lower precision of 2.28%.

Our findings support previously published literature, which has reported similar precision data for whole-body and regional bone density and body composition using iDXA *(2,3,11,12)*. Additionally, both Rothney et al *(11)* and Kaminsky et al *(12)* support our findings of a lower precision in arm FM (2.8% and 4.2%, Rothney et al and Kaminsky et al, respectively). The larger precision error may be due to the repositioning of the participants or the inclusion of breast tissue in the arm region of interest in some rescans, therefore offering the potential for larger errors *(13)*.

Compared to the iDXA, previously published reports from its predecessor, the Prodigy has demonstrated a similar precision for bone density with precisions reported below 2% by Oldroyd et al *(14)* and Krueger et al *(15)*. However, when exploring body composition, both Oldroyd et al and Bilsborough et al *(16)* reported whole-body FM precision values of 2.5% for Prodigy. This is a much lower precision than that of 0.9% for the iDXA in the current study.

These comparisons suggest that the precision of iDXA when measuring bone density remains similar to the Prodigy. However, there appears to be a worthwhile improvement in precision in whole-body and regional FM. This may be due to the improvement in soft tissue assessment as a result of enhanced bone edge detection technology *(17)*.

iDXA vs Prodigy

When scan analysis was carried out using the same software version, significant differences between iDXA and Prodigy were identified in all regions of bone mass, area, and density except for the femoral hip BMD and lumbar spine (L2–L4) bone area, with Prodigy over-reading all values with the exception of hip area. This finding has been similarly observed in other studies *(18–20)* with Hull et al *(19)* reporting significantly higher mean BMC values in the Prodigy than in the iDXA in both males and females (males: 3.11 kg vs 3.06 kg, Prodigy vs iDXA, respectively, and females: 2.37 kg vs 2.31 kg, Prodigy vs iDXA, respectively). Rhodes et al *(20)* also found Prodigy BMC values were significantly higher compared with the iDXA in all regions of bone mass (BMC, 2842 g vs 2651 g, Prodigy vs iDXA, respectively). Furthermore, Morrison et al *(21)* compared iDXA to Prodigy and found significant differences in whole-body and regional bone density (mean whole-body; 1.25 g/cm^2 vs 1.22 g/cm^2, Prodigy vs iDXA, respectively)

When investigating body composition, we also observed significant differences between iDXA and Prodigy, with Prodigy tending to over-read FM and to under-read LM relative to iDXA. The only study we found in the literature to make a similar comparison was that of Morrison et al *(21)*, who reported that only leg LM and arm soft tissue measurements were significantly different between instruments (leg LM mean difference [in kilogram]: 0.586, arm FM: –0.109, arm LM: –0.228).

The significant differences observed between the 2 DXA instruments warranted the development of cross-calibration regression equations. These differences and those observed across the published literature highlight the importance of generating instrument-specific cross-calibration equations when undergoing a system upgrade. It is also important that the cross-calibration equations are relevant to the population under investigation as demonstrated by the apparent outliers at the top end of the FM range.

DXA Accuracy

The accuracy of our DXA FM measurements was evaluated by comparing FM estimated by DXA to that derived from a 4-C model. The 4-C model, as well as whole-body MRI, is a recognized standard in body composition measurements as they account for interindividual variability in TBW and bone mineral mass *(22–24)*. Our results demonstrated a good correlation between iDXA and 4-C-derived FM (r = 0.994), but a systematic bias between the

2 FM estimates was evident. To our knowledge, there is no literature that discusses the accuracy of either iDXA or Prodigy FM measurement using the 4-C model. However, previous literature has reported significant differences between FM (percent) measured by various DXA models (QDR2000, QDR2000W, DPX/L, and Lunar) and the 4-C model *(25)*. When comparing Prodigy and the 4-C model, Williams et al *(25)* found significant differences in FM (1.35, 1.21, and 1.58 kg in nonobese men, women, and obese women, respectively). Williams et al also reported that the FM bias was positively associated with the body mass index. Although it appears that the accuracy of DXA has improved over the years, a systematic bias still remains between the iDXA and the 4-C model.

The differences identified between the 2 methods could have several origins. DXA assumes that the hydration value for fat-free mass remains constant *(26)*; however, this may not be true for participants across a range of masses. Participant mass itself may inflict a bias in soft tissue estimation because of the influence of tissue depth on bone edge detection by DXA; therefore, as subject mass increases, so may the error in detecting soft tissue.

Comparisons between GE software versions (basic and enhanced) for Prodigy and a 4-C model have not been investigated before. There are many publications that demonstrate the transitions between instruments but few that detail the differences when upgrading software versions. In the final part of the present study, we investigated the differences in whole-body FM measurements between basic and enhanced software versions on the Prodigy and compared these to the iDXA and 4-C model.

Prodigy basic analysis mode compared to 4-C demonstrated a good agreement over a wide range of FMs. However, in the highest FMs, the agreement was less good, consistent with previous studies *(25,27,28)*. As referred to earlier, Williams et al *(25)* reported the largest difference between 4-C and Prodigy (Encore 2002) in obese women (mean bias 1.58 kg), and Wells et al *(27)* (Software version not stated) reported that Prodigy significantly overestimated FM compared to 4-C by 0.9 kg with the greatest variability being observed at the highest FMs.

In summary, the latest DXA instrument from GE, the iDXA, comes with new hardware in the form of a more powerful X-ray tube, enhanced image resolution, and therefore better bone edge detection. Furthermore, the latest software, Encore version 15 and 16, comes with developed soft tissue algorithms. This enhancement in technology has led to an improvement in both the accuracy and the precision of the new instrument. However, this finding means that differences exist between the iDXA and the Prodigy instruments, and therefore cross-calibration equations are essential if comparisons between instruments are unavoidable. Even with these improvements, accuracy issues remain at the highest FMs, reinforcing the importance of deriving cross-calibration equations that are relevant to the population under investigation, and also, further comparative studies are warranted in an obese population.

Acknowledgments

LPEW and PRM are supported by the NIHR/Wellcome Trust Clinical Research Facility Cambridge. MCV is supported by the MRC Elsie Widdowson Laboratory (Programme numbers: Physiological Modelling of Metabolic Risk, MC_UP_A090_1005, and Nutrition, Surveys and Studies, MC_U105960384).

The authors thank all of the participants without whom we could not have completed this study. We would also like to thank Katie Bird and Liz Blower at the NIHR/Wellcome Trust Clinical Research Facility for their assistance with the DXA measurements and dose administration, and Priya Singh and Elise Orford at the Medical Research Council Elsie Widdowson Laboratory for their assistance in the deuterium analysis. Of course, we will remain forever indebted to Dr Les Bluck for all of his scientific excellence and help in conceptualizing the study and for many other worthy contributions before his untimely death.

Appendix: Supplementary material

Supplementary data to this article can be found online at doi:10.1016/j.jocd.2017.06.029.

References

1. Toombs RJ, Ducher G, Shepherd JA, De Souza MJ. 2012 The impact of recent technological advances on the trueness and precision of DXA to assess body composition. Obesity (Silver Spring) 20(1):30–39.
2. Hind K, Oldroyd B, Truscott JG. 2011 In vivo precision of the GE Lunar iDXA densitometer for the measurement of total body composition and fat distribution in adults. Eur J Clin Nutr 65(1):140–142.
3. Hind K, Oldroyd B, Truscott JG. 2010 In vivo precision of the GE Lunar iDXA densitometer for the measurement of total-body, lumbar spine, and femoral bone mineral density in adults. J Clin Densitom 13(4):413–417.
4. Shepherd JA, Lu Y, Wilson K, et al. 2006 Cross-calibration and minimum precision standards for dual-energy X-ray absorptiometry: the 2005 ISCD Official Positions. J Clin Densitom 9(1):31–36.
5. Baim S, Wilson CR, Lewiecki EM, et al. 2005 Precision assessment and radiation safety for dual-energy X-ray absorptiometry: position paper of the International Society for Clinical Densitometry. J Clin Densitom 8(4):371–378.
6. Chen X, Iqbal N, Boden G. 1999 The effects of free fatty acids on gluconeogenesis and glycogenolysis in normal subjects. J Clin Invest 103(3):365–372.
7. Fuller NJ, Jebb SA, Laskey MA, et al. 1992 Four-component model for the assessment of body composition in humans: comparison with alternative methods, and evaluation of the density and hydration of fat-free mass. Clin Sci 82(6):687–693.
8. IAEA. 2009 Assessment of body composition and total energy expenditure in humans using stable isotope techniques. In: IAEA Human Health Series. Vienna: IAEA, 146.
9. Coward WA. 1991 Measurement of energy expenditure: the doubly-labelled-water method in clinical practice. Proc Nutr Soc 50(2):227–237.

10. Schoeller DA, Hnilicka JM. 1996 Reliability of the doubly labeled water method for the measurement of total daily energy expenditure in free-living subjects. J Nutr 126(1):348S–354S.
11. Rothney MP, Martin FP, Xia Y, et al. 2012 Precision of GE Lunar iDXA for the measurement of total and regional body composition in nonobese adults. J Clin Densitom 15(4):399–404.
12. Kaminsky LA, Ozemek C, Williams KL, Byun W. 2014 Precision of total and regional body fat estimates from dual-energy X-ray absorptiometer measurements. J Nutr Health Aging 18(6):591–594.
13. Knapp KM, Welsman JR, Hopkins SJ, et al. 2015 Obesity increases precision errors in total body dual-energy x-ray absorptiometry measurements. J Clin Densitom 18(2):209–216.
14. Oldroyd B, Smith AH, Truscott JG. 2003 Cross-calibration of GE/Lunar pencil and fan-beam dual energy densitometers–bone mineral density and body composition studies. Eur J Clin Nutr 57(8):977–987.
15. Krueger D, Vallarta-Ast N, Checovich M, et al. 2012 BMD measurement and precision: a comparison of GE Lunar Prodigy and iDXA densitometers. J Clin Densitom 15(1):21–25.
16. Bilsborough JC, Greenway K, Opar D, et al. 2014 The accuracy and precision of DXA for assessing body composition in team sport athletes. J Sports Sci 32(19):1821–1828.
17. GE Healthcare 2006 Lunar iDXA: Intelligent DXA. Belgium: GE Healthcare, 10.
18. Hind K, Cooper W, Oldroyd B, et al. 2013 A cross-calibration study of the GE-Lunar iDXA and prodigy for the assessment of lumbar spine and total hip bone parameters via three statistical methods. J Clin Densitom 18(1):86–92.
19. Hull H, He Q, Thornton J, et al. 2009 iDXA, Prodigy, and DPXL dual-energy X-ray absorptiometry whole-body scans: a cross-calibration study. J Clin Densitom 12(1):95–102.
20. Rhodes LA, Cooper W, Oldroyd B, Hind K. 2013 Cross-calibration of a GE iDXA and Prodigy for total and regional body bone parameters: the importance of using cross-calibration equations for longitudinal monitoring after a system upgrade. J Clin Densitom 17(4):496–504.
21. Morrison SA, Petri RM, Hunter HL, et al. 2016 Comparison of the lunar prodigy and iDXA dual-energy X-ray absorptiometers for assessing total and regional body composition. J Clin Densitom 19(3):290–297.
22. Lohman TG, Harris M, Teixeira PJ, Weiss L, et al. 2000 Assessing body composition and changes in body composition. Another look at dual-energy X-ray absorptiometry. Ann N Y Acad Sci 904:45–54.
23. Muller MJ, Braun W, Pourhassan M, et al. 2016 Application of standards and models in body composition analysis. Proc Nutr Soc 75(2):181–187.
24. Heymsfield SB, Ebbeling CB, Zheng J, et al. 2015 Multi-component molecular-level body composition reference methods: evolving concepts and future directions. Obes Rev 16(4):282–294.
25. Williams JE, Wells JK, Wilson CM, et al. 2006 Evaluation of lunar prodigy dual-energy X-ray absorptiometry for assessing body composition in healthy persons and patients by comparison with the criterion 4-component model. Am J Clin Nutr 83(5):1047–1054.
26. Wang Z, Heymsfield SB, Chen Z, et al. 1999 Hydration of fat-free body mass: review and critique of a classic body-composition constant. Am J Clin Nutr 69(5):833–841.
27. Wells JC, Williams JE, Chomtho S, et al. 2012 Body-composition reference data for simple and reference techniques and a 4-component model: a new UK reference child. Am J Clin Nutr 96(6):1316–1326.
28. Wells JC, Haroun D, Williams JE, et al. 2015 Body composition in young female eating-disorder patients with severe weight loss and controls: evidence from the four-component model and evaluation of DXA. Eur J Clin Nutr 69(12):1330–1335.